Breaking the Barrier: An Osmium Photosensitizer with Unprecedented Hypoxic Phototoxicity for Real World Photodynamic Therapy

John A. Roque III,[a,b] Patrick C. Barrett,[a] Houston D. Cole,[b] Liubov M. Lifshits,[b] Ge Shi,[c] Susan Monro,[c] David von Dohlen,[a] Susy Kim,[d] Nino Russo,[e] Gagan Deep,[d] Colin G. Cameron,*[a,b] Marta E. Alberto,*[e] Sherri A. McFarland*[a,b,c]

[a] *Department of Chemistry and Biochemistry, The University of North Carolina at Greensboro, Greensboro, North Carolina, 27402 USA*
[b] *Department of Chemistry and Biochemistry, The University of Texas at Arlington, Arlington, Texas, 76019 USA*
[c] *Department of Chemistry, Acadia University, Wolfville, Nova Scotia, B4P 2R6 Canada*
[d] *Department of Cancer Biology, Wake Forest School of Medicine, Winston Salem, NC, 27157 USA*
[e] *Dipartimento di Chimica e Tecnologie Chimiche, Università della Calabria, Arcavacata di Rende, 87036 Italy*
* Corresponding Authors: C.G.C <colin.cameron@uta.edu> ORCID 0000-0003-0978-0894; M.E.A. <marta.alberto@unical.it> ORCID 0000-0001-9925-7233; S.A.M. <sherri.mcfarland@uta.edu> ORCID 0000-0002-8028-5055

Supplemental Methods (SM)

Figures

Table(s)

Supplemental Methods (SM)

SM-1 Standard assay on 384-well plates

A miniaturized format for drug screening by hand. An electronic multichannel pipettor is strongly recommended for successful set-up by hand. Volumes of our standard assay in 96-well plates approximately decrease to 40%. Into 384-well plates (Greiner Bio-One 781182), a DPBS perimeter of 100 µL/well was installed into the outmost two wells (144 well count). After this, 10 µL/well of DPBS was dispensed into all control wells (12 count). For sample and control wells (240 well count), 10 µL/well of complete media was added. An additional 20 µL/well media was dispensed into negative cell controls. At this point, sample wells have 10 µL/well complete media, positive controls 20 µL/well media and DPBS, and negative controls 40 µL/well of mainly media. It is optional to equilibrate plates in a humidified incubator (37°C, 5% CO_2, ≥ 90% RH) to aid initial aliquots. For light treated compounds of greater potency (pM activity), controls are excluded to expand the concentration range on any given plate.

After media is dispensed, plates are equilibrated in the incubator for a minimum 15 mins before addition of cellular slurry. In the case of our cell line SK-MEL-28, seeding density is slightly lower than 96-well format at 150,000 cells mL^{-1} (3000 cells $well^{-1}$). Several seed densities with **Os-4T** were tested ranging from 50,000–200,000 cells mL^{-1} and found to produce similar dose-response curves. However, the lower seed density was a better fit for the linear portion of a standard curve over our assay's timeline (3–4 days). Plates were seeded 20 µL/well across four plates at a time for sample and positive control wells. They were mixed twice (up, down, left, right - mild inversions) at both the biosafety cabinet and before placing inside the incubator.

Following 1–3 h of incubation, cells are either left to incubate further (normoxia runs) or transferred to a 1% O_2 culture chamber (Biospherix, XVivo 2) for 2–3 h incubation. While waiting, compound serial dilutions are prepared in sterile 0.8 mL 96-deep well plates (VWR 76210-522) using DPBS as solvent. For compounds of lower solubility like **Os-4T**, initial aliquots are dispensed via reverse pipette due to increased viscosity at 25 mM in DMSO. Dilutions are prepared in serial across 9–20 concentrations ranging from 1200–4×10^{-14} µM. Covered deep-well plates are incubated for 0.5–1 h before final dispensing (d_f = 4) at 10 µL/well. All sample and control wells have 40 µL/well at this point. Replicates are generally dispensed row-wise and spaced every 4 (triplicates) or 6 (duplicates) rows. Repeats across experiments change plate maps for compound and replicate locations. For a standard 12-channel pipettor, compounds are dispensed every other column. Therefore, it is important to plan liquid dispensing and an appropriate plate map ahead of time.

Following dark (sham) or light treatments (16–20 h drug-to-light interval, DLI), plates are further incubated overnight before final viability measurements. One day is removed from the post-PDT period of our standard 96-well plate assay to mitigate edge effects. At this point, 10 µL/well of 0.3 mM sterifiltered resazurin in 0.2 M phosphate buffer (pH = 7.4) is aliquoted across all well plates. Generally, 4–6 plates are handled at a time in the biosafety cabinet. Resazurin dyed plates were incubated further for 4 h before reading fluorometrically on a Molecular Devices M2e (30 s shake, bottom-read, λ_{exc} 530 nm, long-pass 570 nm, λ_{em} 620 nm). Whereas unnecessary for a 96-well plate, it was found that assay S/N drastically improved if the reader's plate adaptor was removed prior to the read (shorter distance from sample to detector).

Following resazurin, the sulforhodamine B (SRB) assay would likewise be performed as described in the main text at this point. All volumes are half of those used in a 96-well plate. However, it was not performed for any data reported in these works on a 384-well plate.

Data from 384-well plates was generally processed via custom R[1] scripts using the plater,[2] dplyr,[3] readxl,[4] openxlsx,[5] and tidyr[6] packages.

References

1 R Core Team, *R: A Language and Environment for Statistical Computing*, R Foundation for Statistical Computing, Vienna, Austria, 2020.
2 S. M. Hughes, *J. Open Source Softw.*, 2016, **1**, 106.
3 H. Wickham, R. François, L. Henry and K. Müller, *dplyr: A Grammar of Data Manipulation*, 2020.
4 H. Wickham and J. Bryan, *readxl: Read Excel Files*, 2019.
5 P. Schauberger and A. Walker, *openxlsx: Read, Write and Edit xlsx Files*, 2019.
6 H. Wickham and L. Henry, *tidyr: Tidy Messy Data*, 2020.

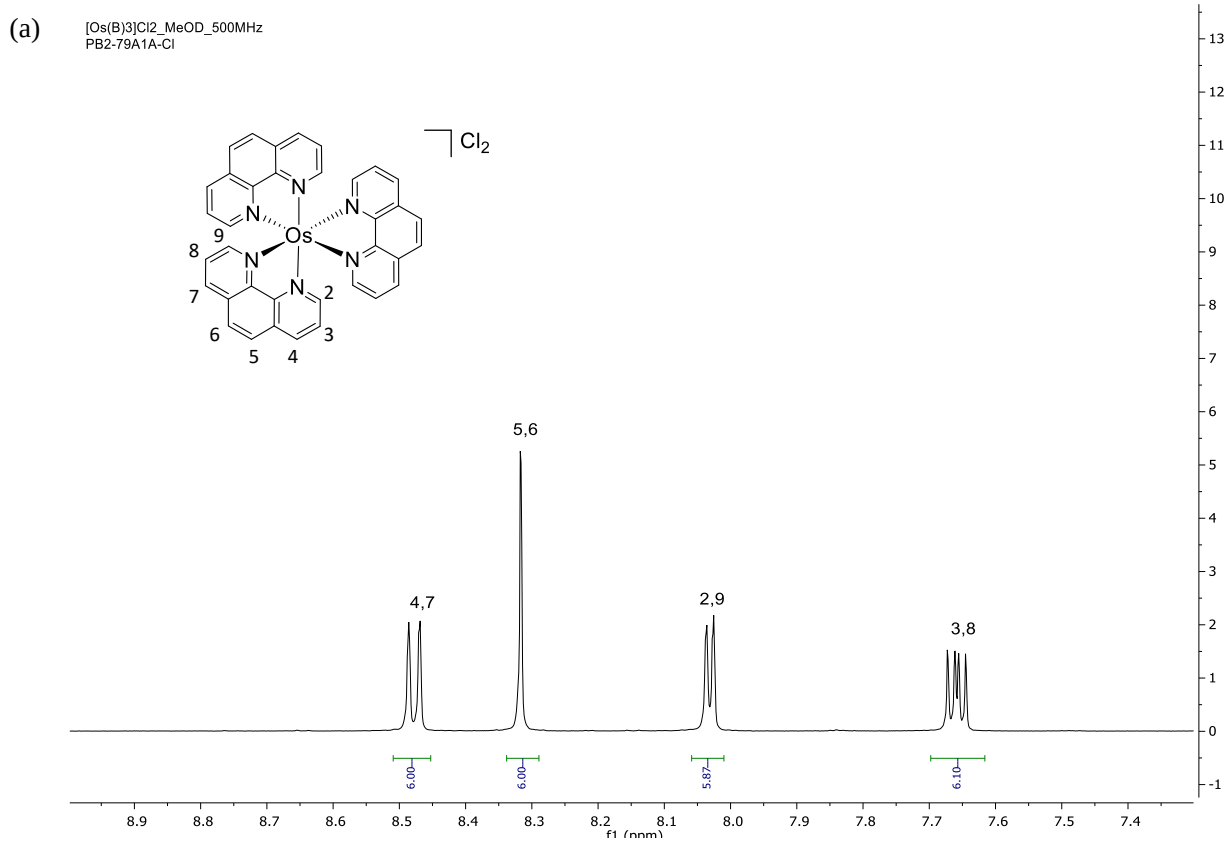

Figure S-1 500 MHz ^{1}H NMR spectra of $[Os(phen)_3]^{2+}$ (Cl^- salt) in MeOD-d_3 at 298 K with structure labelling and ^{1}H NMR assignments. Zoom of ^{1}H NMR spectrum, aromatic region.

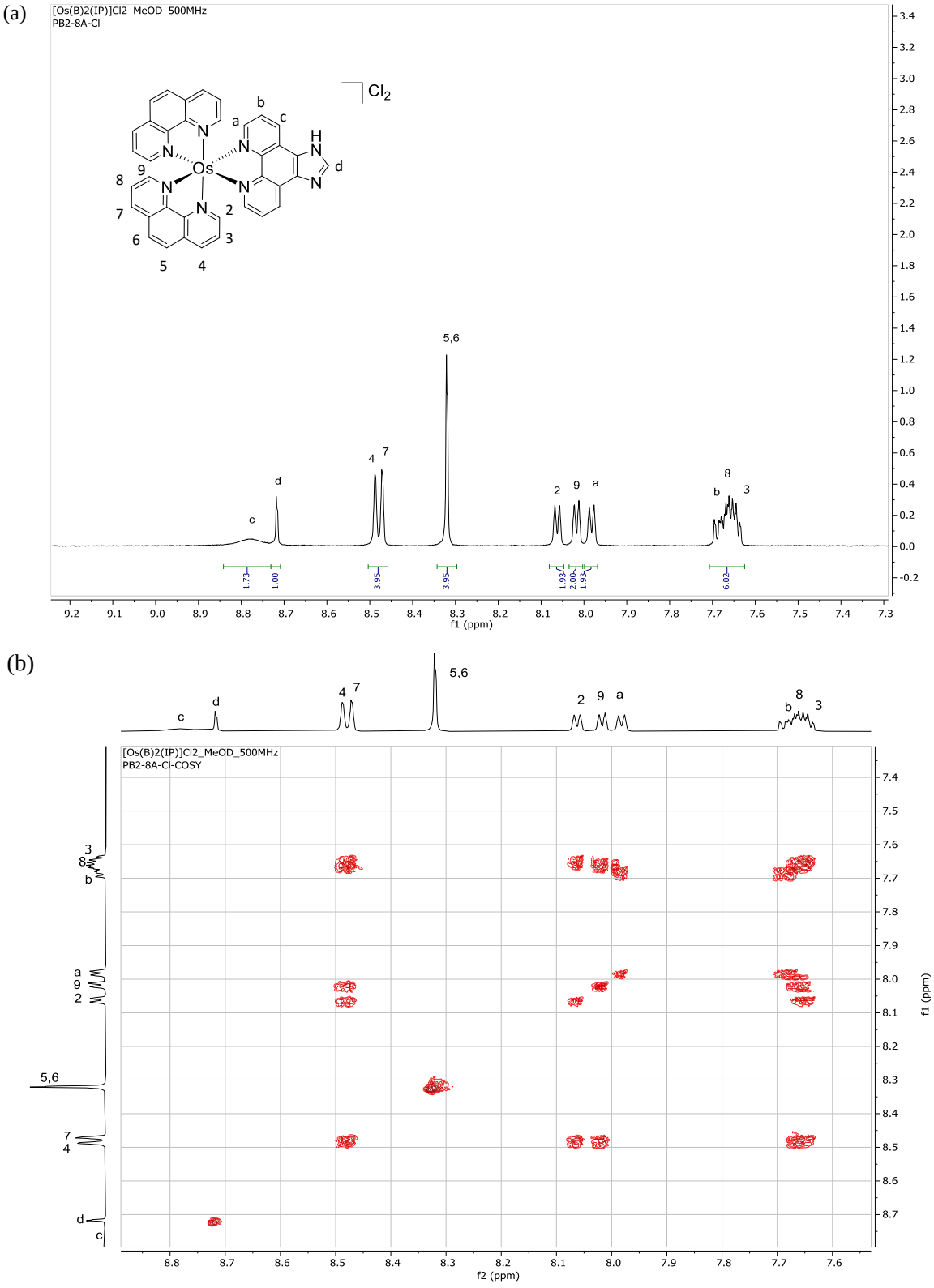

Figure S-2 500 MHz ^{1}H NMR spectra of **Os-0T** (Cl^{-} salt) in MeOD-d_3 at 298 K with structure labelling and ^{1}H NMR assignments. (a) Zoom of ^{1}H NMR spectrum, aromatic region. (b) ^{1}H–^{1}H COSY NMR spectrum, aromatic region.

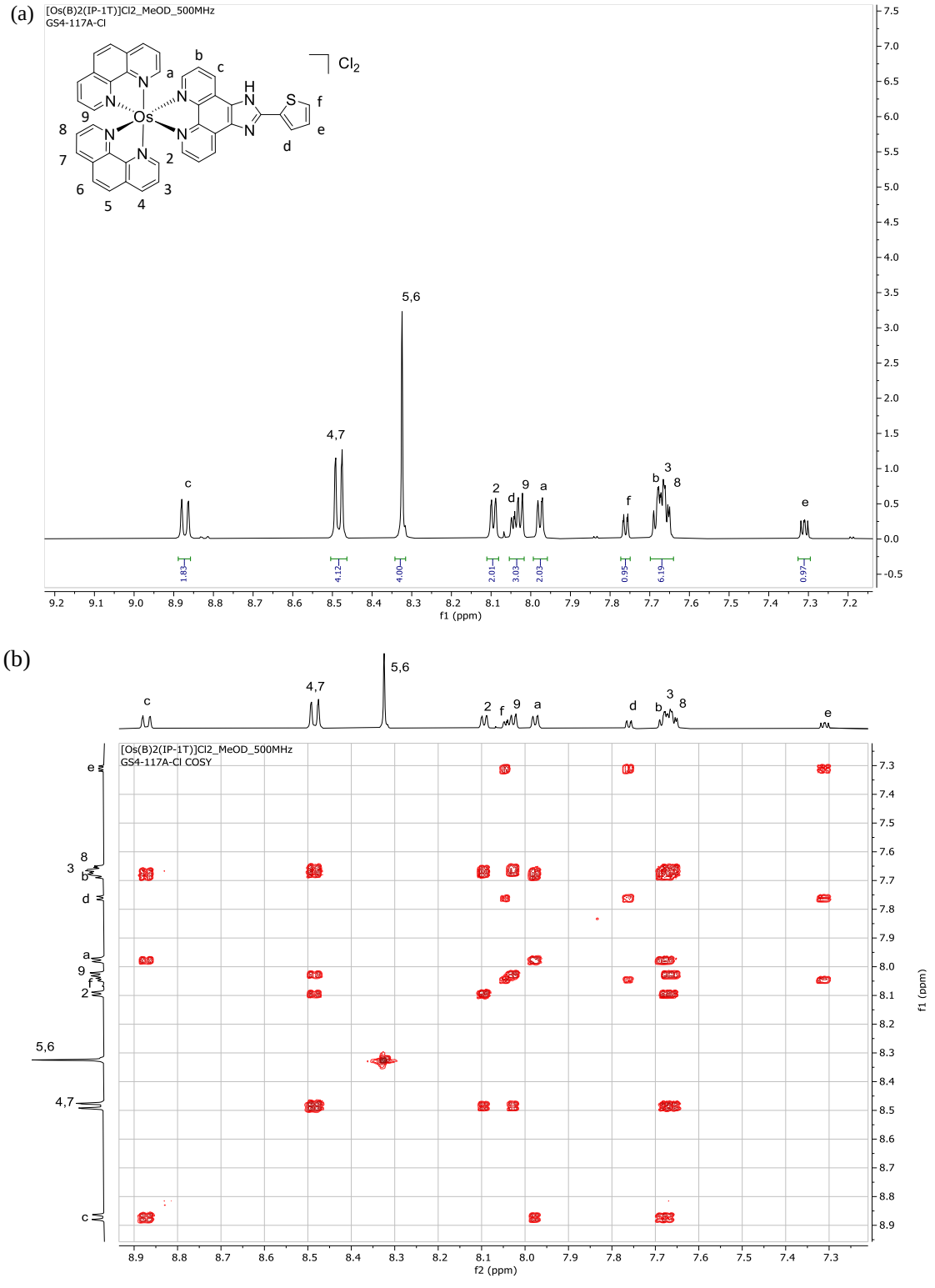

Figure S-3 500 MHz ^{1}H NMR spectra of **Os-1T** (Cl^{-} salt) in MeOD-d_3 at 298 K with structure labelling and ^{1}H NMR assignments. (a) Zoom of ^{1}H NMR spectrum, aromatic region. (b) ^{1}H–^{1}H COSY NMR spectrum, aromatic region.

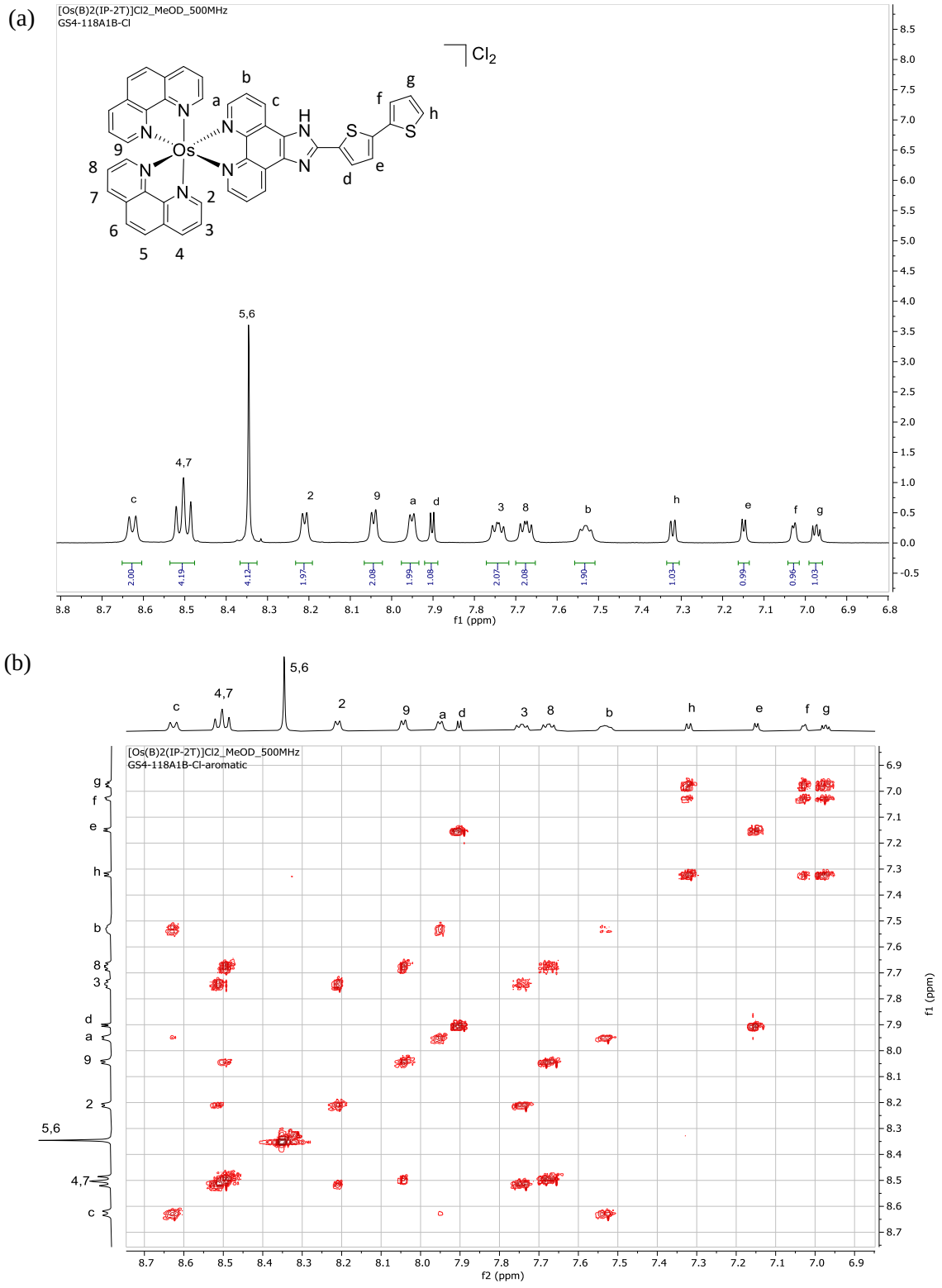

Figure S-4 500 MHz ^{1}H NMR spectra of **Os-2T** (Cl^{-} salt) in MeOD-d_3 at 298 K with structure labelling and ^{1}H NMR assignments. (a) Zoom of ^{1}H NMR spectrum, aromatic region. (b) ^{1}H–^{1}H COSY NMR spectrum, aromatic region.

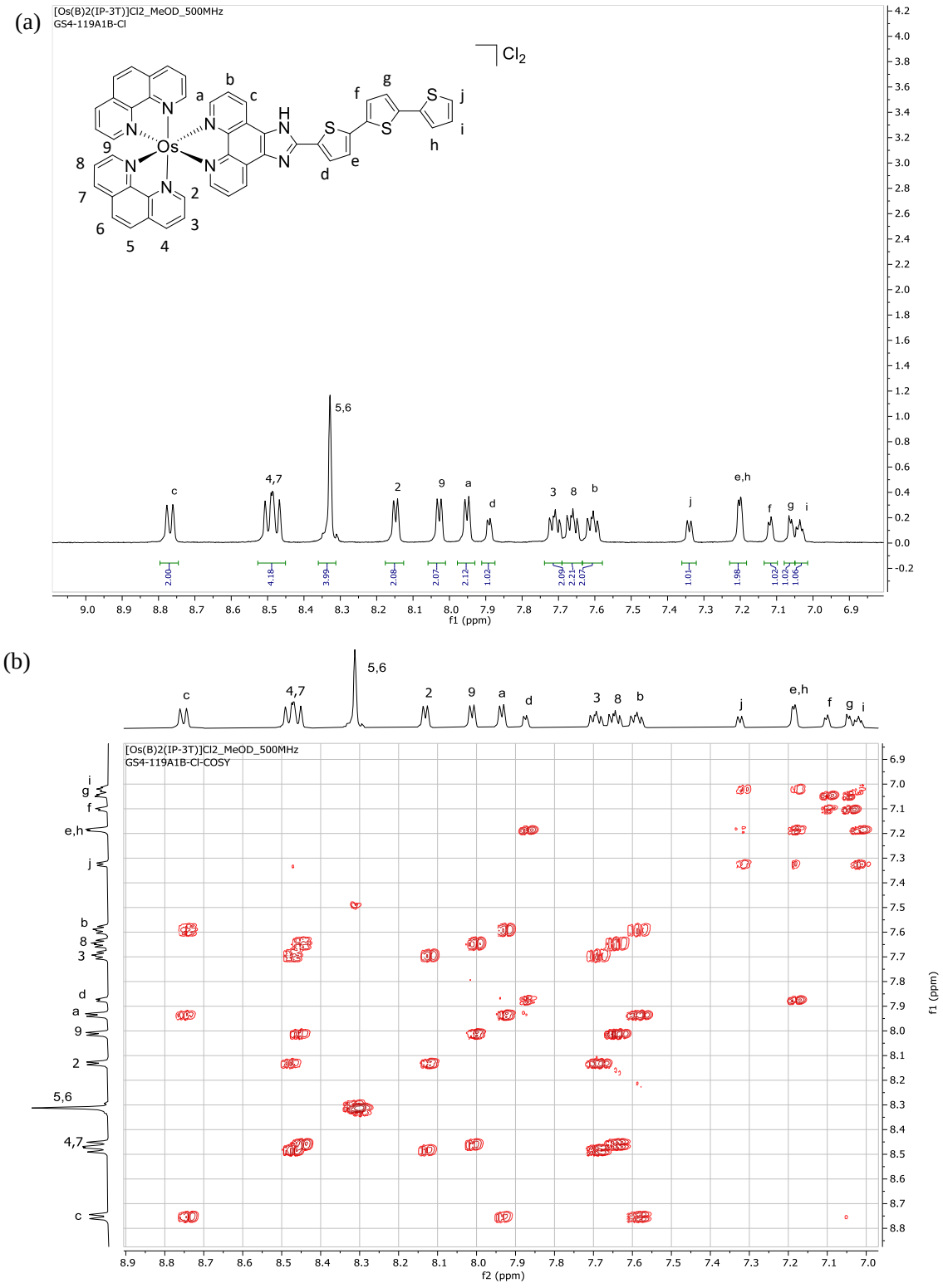

Figure S-5 (a) 500 MHz ^{1}H NMR spectra of **Os-3T** (Cl^{-} salt) in MeOD-d_3 at 298 K with structure labelling and ^{1}H NMR assignments. (a) Zoom of ^{1}H NMR spectrum, aromatic region. (b) ^{1}H–^{1}H COSY NMR spectrum, aromatic region.

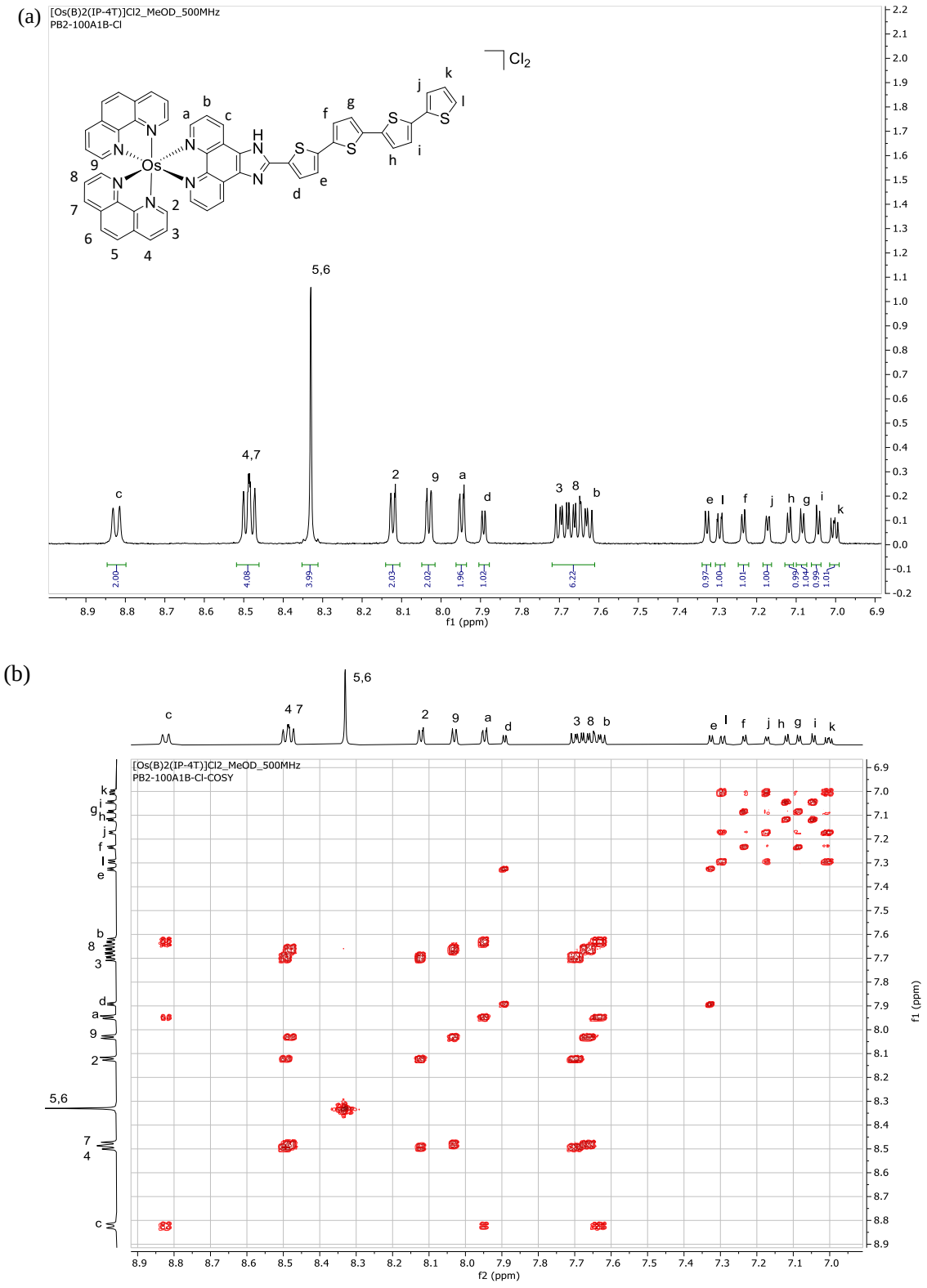

Figure S-6 500 MHz ^{1}H NMR spectra of **Os-4T** (Cl^{-} salt) in MeOD-d_3 at 298 K with structure labelling and ^{1}H NMR assignments. (a) Zoom of ^{1}H NMR spectrum, aromatic region. (b) ^{1}H–^{1}H COSY NMR spectrum, aromatic region.

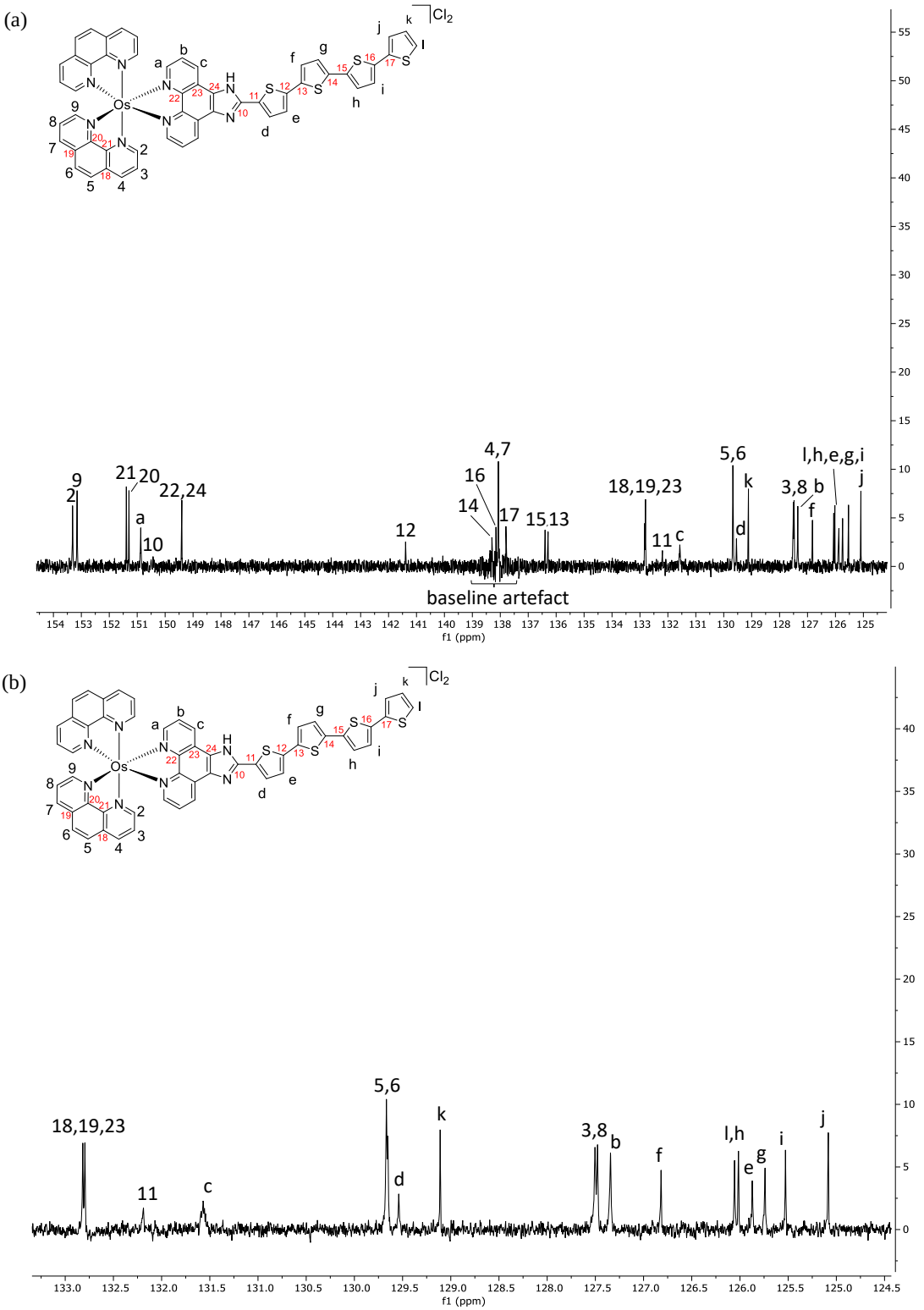

Note: The noise at the region 138.5–137.7 ppm is an artifact caused by nearby radio transmitters.

Figure S-7 175 MHz ^{13}C NMR spectrum of **Os-4T** (Cl^- salt) in MeOD-d_3 at 298 K with structure labelling and ^{13}C NMR assignments. (a) Zoom of 124.4-154.5 ppm region. (b) Zoom of 124.5-133.3 ppm region.

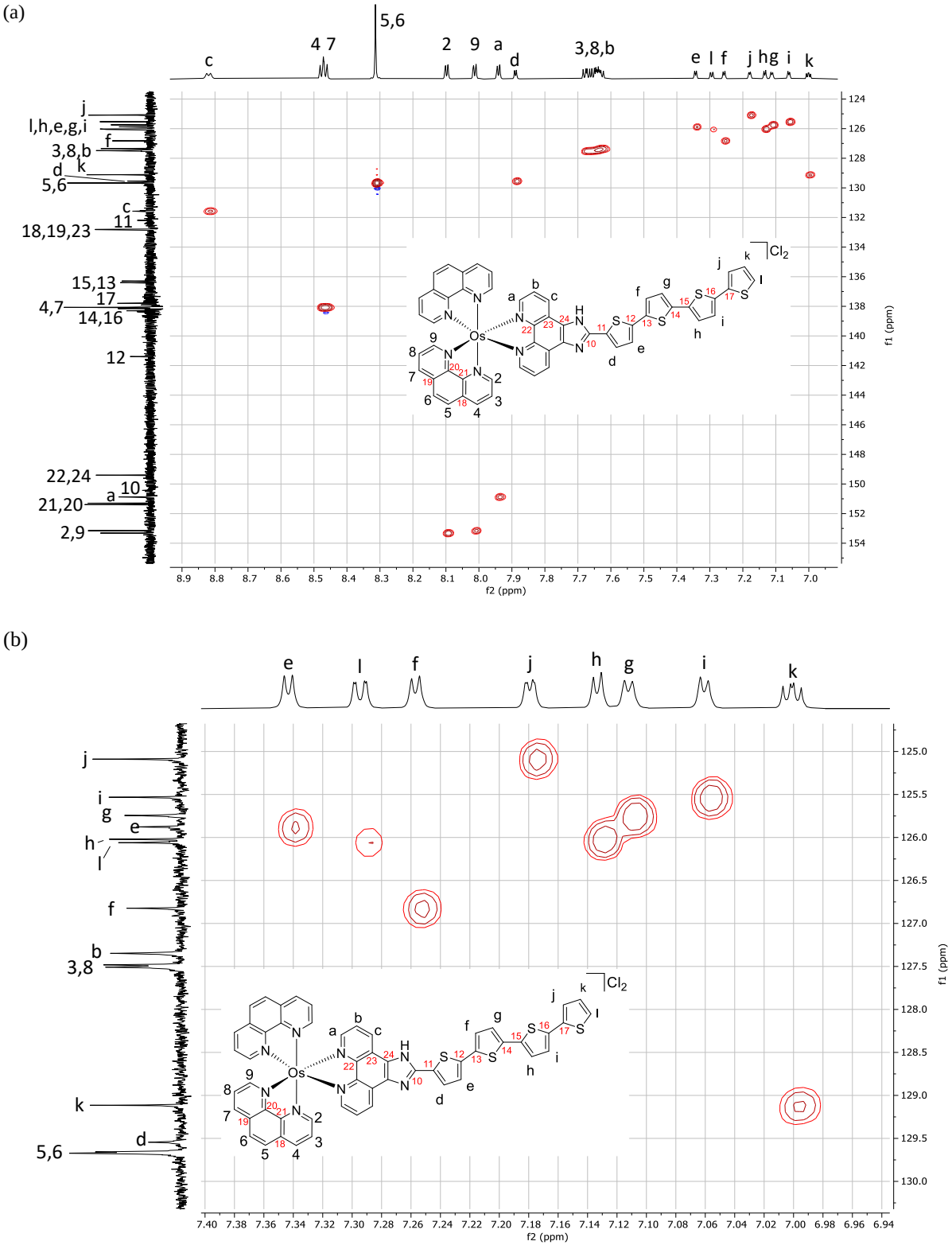

Figure S-8 (a) 700 MHz ^{13}C–^{1}H HSQC NMR spectrum of **Os-4T** (Cl^- salt) in MeOD-d_3 at 298 K with structure labelling and ^{1}H and ^{13}C NMR assignments. (b) Zoom of ^{13}C –^{1}H HSQC NMR spectrum.

(a)

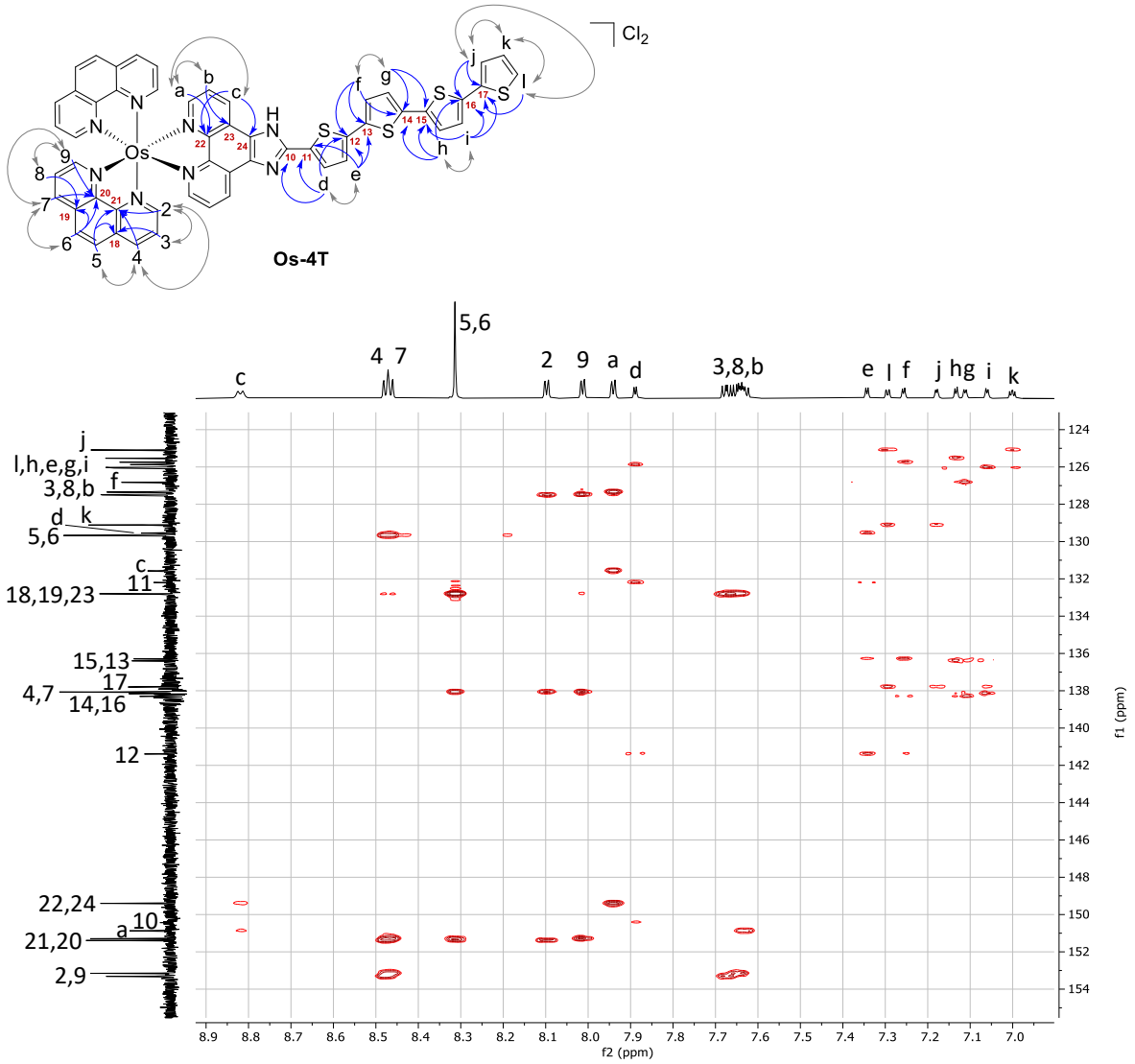
Cl2
Os-4T
5,6
4 7
2 9 a d
3,8,b
e l f j hg i k
c
j
l,h,e,g,i
3,8,b
f
d k
5,6
c
11
18,19,23
15,13
17
4,7
14,16
12
22,24
a 10
21,20
2,9
f1 (ppm)
f2 (ppm)

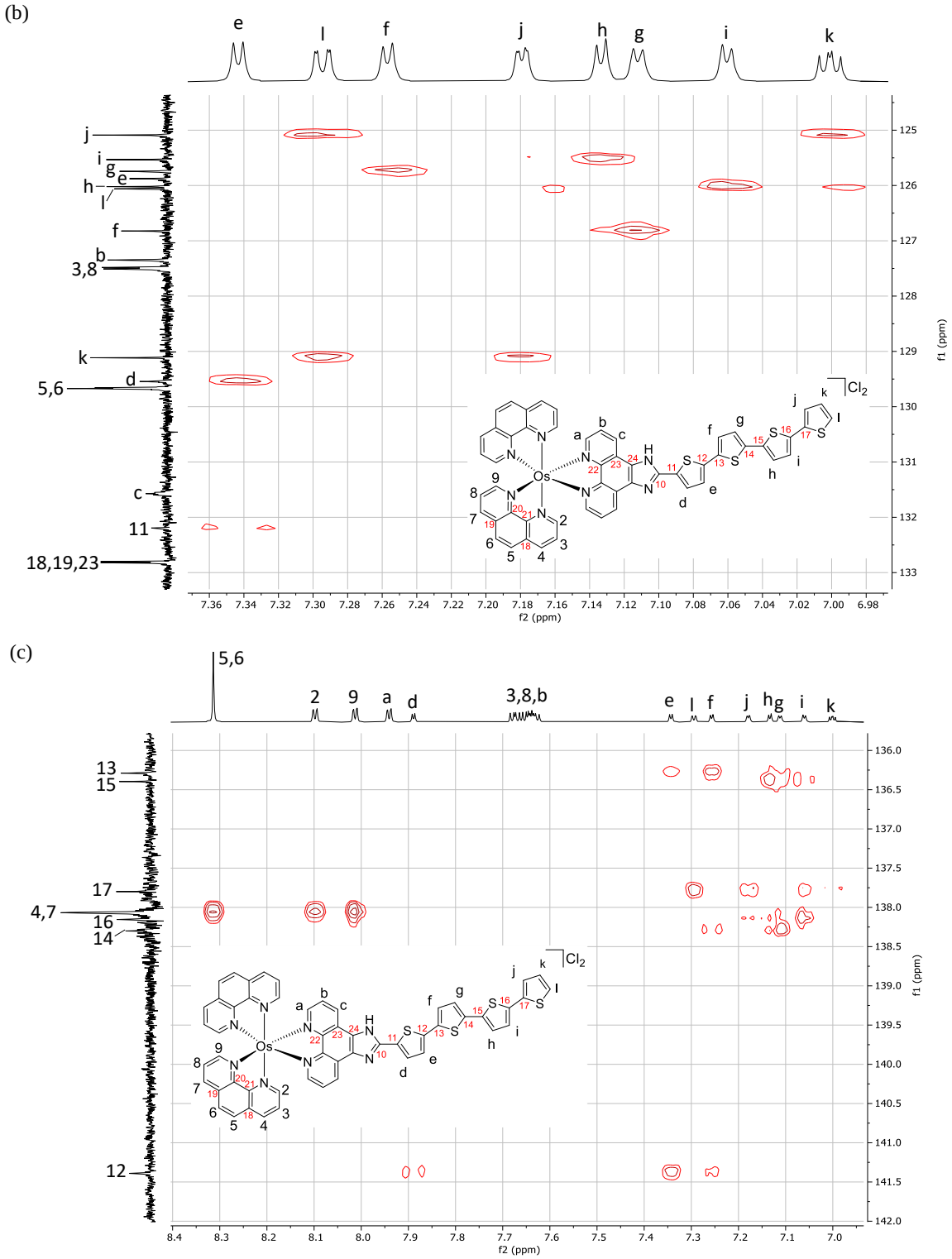

Figure S-9. (a) 700 MHz ^{13}C–^{1}H HMBC NMR spectrum of **Os-4T** (Cl^- salt) in MeOD-d_3 at 298 K with structure labelling and ^{1}H and ^{13}C NMR assignments. A representative drawing of the HMBC correlations is shown at the top (grey arrows show ^{1}H–^{13}C correlations to tertiary carbons, blue arrows show ^{1}H–^{13}C correlations to quaternary carbons). (b) Zoom of ^{13}C–^{1}H HMBC NMR spectrum. (c) Zoom of ^{13}C–^{1}H HMBC NMR spectrum.

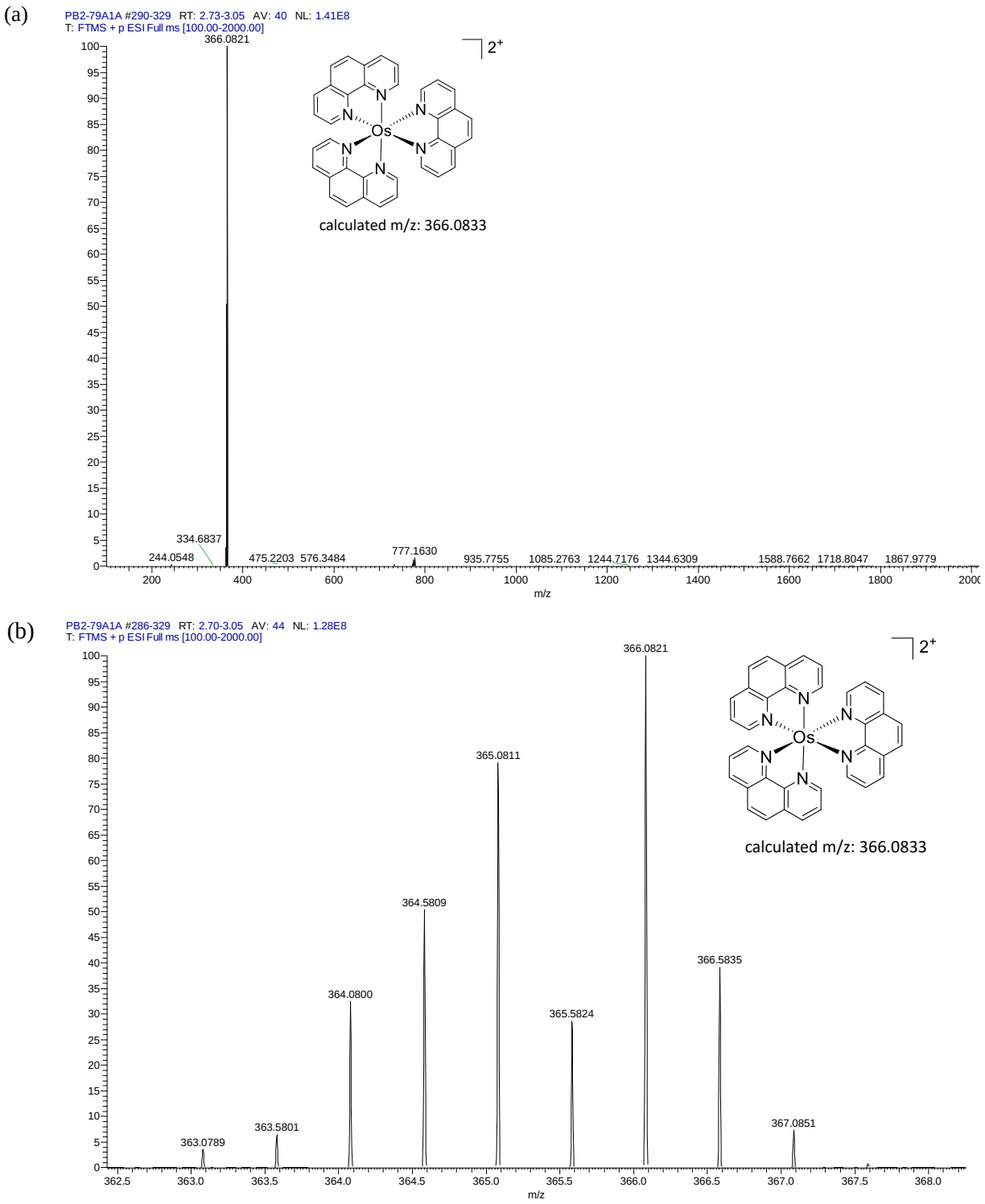

Figure S-10 (a) High resolution ESI^{+}–MS spectrum for $[Os(phen)_3]^{2+}$ (Cl^{-} salt). (b) Zoom of 366.0821 peak showing isotopic distribution.

(a)

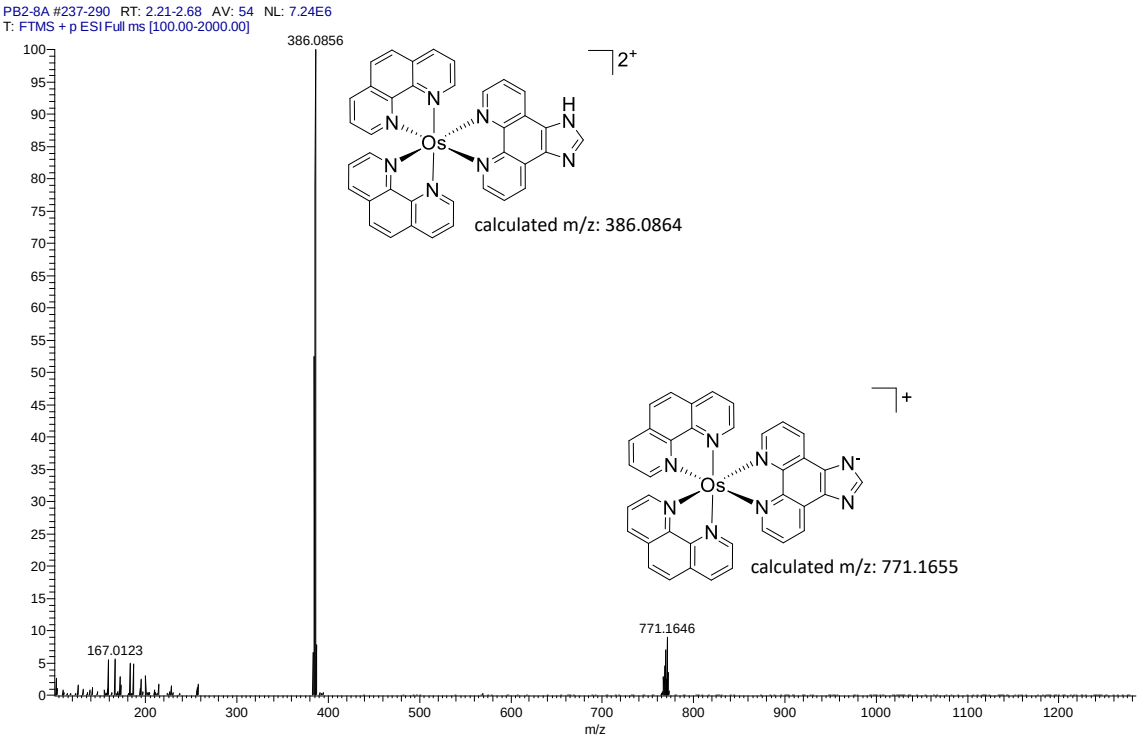
PB2-8A #237-290 RT: 2.21-2.68 AV: 54 NL: 7.24E6
T: FTMS + p ESI Full ms [100.00-2000.00]
386.0856
2+
calculated m/z: 386.0864
+
calculated m/z: 771.1655
771.1646
167.0123
m/z

(b)

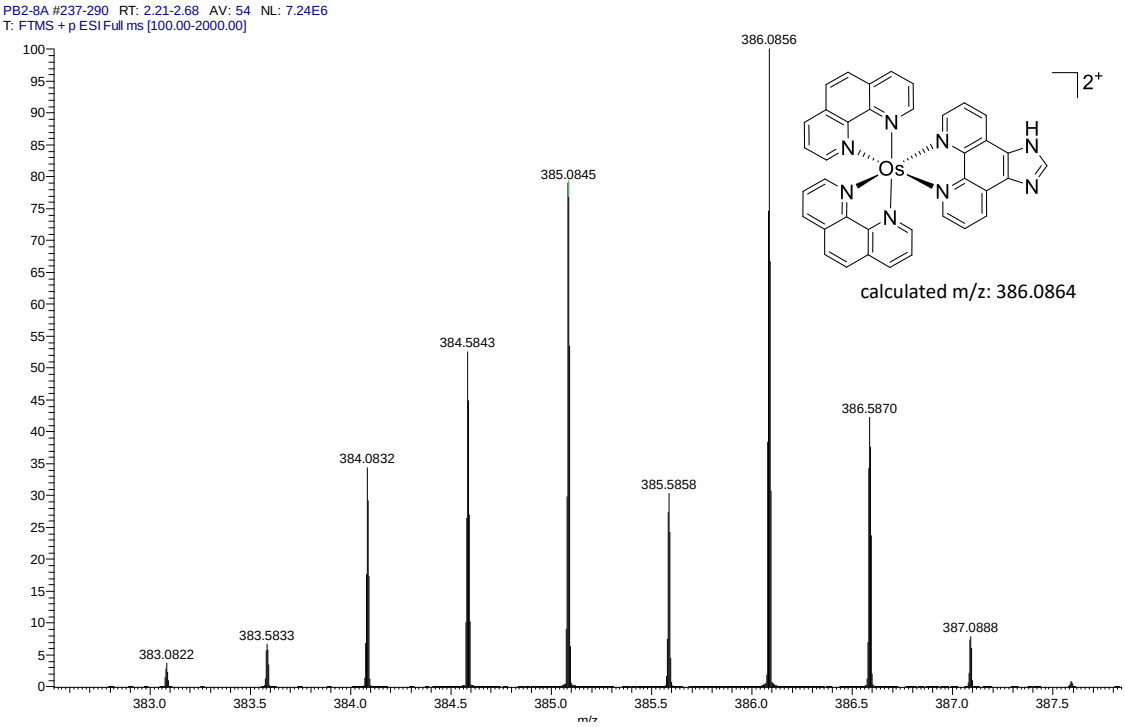
PB2-8A #237-290 RT: 2.21-2.68 AV: 54 NL: 7.24E6
T: FTMS + p ESI Full ms [100.00-2000.00]
386.0856
385.0845
384.5843
384.0832
386.5870
385.5858
383.5833
383.0822
387.0888
2+
calculated m/z: 386.0864
m/z

(c)

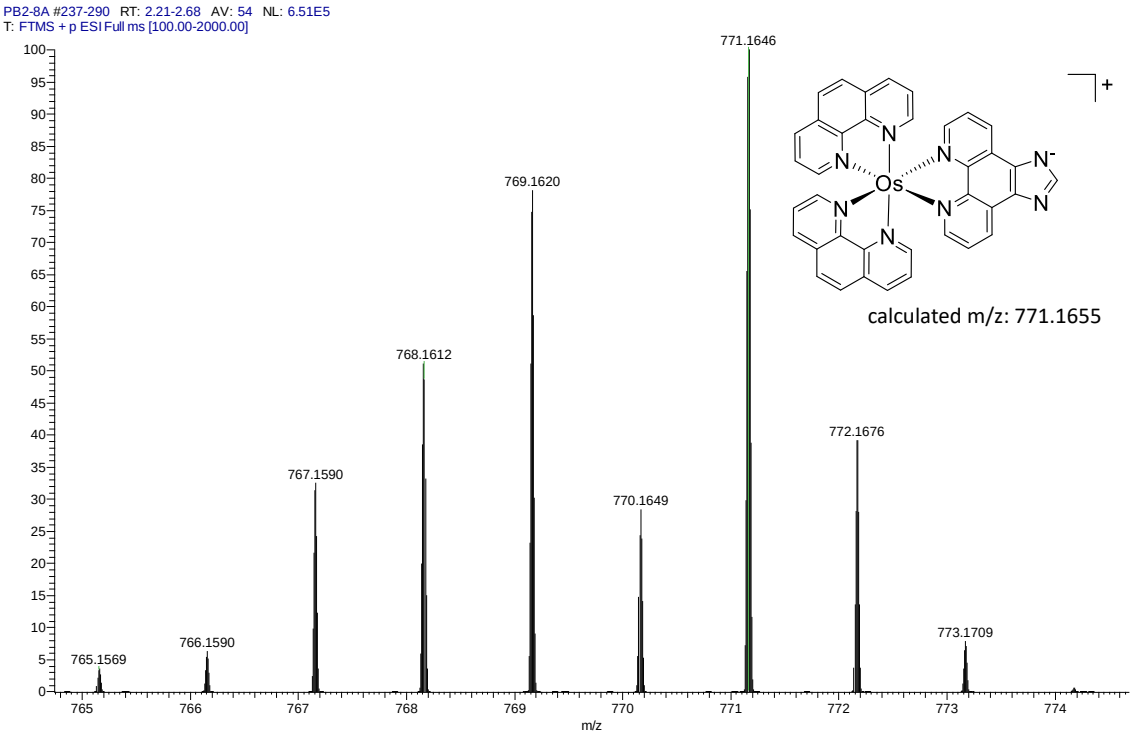

Figure S-11 (a) High resolution ESI^{+}–MS spectrum for **Os-0T** (Cl^{-} salt). (b) Zoom of 386.0856 peak showing isotopic distribution. (c) Zoom of 771.1646 peak showing isotopic distribution.

(a)

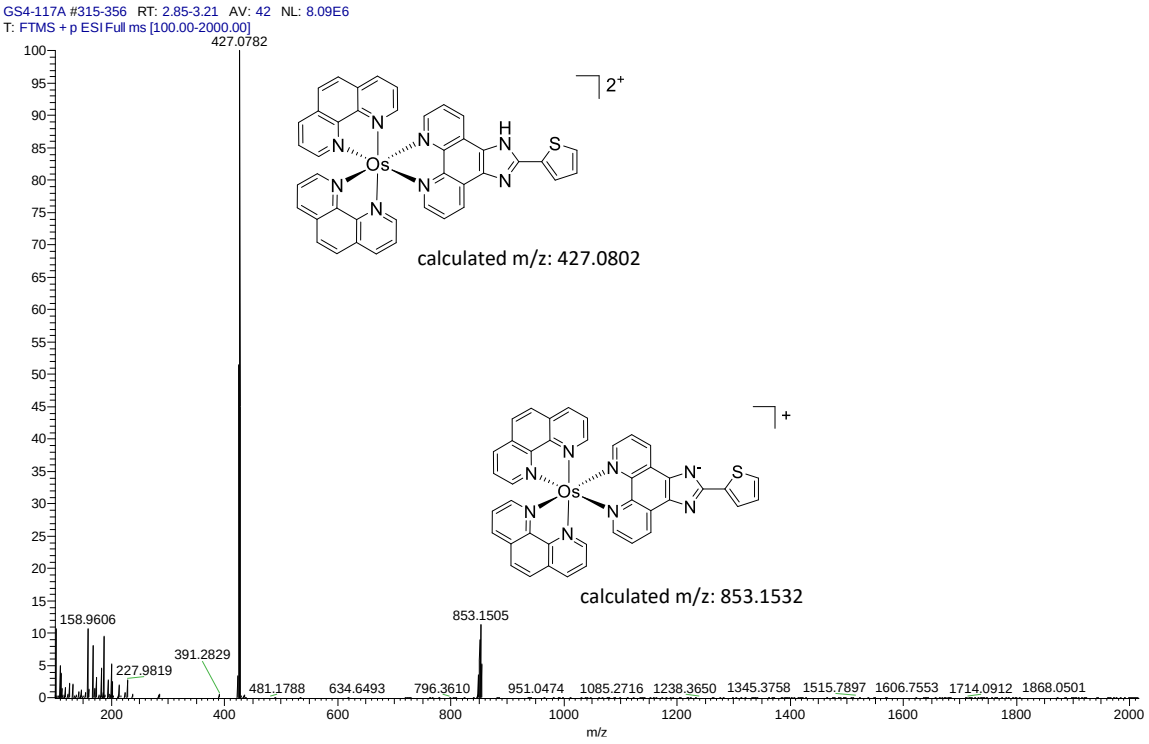
GS4-117A #315-356 RT: 2.85-3.21 AV: 42 NL: 8.09E6
T: FTMS + p ESI Full ms [100.00-2000.00]
427.0782
2+
calculated m/z: 427.0802
+
calculated m/z: 853.1532
158.9606
227.9819
391.2829
481.1788
634.6493
796.3610
853.1505
951.0474
1085.2716
1238.3650
1345.3758
1515.7897
1606.7553
1714.0912
1868.0501
m/z

(b)

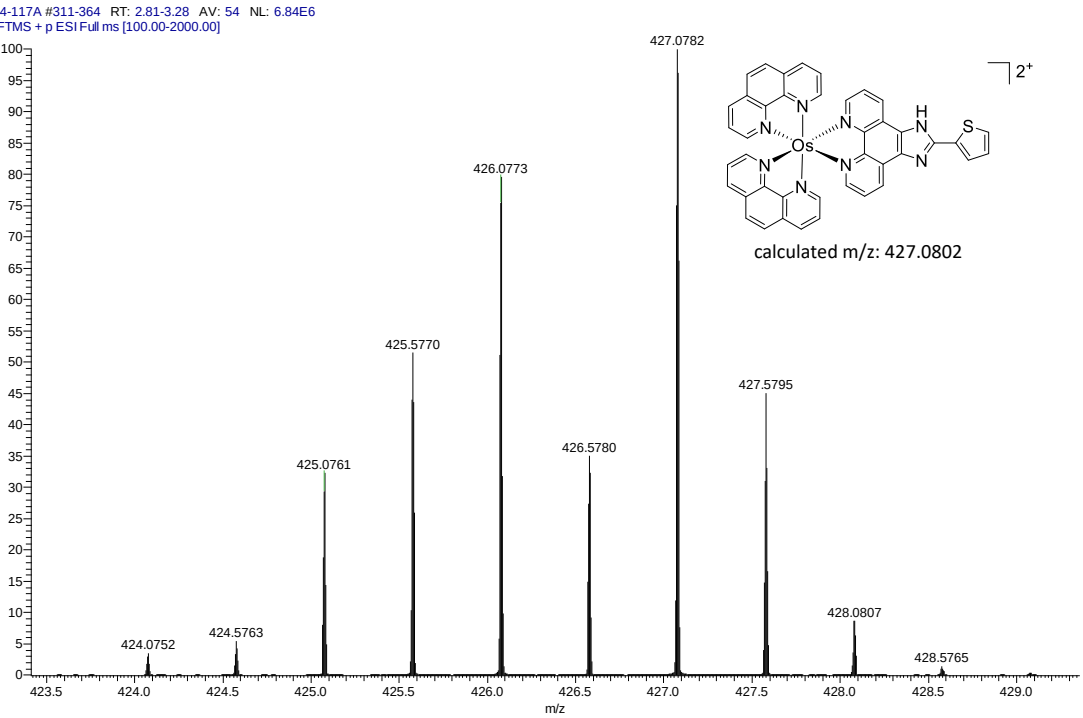
GS4-117A #311-364 RT: 2.81-3.28 AV: 54 NL: 6.84E6
T: FTMS + p ESI Full ms [100.00-2000.00]
427.0782
426.0773
425.5770
427.5795
426.5780
425.0761
428.0807
424.5763
424.0752
428.5765
2+
calculated m/z: 427.0802
m/z

(c)

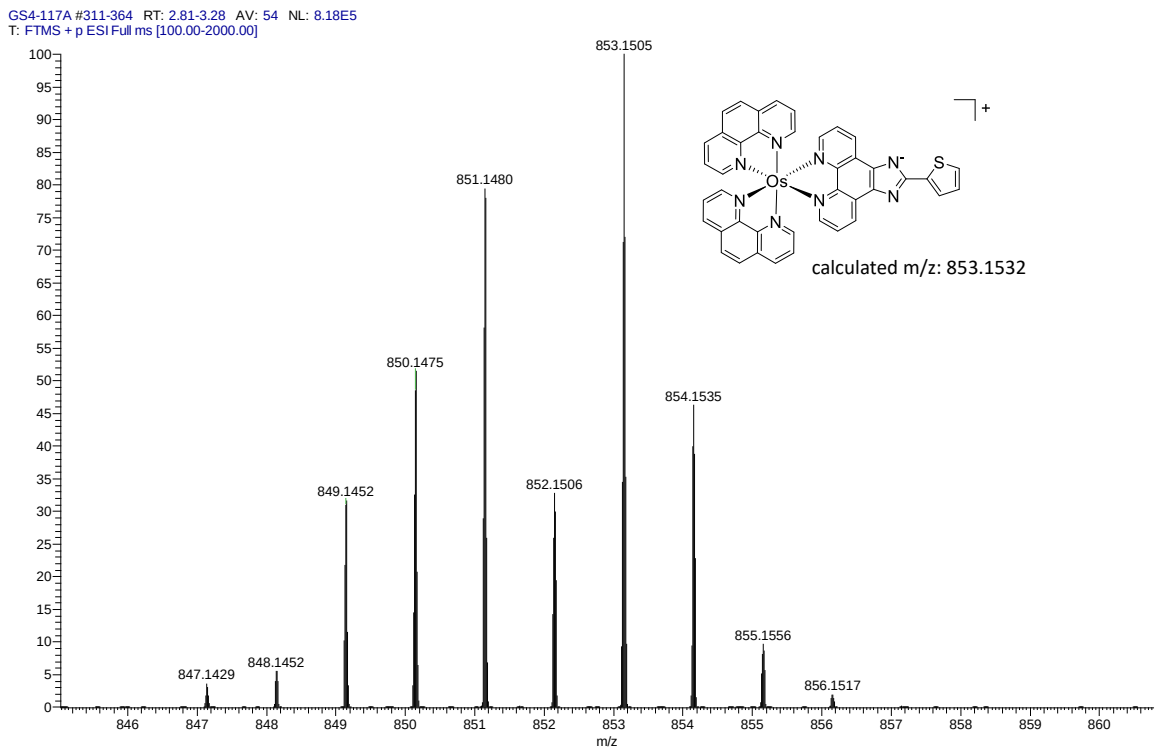

Figure S-12 (a) High resolution ESI$^+$–MS spectrum for **Os-1T** (Cl^- salt). (b) Zoom of 427.0782 peak showing isotopic distribution. (c) Zoom of 853.1505 peak showing isotopic distribution

(a)

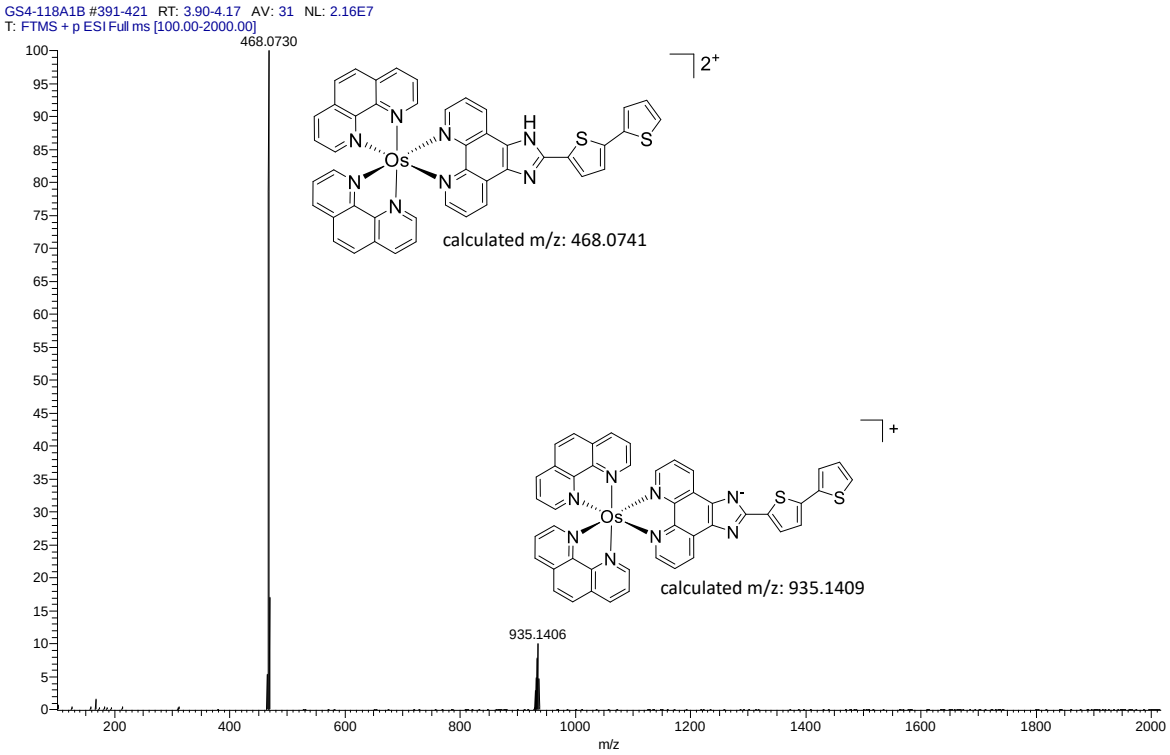
GS4-118A1B #391-421 RT: 3.90-4.17 AV: 31 NL: 2.16E7
T: FTMS + p ESI Full ms [100.00-2000.00]
468.0730
2+
calculated m/z: 468.0741
+
calculated m/z: 935.1409
935.1406
m/z

(b)

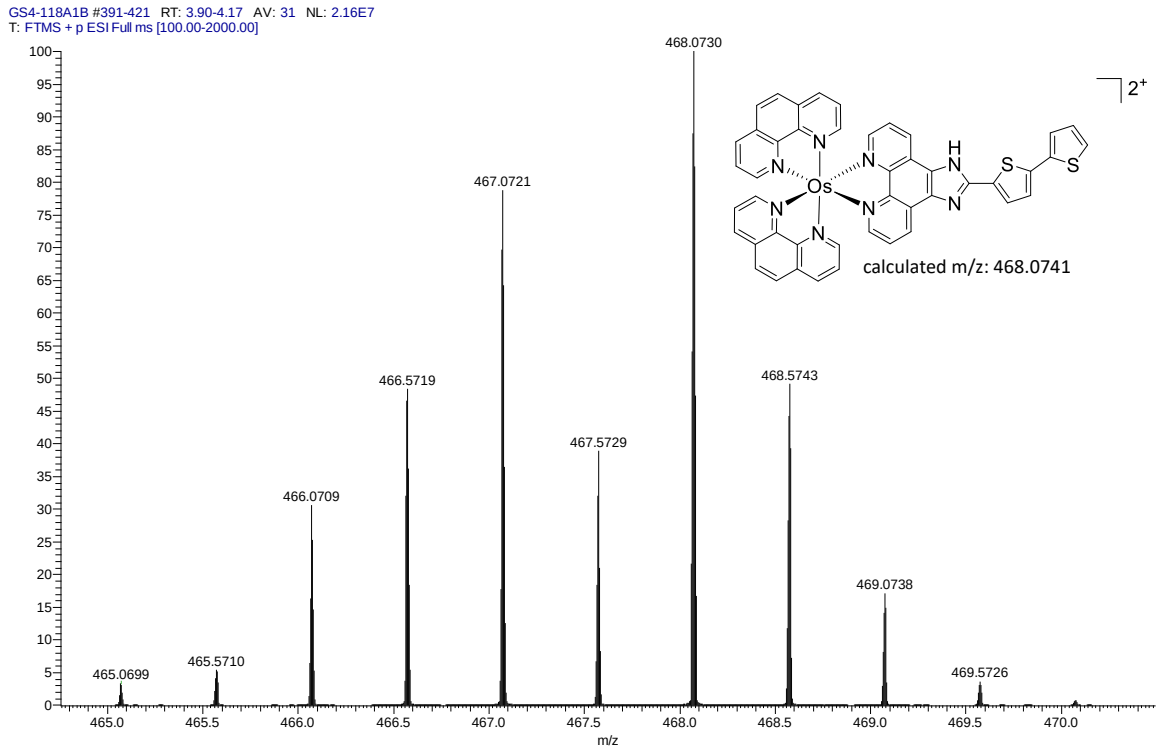
GS4-118A1B #391-421 RT: 3.90-4.17 AV: 31 NL: 2.16E7
T: FTMS + p ESI Full ms [100.00-2000.00]
468.0730
467.0721
466.5719
468.5743
467.5729
466.0709
469.0738
465.5710
465.0699
469.5726
2+
calculated m/z: 468.0741
m/z

(c)

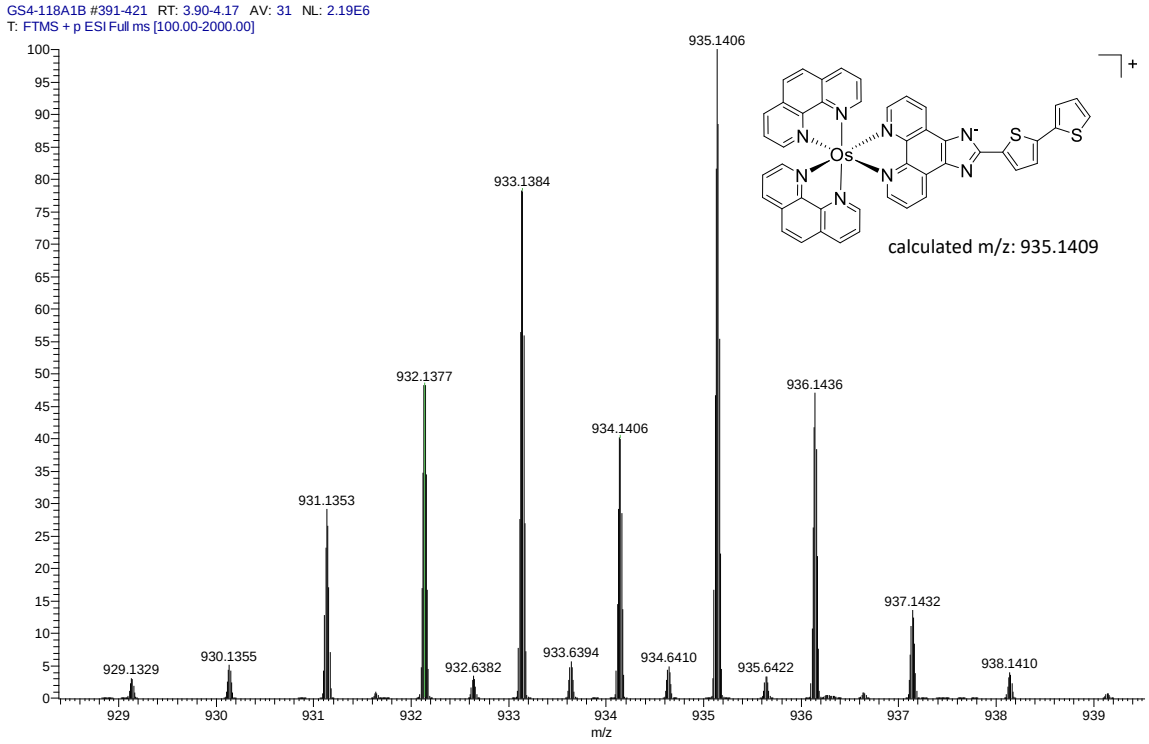

Figure S-13 (a) High resolution ESI^+–MS spectrum for **Os-2T** (Cl^- salt). (b) Zoom of 468.0730 peak showing isotopic distribution. (c) Zoom of 935.1406 peak showing isotopic distribution.

(a)

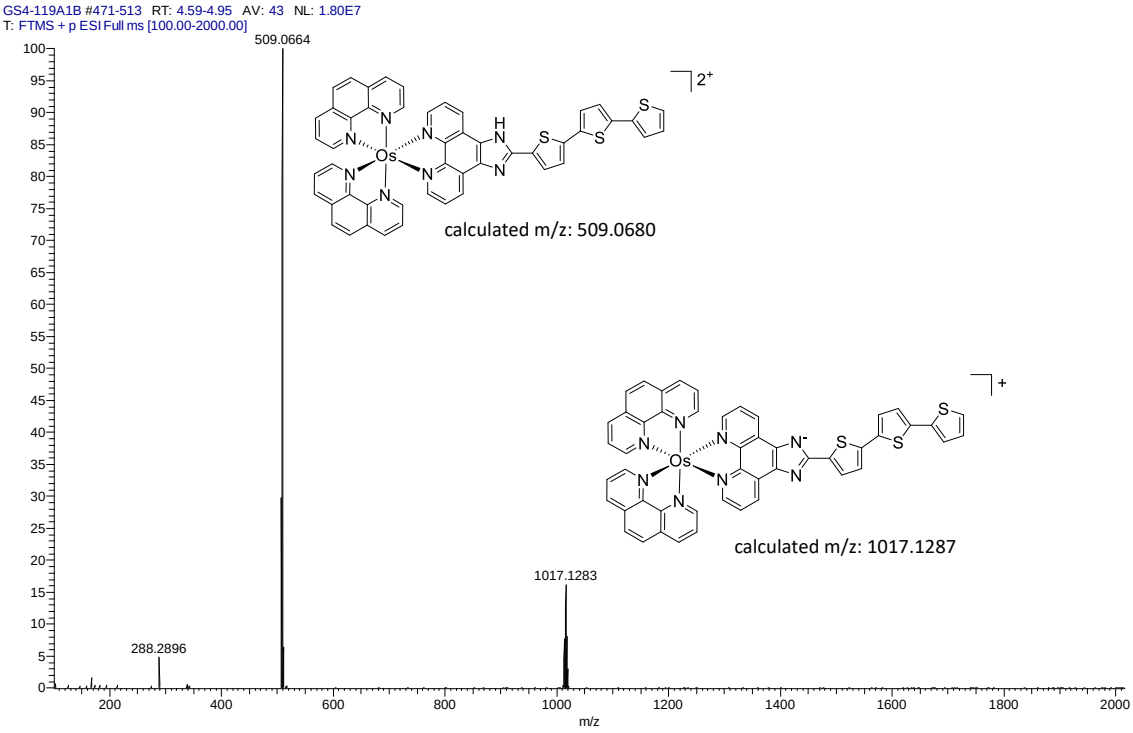
GS4-119A1B #471-513 RT: 4.59-4.95 AV: 43 NL: 1.80E7
T: FTMS + p ESI Full ms [100.00-2000.00]
509.0664
2+
calculated m/z: 509.0680
+
calculated m/z: 1017.1287
1017.1283
288.2896
m/z

(b)

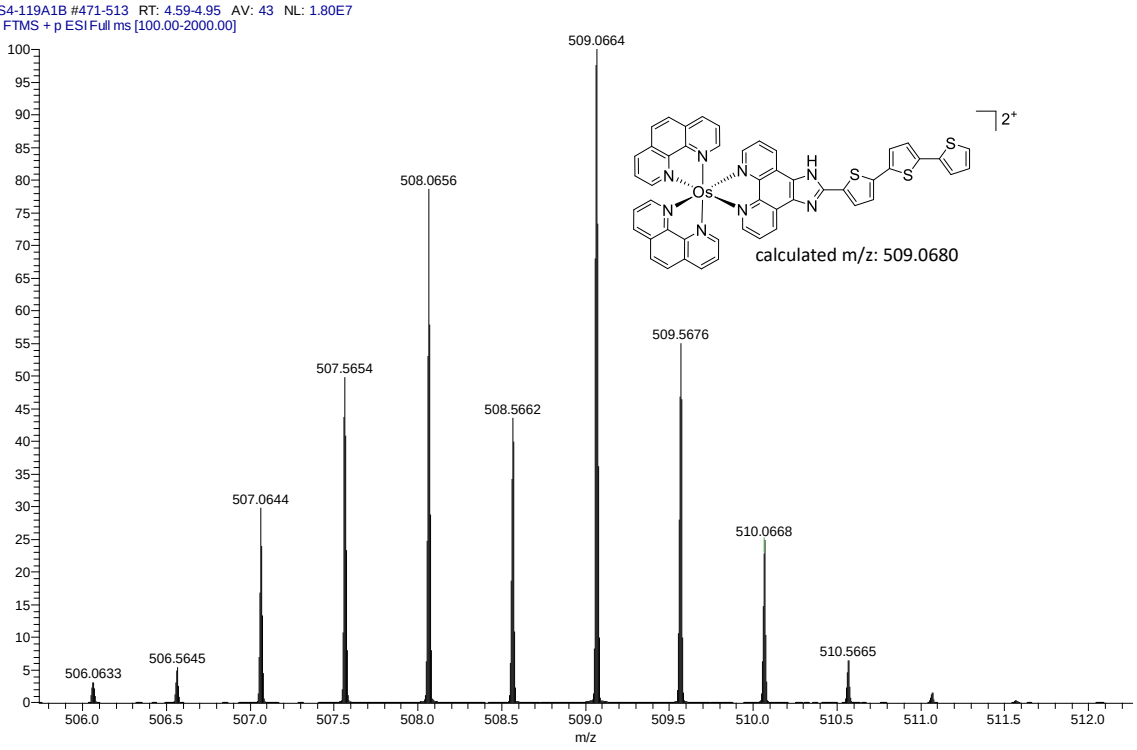
GS4-119A1B #471-513 RT: 4.59-4.95 AV: 43 NL: 1.80E7
T: FTMS + p ESI Full ms [100.00-2000.00]
509.0664
508.0656
509.5676
507.5654
508.5662
507.0644
510.0668
506.5645
510.5665
506.0633
2+
calculated m/z: 509.0680
m/z

(c)

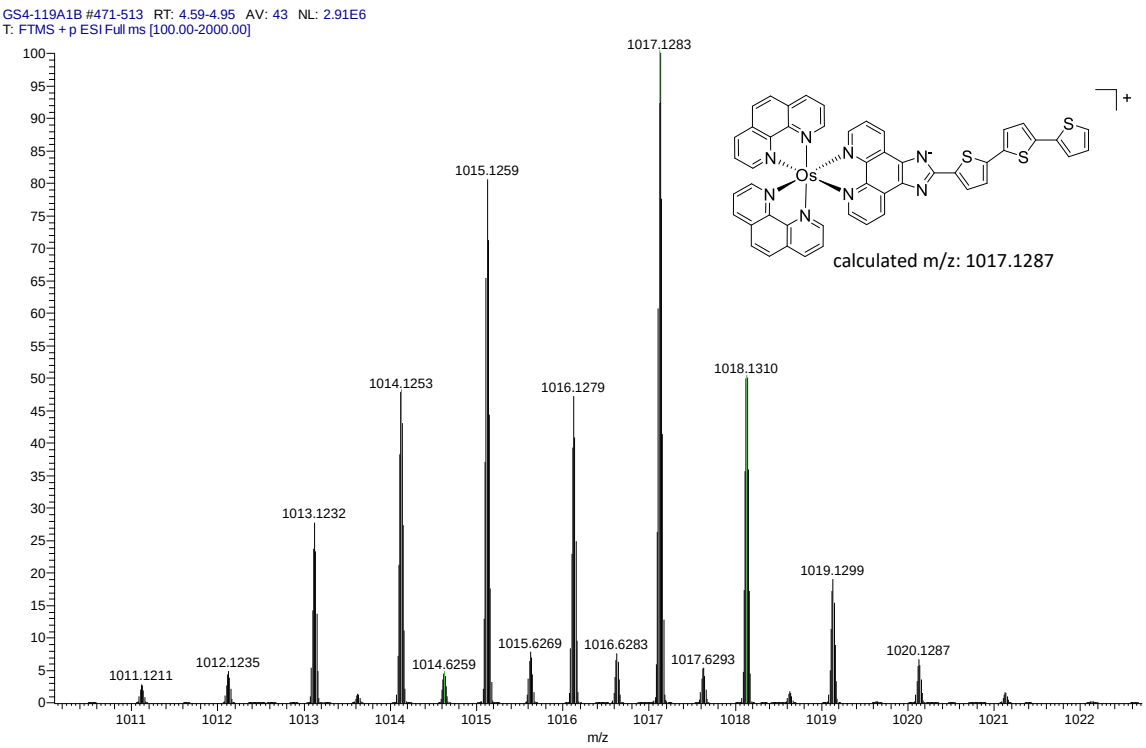

Figure S-14 (a) High resolution ESI^+–MS spectrum for **Os-3T** (Cl^- salt). (b) Zoom of 509.0664 peak showing isotopic distribution. (c) Zoom of 1017.1283 peak showing isotopic distribution.

(a)

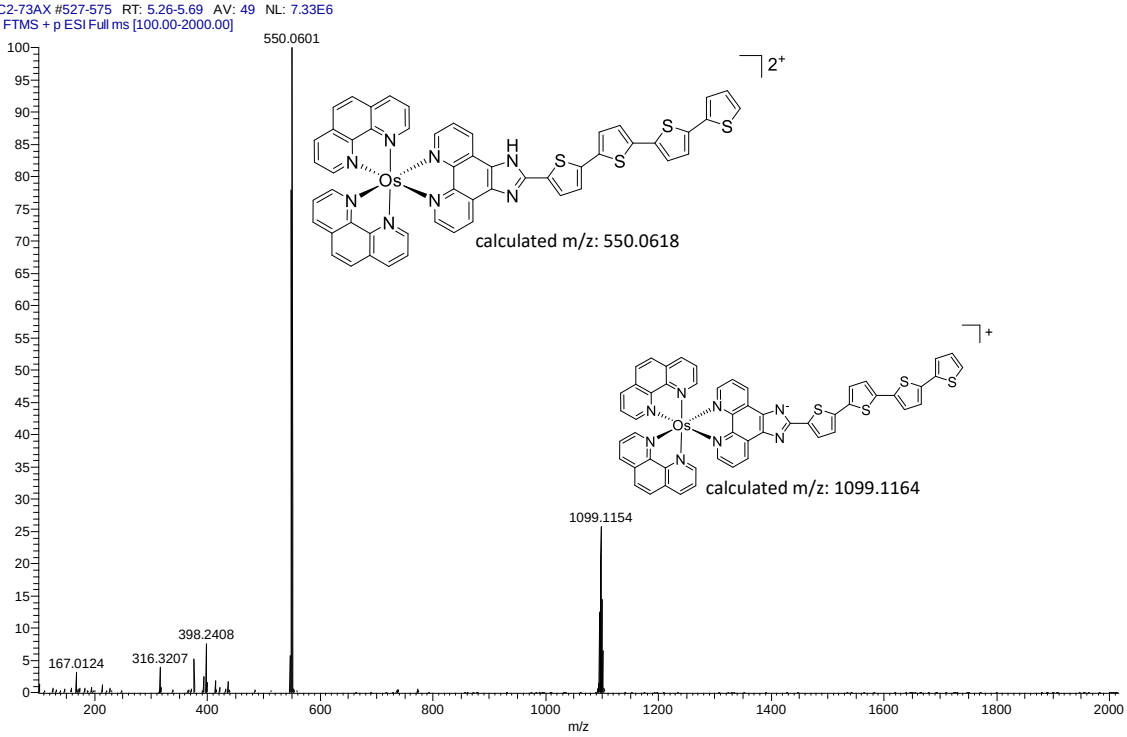
HC2-73AX #527-575 RT: 5.26-5.69 AV: 49 NL: 7.33E6
T: FTMS + p ESI Full ms [100.00-2000.00]
550.0601
2+
calculated m/z: 550.0618
1099.1154
+
calculated m/z: 1099.1164
398.2408
316.3207
167.0124
m/z

(b)

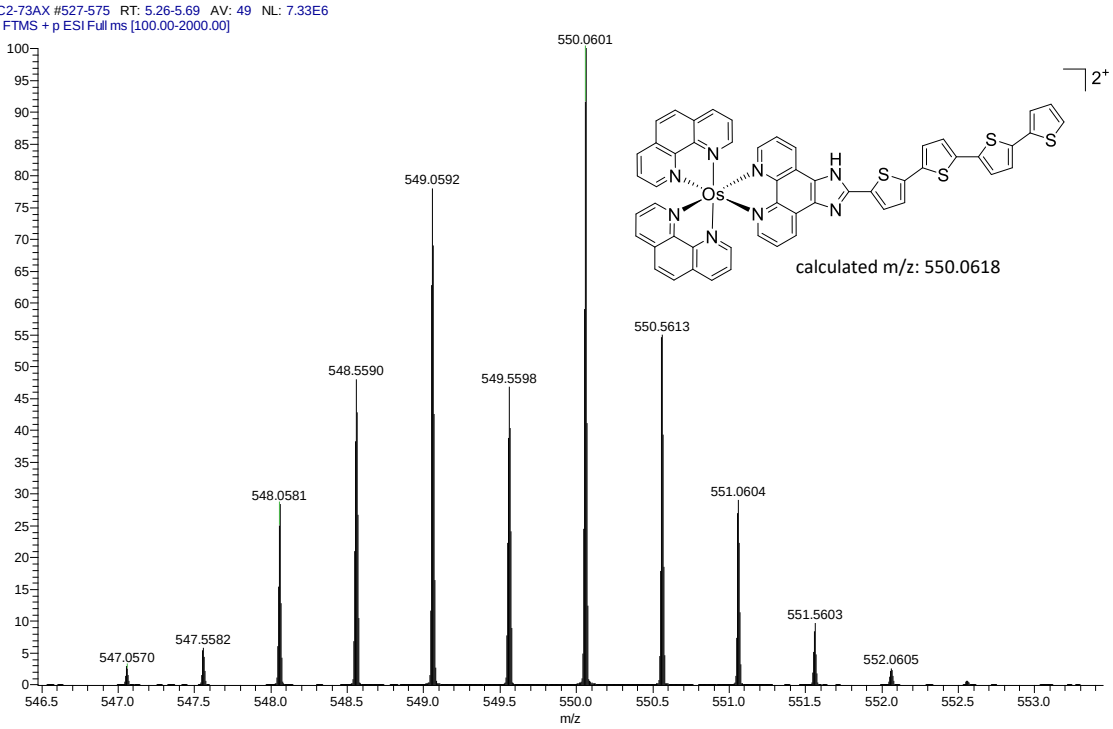
HC2-73AX #527-575 RT: 5.26-5.69 AV: 49 NL: 7.33E6
T: FTMS + p ESI Full ms [100.00-2000.00]
550.0601
2+
calculated m/z: 550.0618
549.0592
550.5613
548.5590
549.5598
548.0581
551.0604
551.5603
547.5582
547.0570
552.0605
m/z

(c)

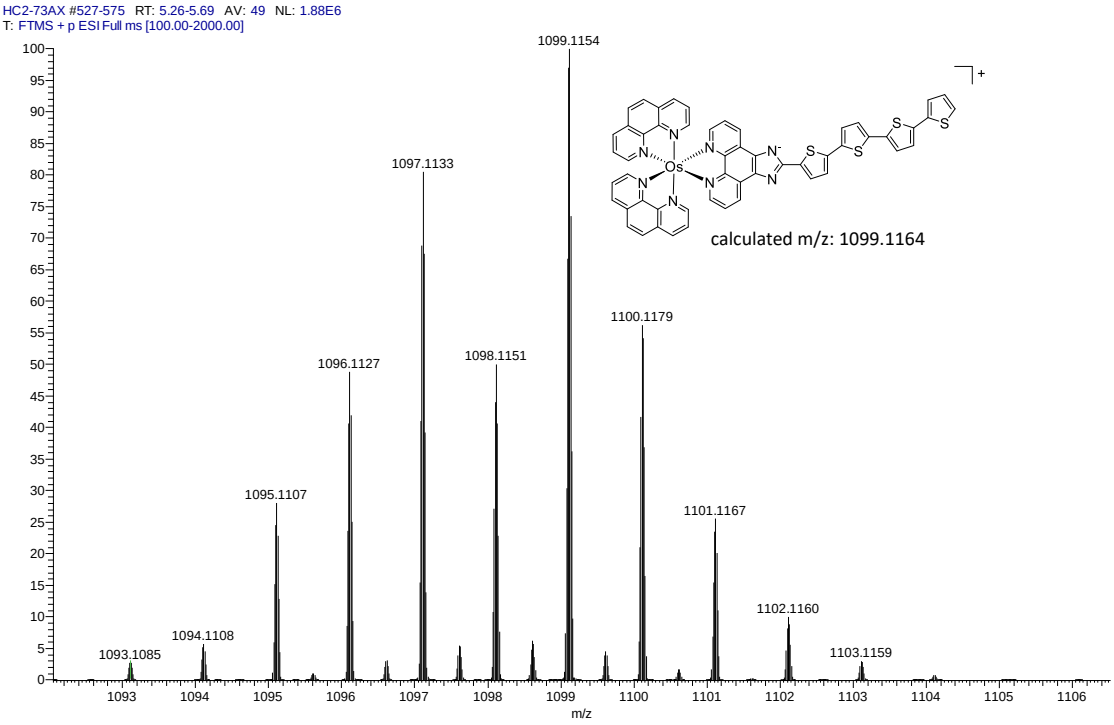

Figure S-15 (a) High resolution ESI^{+}–MS spectrum for **Os-4T** (Cl^{-} salt). (b) Zoom of 550.0601 peak showing isotopic distribution. (c) Zoom of 1099.1154 peak showing isotopic distribution.

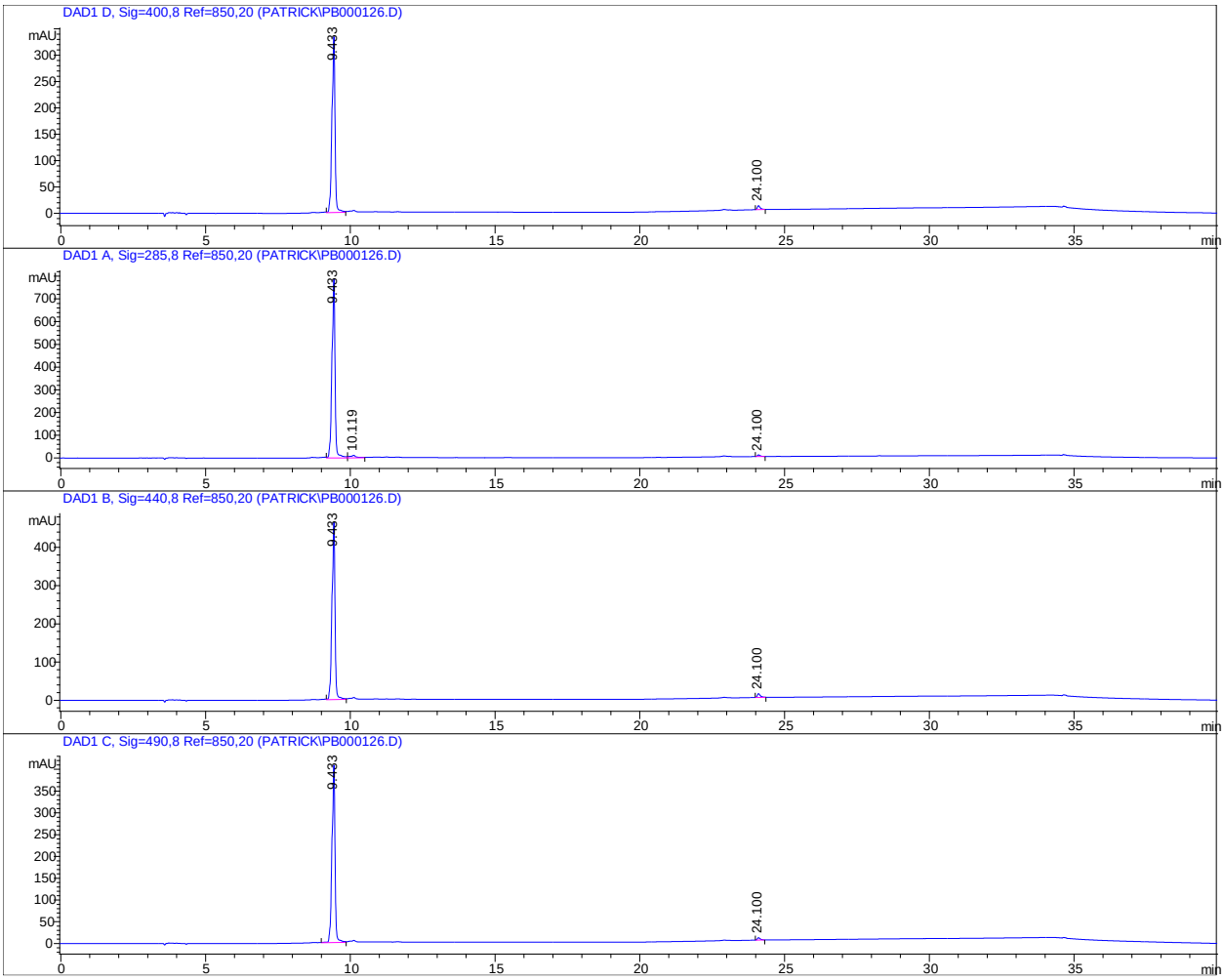

Figure S-16 HPLC chromatogram for $[Os(phen)_3]^{2+}$ (Cl^- salt) collected at the following wavelengths: 400, 285, 440, and 490 nm.

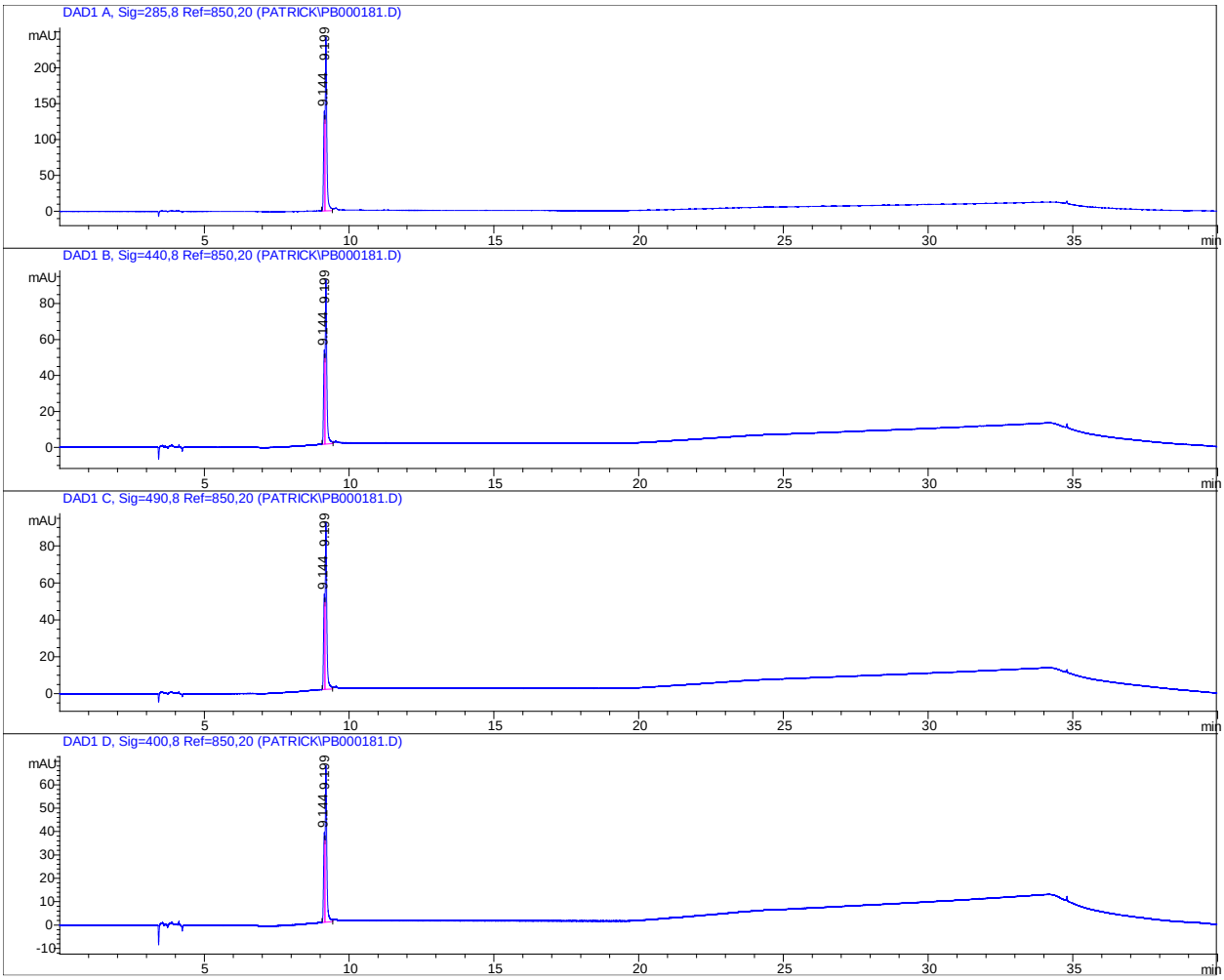

Figure S-17 HPLC chromatogram for **Os-0T** (Cl^- salt) collected at the following wavelengths: 285, 440, 490, and 400 nm.

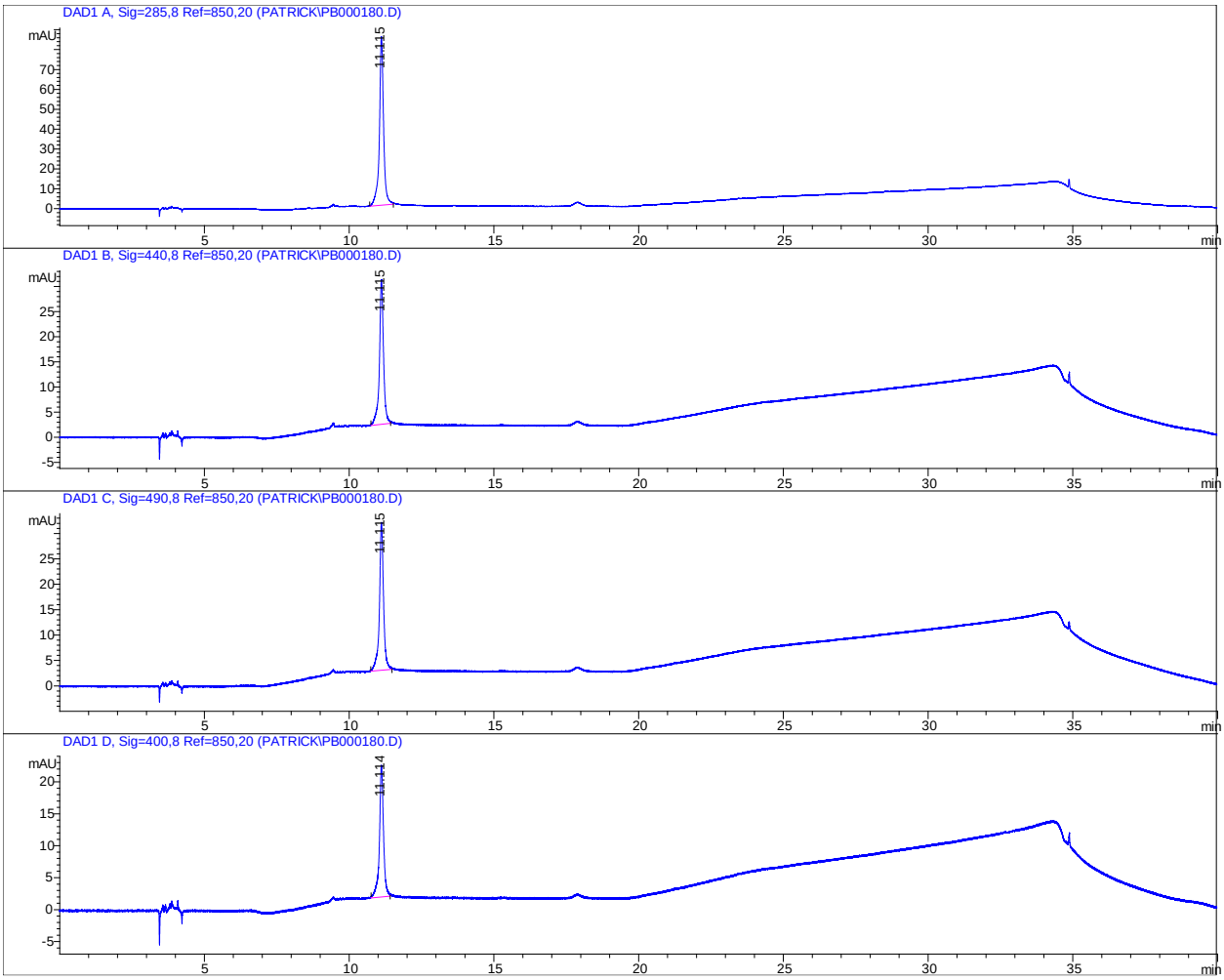

Figure S-18 HPLC chromatogram for **Os-1T** (Cl^- salt) collected at the following wavelengths: 285, 440, 490, and 400 nm.

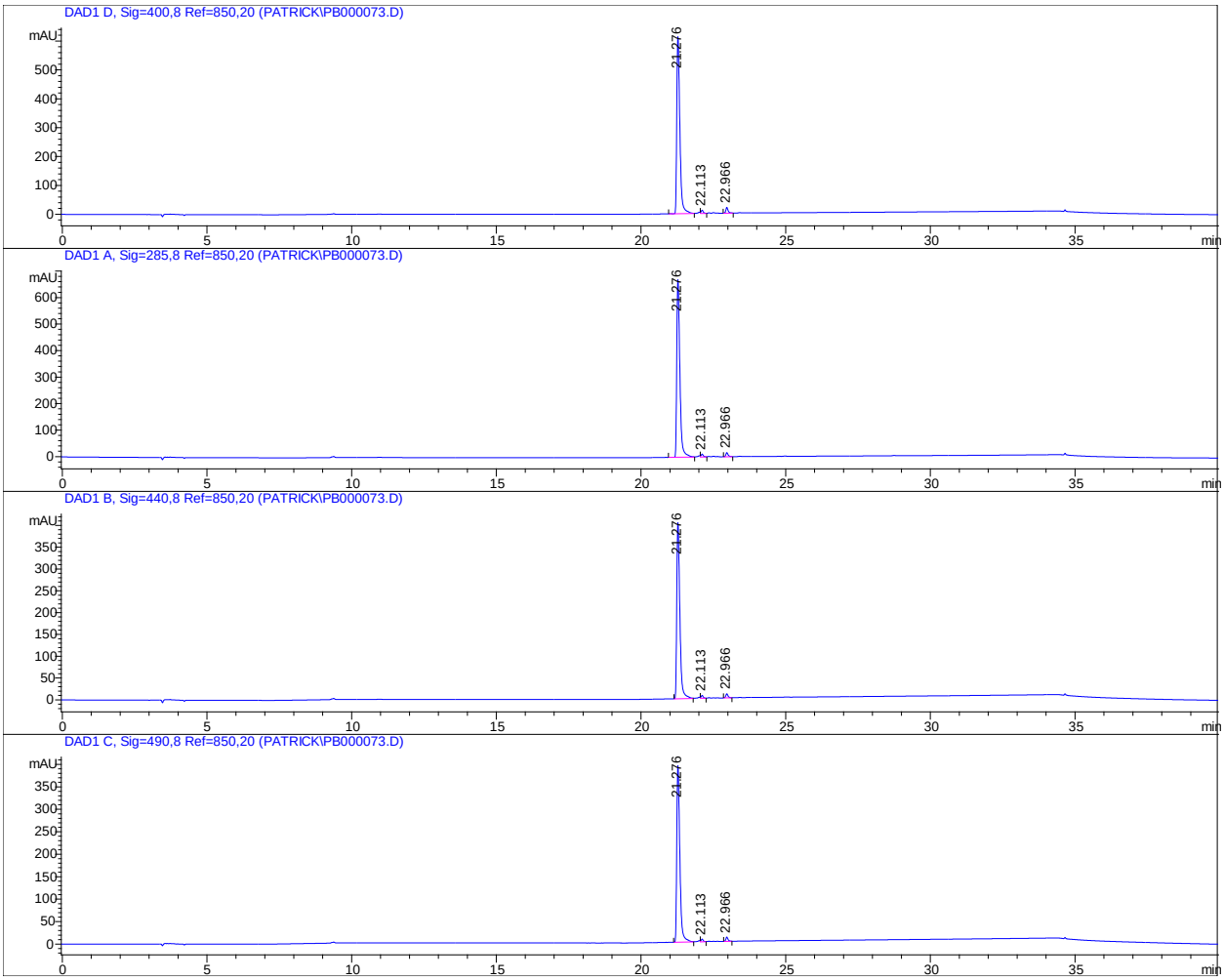

Figure S-19 HPLC chromatogram for **Os-2T** (Cl^- salt) collected at the following wavelengths: 400, 285, 440, and 490 nm.

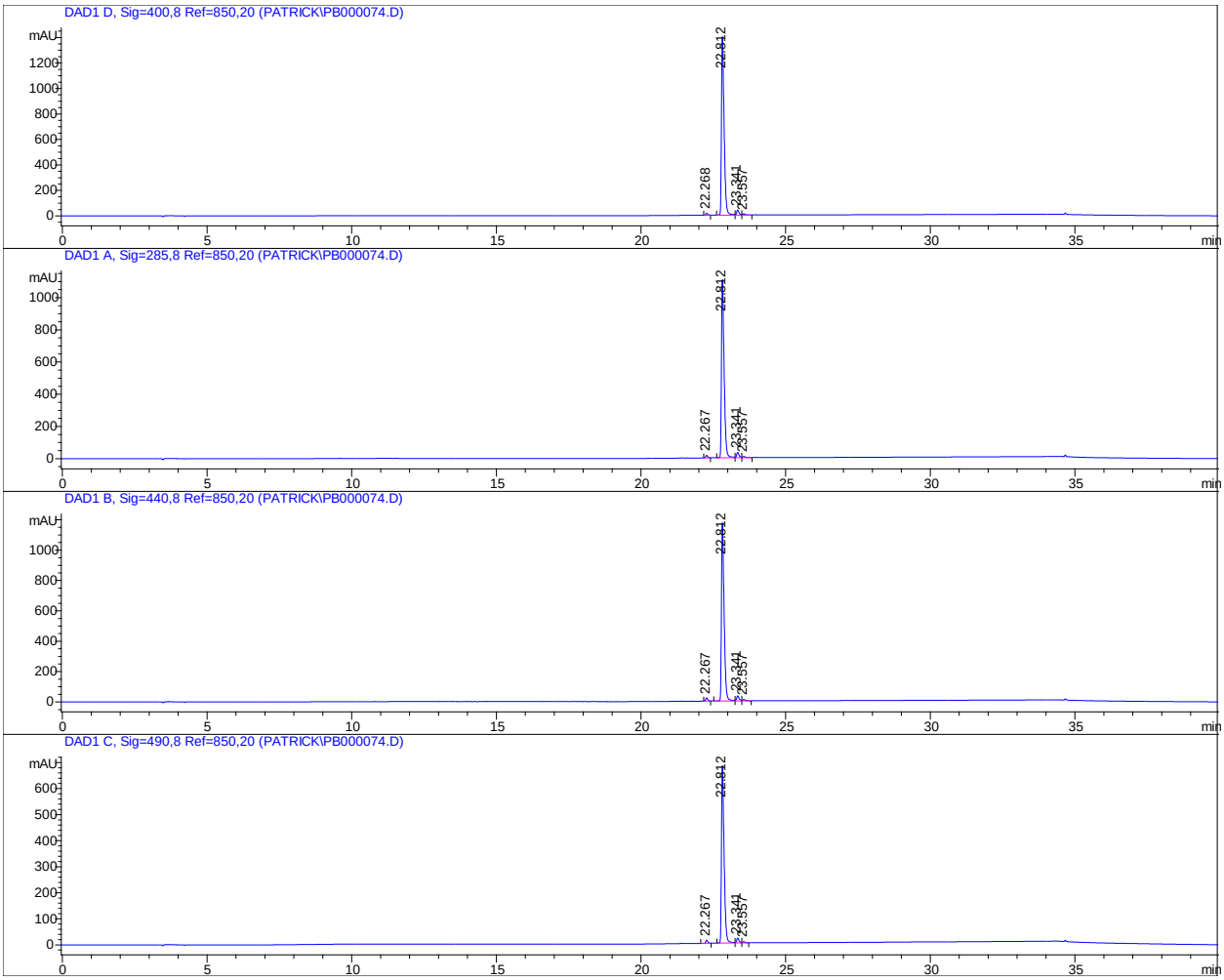

Figure S-20 HPLC chromatogram for **Os-3T** (Cl^- salt) collected at the following wavelengths: 400, 285, 440, and 490 nm.

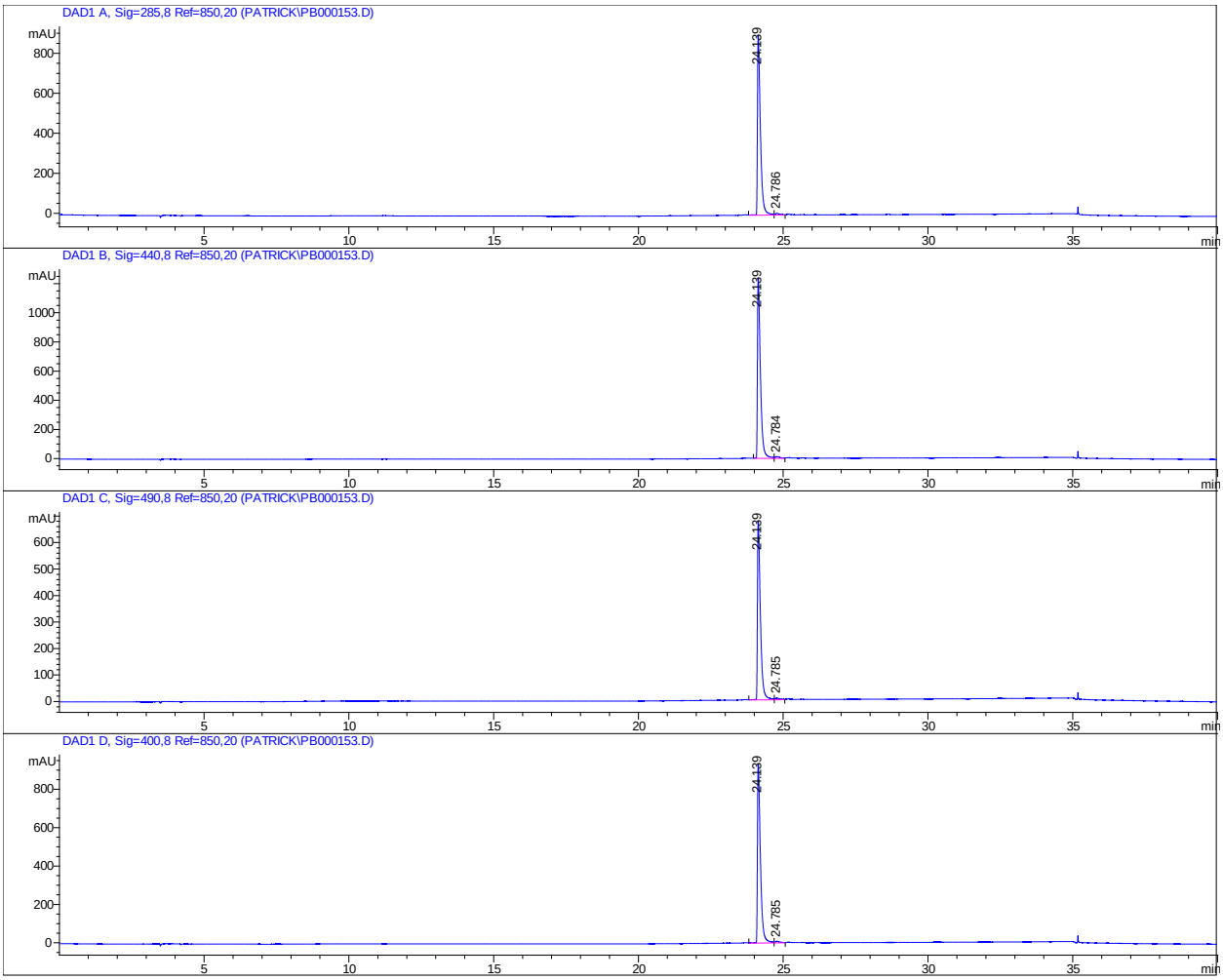

Figure S-21 HPLC chromatogram for **Os-4T** (Cl^- salt) collected at the following wavelengths: 285, 440, 490, and 400 nm.

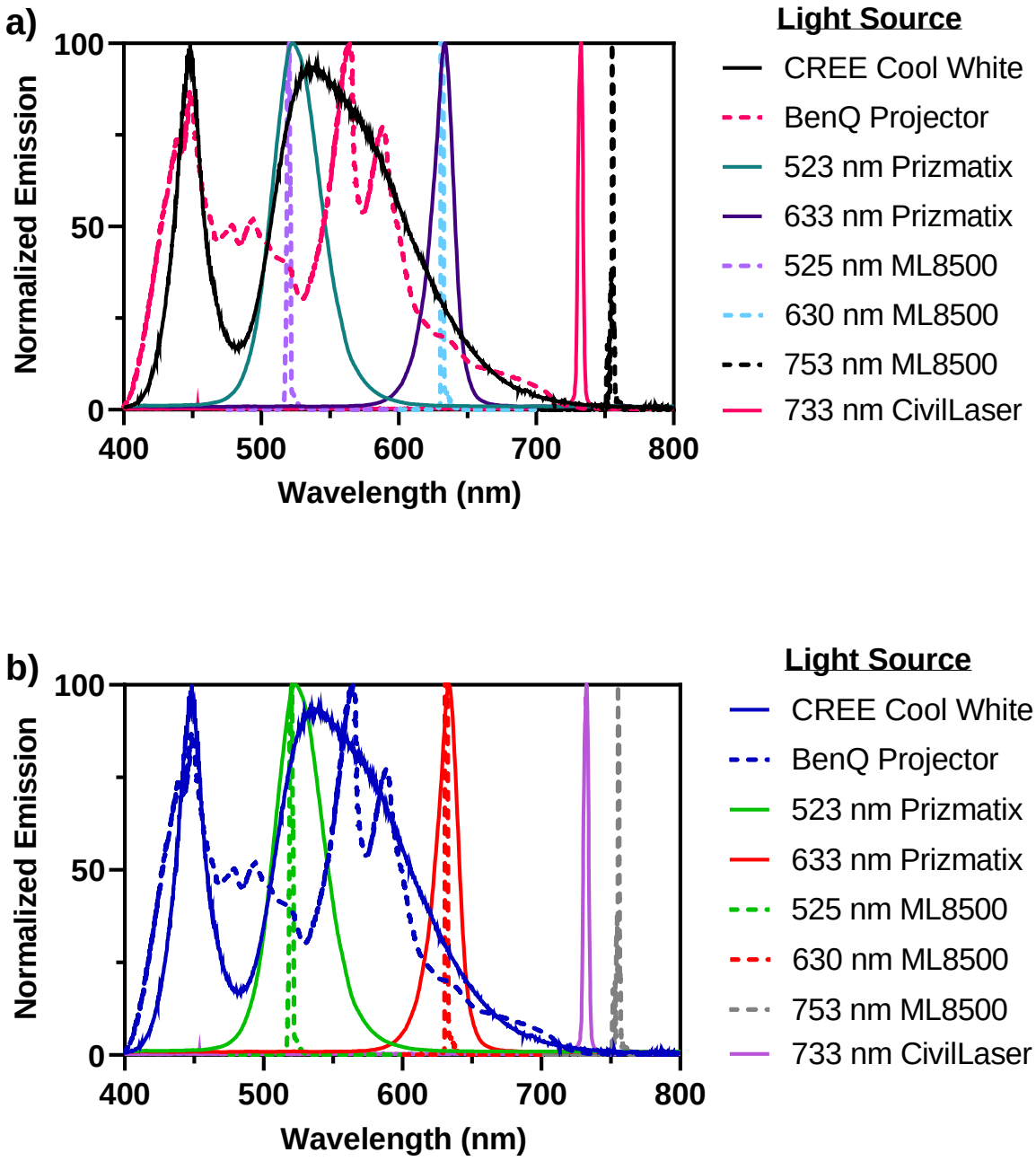

Figure S-22 Light source emissions used for photobiological studies where a) includes a color-blind friendly scheme and b) approximately matches colors to visible emission maxima.

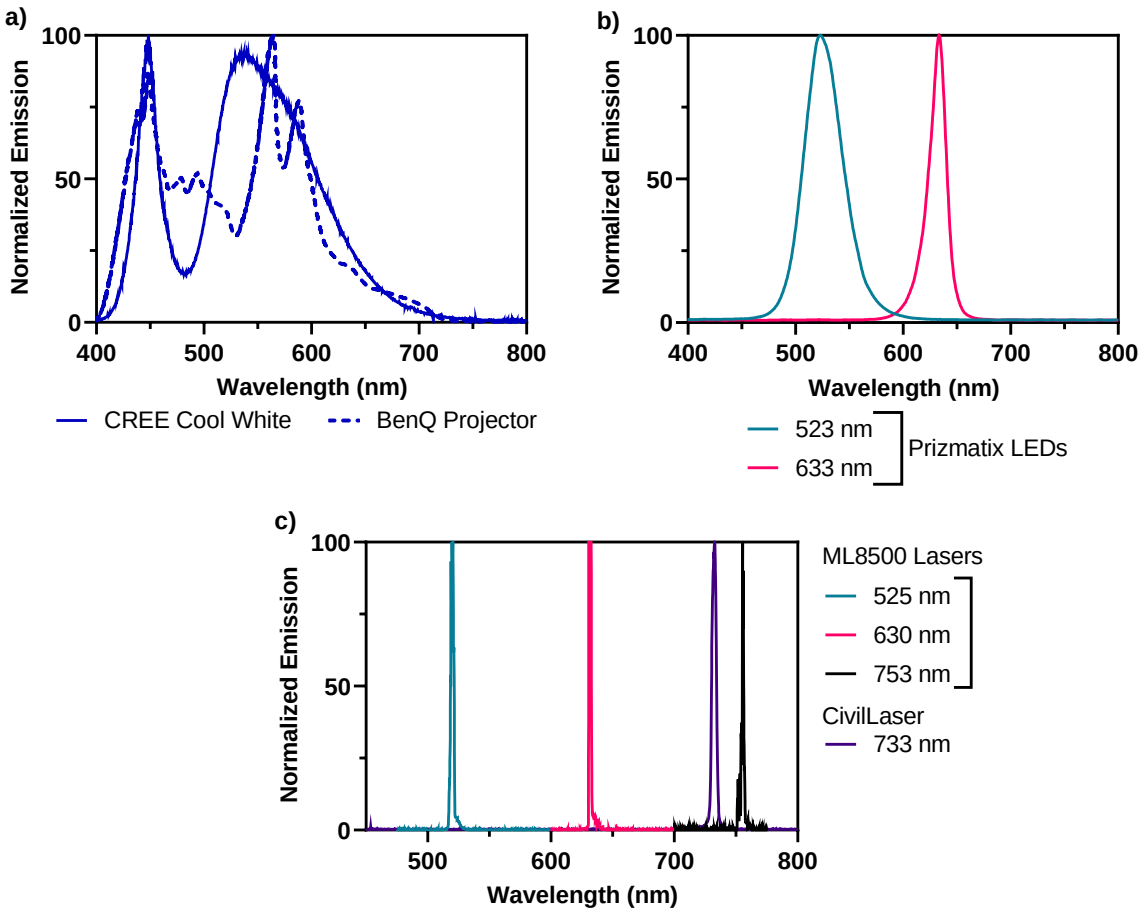

Figure S-23 Alternative plotting of light sources used in photobiological studies. a) broad white visible, b) Prizmatix LEDs, and c) lasers on the Modulight ML8500 or from CivilLaser.

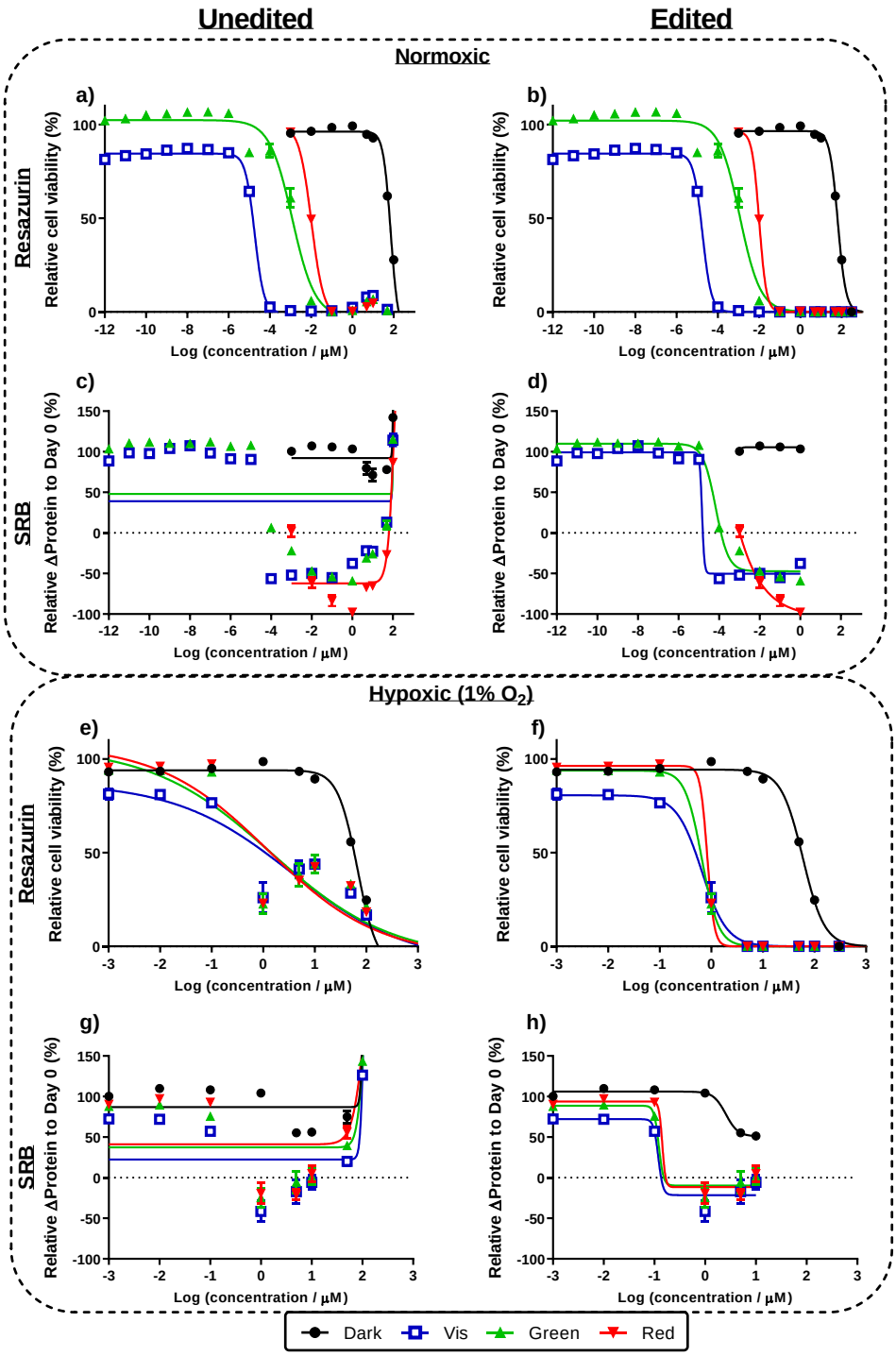

Figure S-24 Comparison of resazurin ($\lambda_{exc/em}$ = 530/620 nm; a–b, e–f) and sulforhodamine B (SRB, λ_{abs} = 565 nm; c–d, g–h) stains in normoxic- (a–d) and hypoxic-incubated (e–h) SK-MEL-28 human melanoma cells treated with **Os-4T**. Interference, mainly due to a combination of spectral overlap and resazurin reduction (left column), is corrected either by manual zeroing (resazurin) or data exclusion at the highest compound concentrations (right column) after microscopic verification. Fits in all cases are four-parameter logistic curves with points referenced to a positive (sham) growth control.

Table S-1 Lipophilicities of $[Os(phen)_3]^{2+}$ and **Os-*n*T** (***n*=0–4**) as chloride salts in 1-octanol and phosphate buffer (pH = 7.4), each solvent saturated with the other. [a]n.d. = not determined; **Os-4T** was not determined due to precipitation.

Complex	log ($D_{o/w}$ ± SD)
$[Os(phen)_3]^{2+}$	−1.697 ± 0.035
Os-0T	−2.243 ± 0.063
Os-1T	−0.794 ± 0.007
Os-2T	−0.341 ± 0.027
Os-3T	0.726 ± 0.043
Os-4T	n.d.[a]

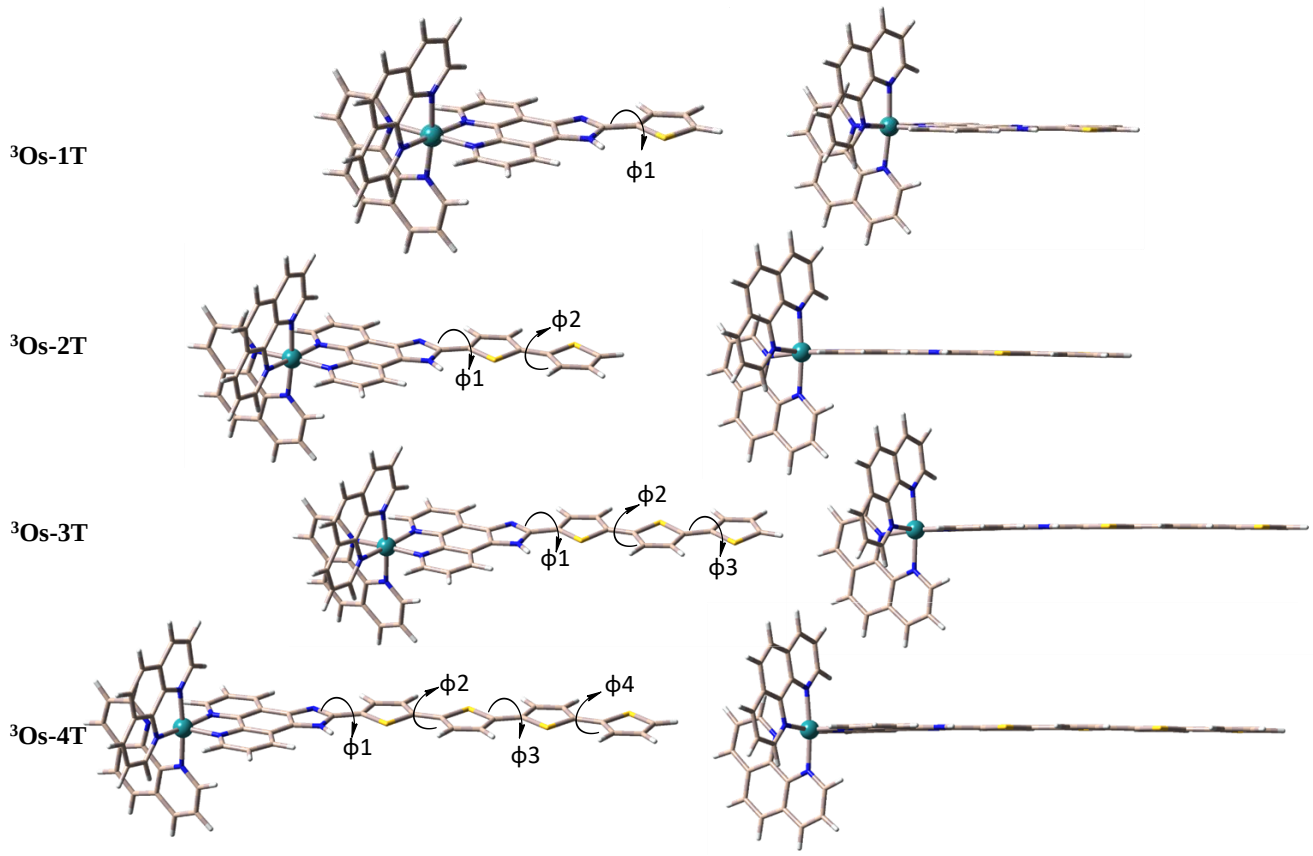

Figure S-25 Triplet States Geometry Optimizations of **^{3}Os-1T**, **^{3}Os-2T**, **^{3}Os-3T** and **^{3}Os-4T** obtained in a water environment at PBE0/6-31+G**/SDD/level of theory, each reported in two different orientations.

Table S-2 Dihedral angles ϕ1–ϕ4 (degree) for singlet and triplet optimized **Os-1T**–**Os-4T** geometries in a water environment at PBE0/6-31+G**/SDD/level of theory

	Dihedral Angles (° Degree)							
	ϕ1		ϕ2		ϕ3		ϕ4	
	Singlet	Triplet	Singlet	Triplet	Singlet	Triplet	Singlet	Triplet
Os-1T	−179.56	−179.68	\	\	\	\	\	\
Os-2T	179.61	−179.49	−164.61	179.88	\	\	\	\
Os-3T	−179.73	−179.45	−169.86	179.71	162.53	−179.92	\	\
Os-4T	−178.67	−179.21	−176.79	179.43	170.67	−179.72	−161.78	179.87

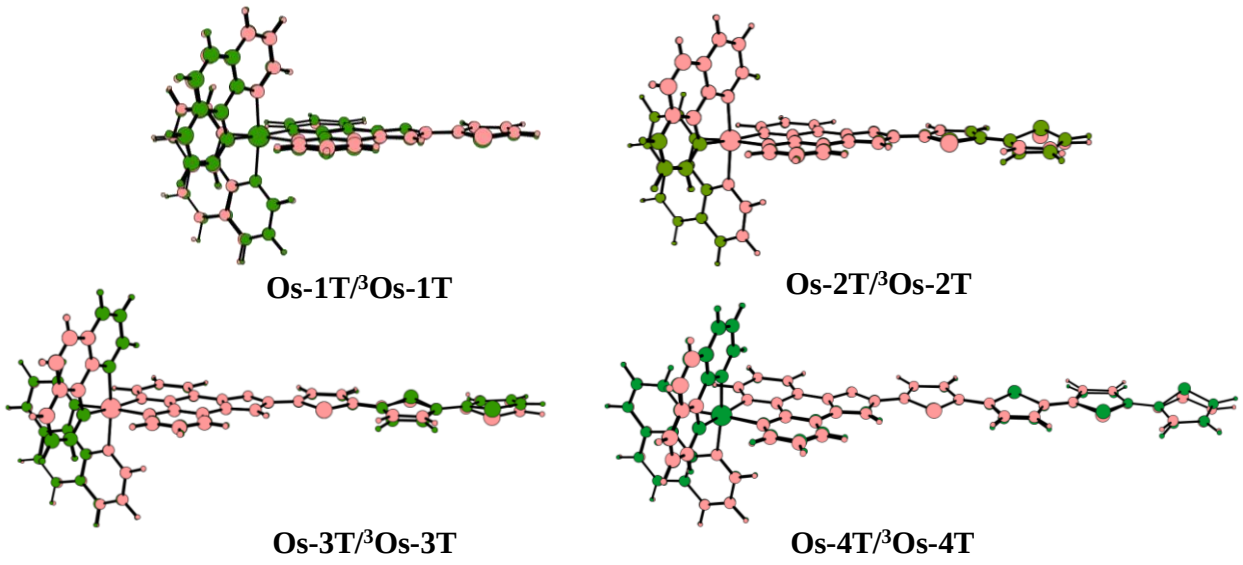

Figure S-26 Superpositions of ground (green) and excited states (pink), for **Os-1T**–**Os-4T** in a water environment at PBE0/6-31+G**/SDD/level of theory

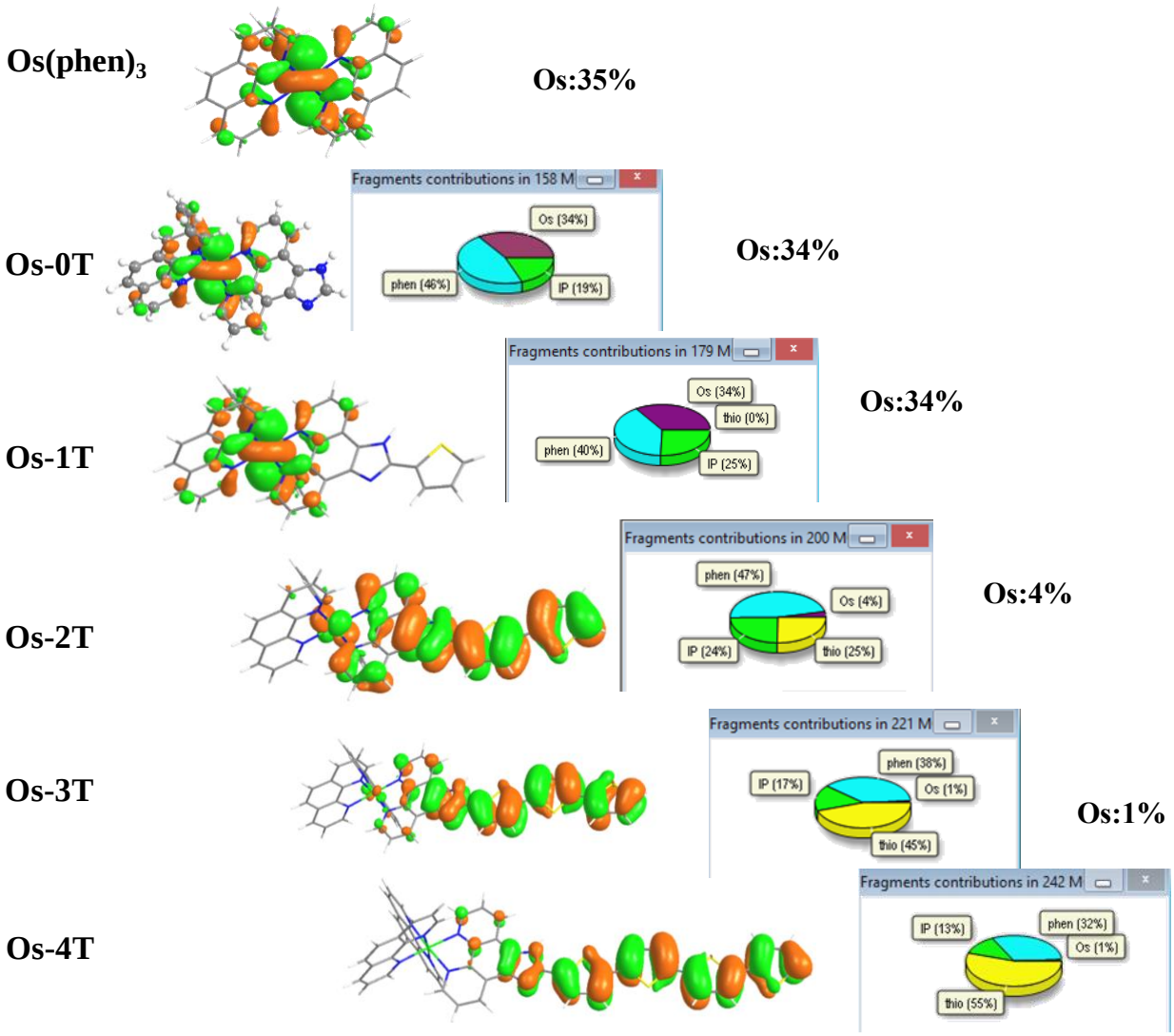

Figure S-27 MO plots of metal-based $[Os(phen)_3]^{2+}$ and **Os-*n*T** (***n*=0–1**) and ligand-based **Os-*n*T** (***n*=2–4**) **HOMO**, with the fraction of phen (cyan), IP (green) and Os (purple) components in each MO.

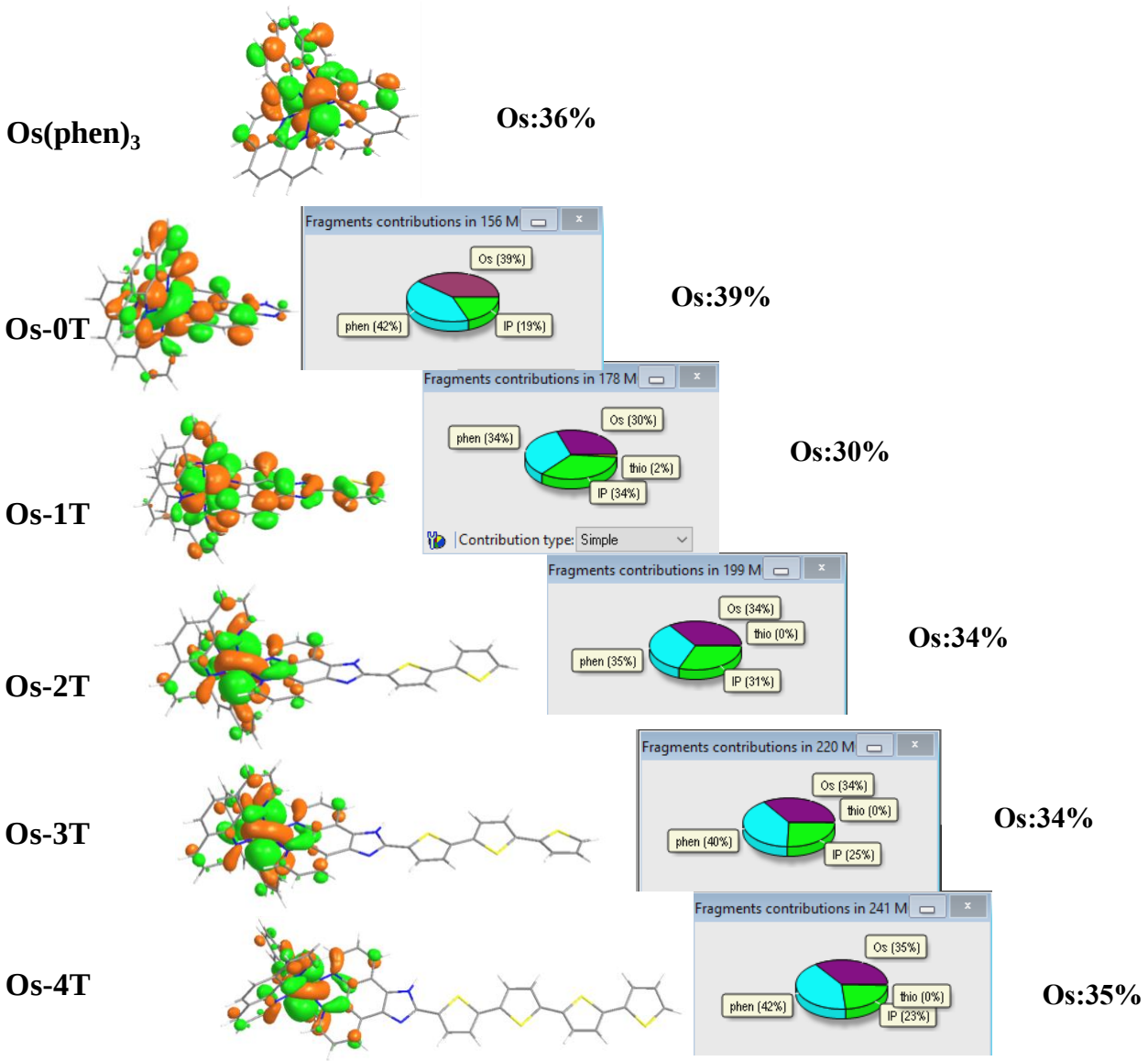

Figure S-28 MO plots of metal-based **HOMO-1**, with the fraction of phen (cyan), IP (green) and Os (purple) components in each MO.

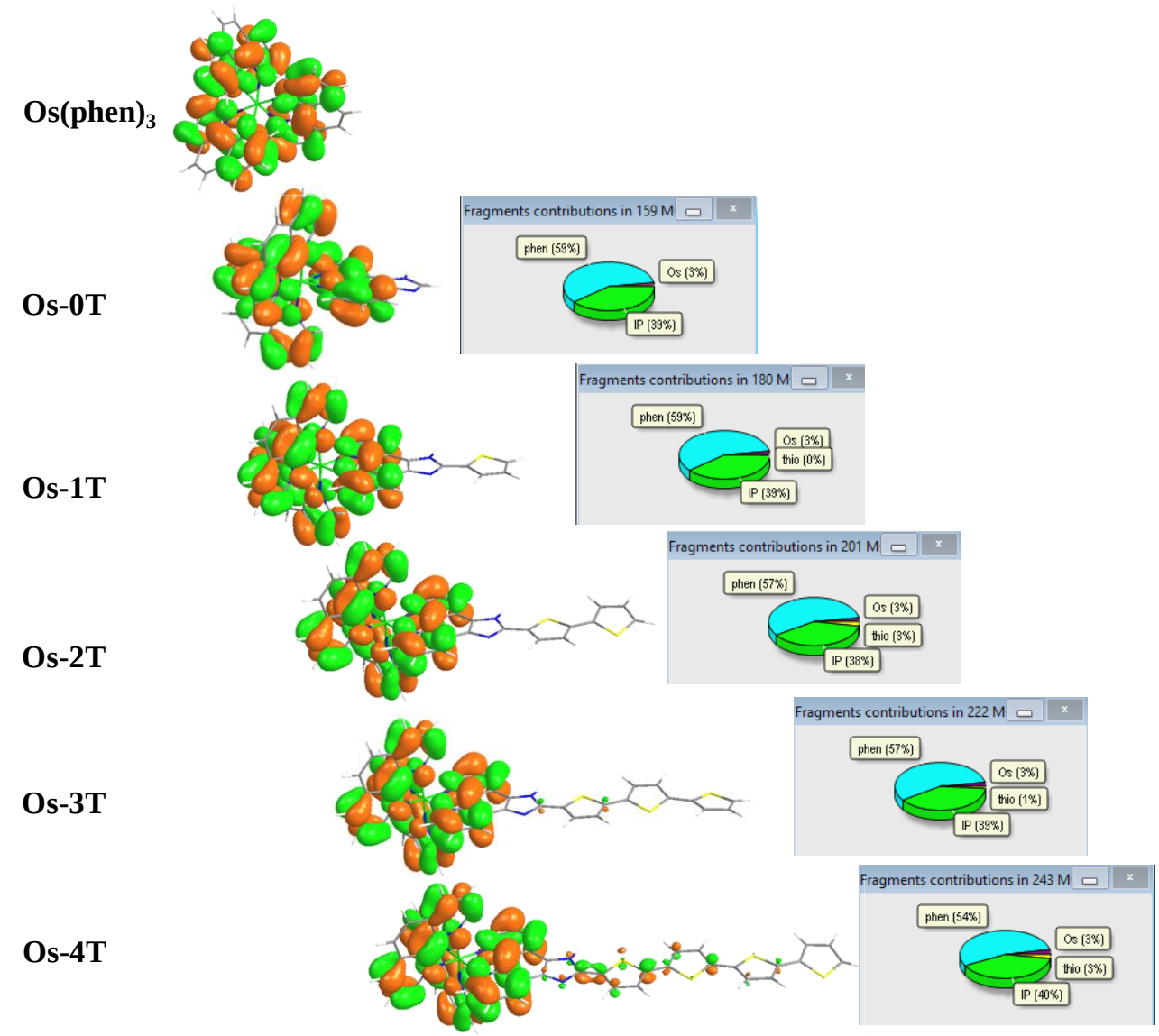

Figure S-29 MO plots of phen-based **LUMO**, with the fraction of phen (cyan), IP (green) and Os (purple) components in each MO.

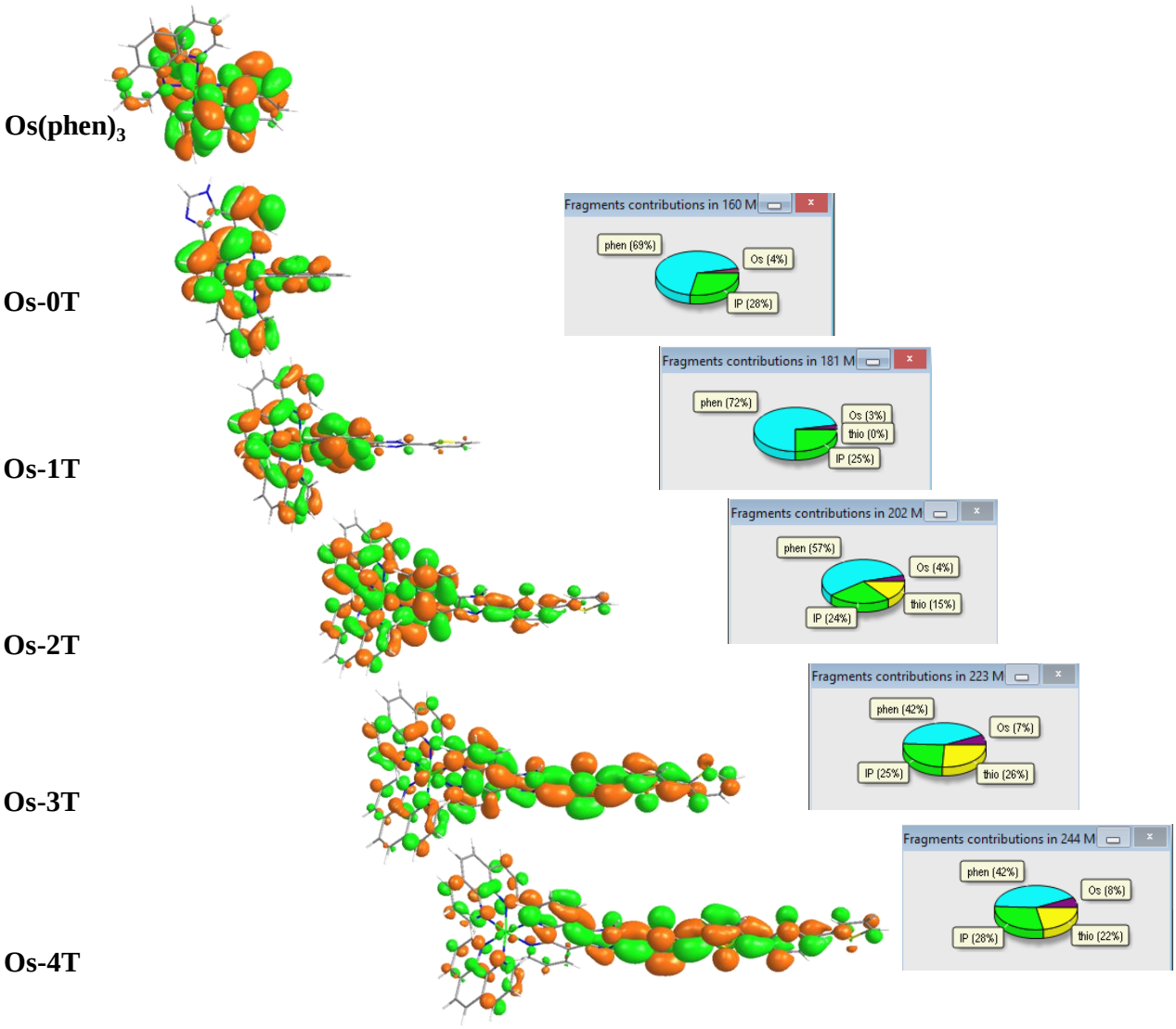

Figure S-30 MO plots of ligand-based **LUMO+1**, with the fraction of phen (cyan), IP (green) and Os (purple) components in each MO.

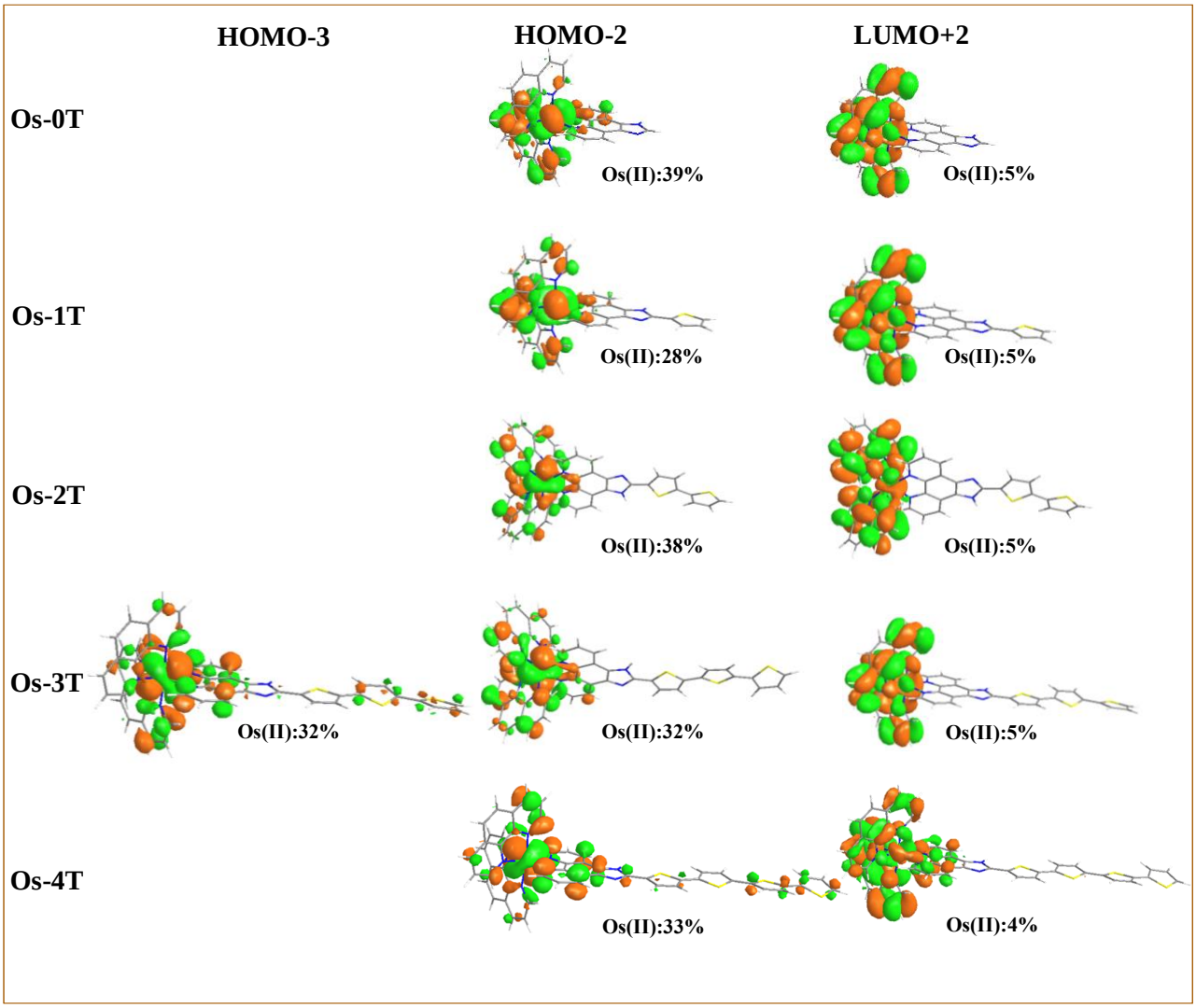

Figure S-31 Additional plots of involved MOs in the UV-Vis spectra

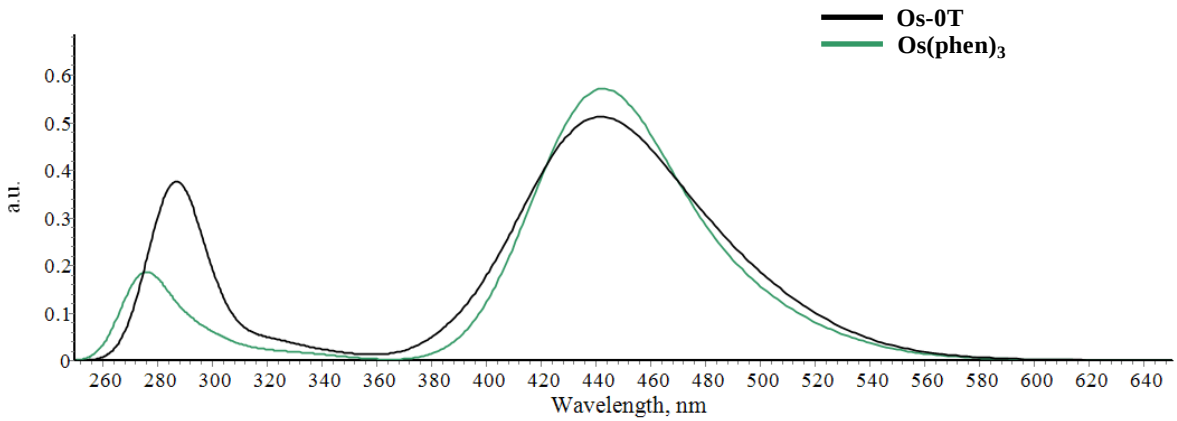

Figure S-32 Comparison of the computed UV-Vis spectra of **Os-0T** and $[Os(phen)_3]^{2+}$ in water at M06/6-31+G(d,p)/SDD/level of theory.

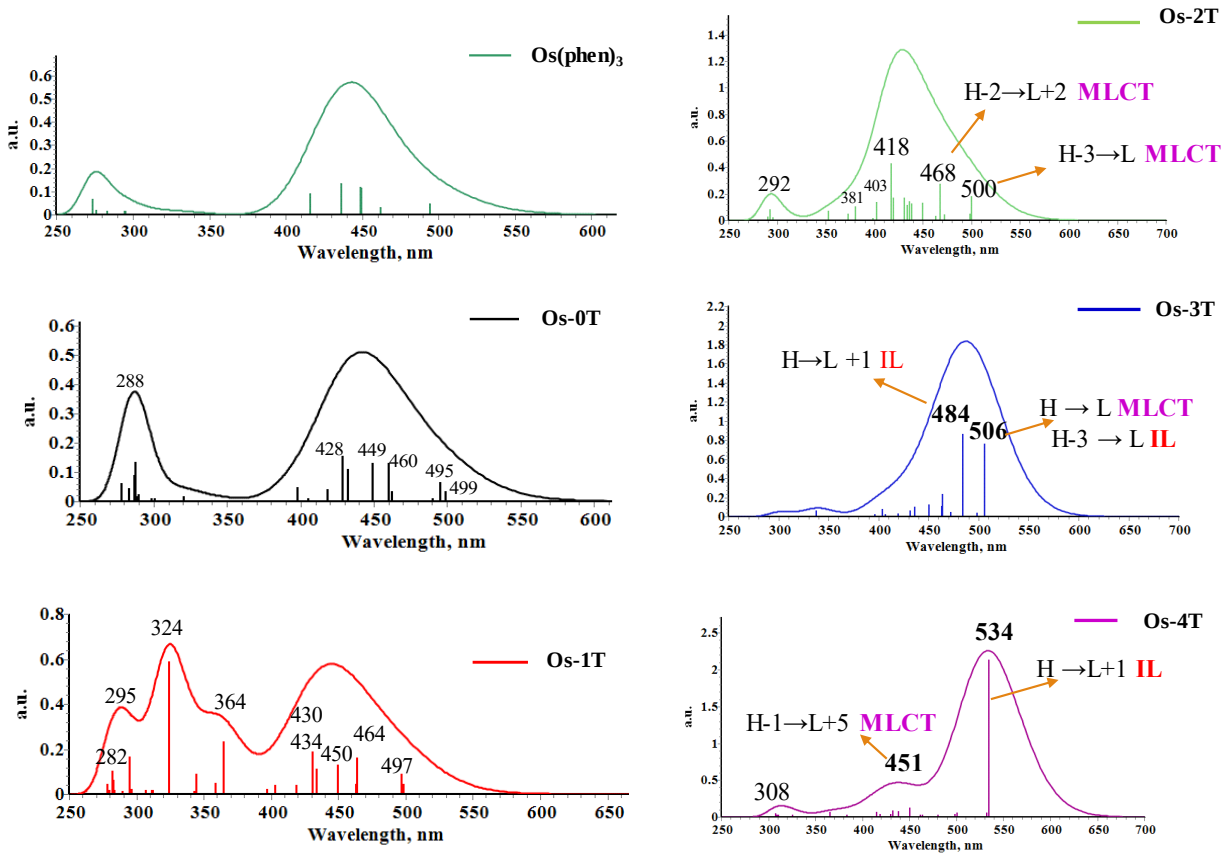

Figure S-33 Individual computed UV-Vis spectra of **Os-*n*T** (***n*=0–4**), in water, at the M06/6-31+G(d,p) / SDD level of theory.

Table S-3 Computed Excitation Energies of the lowest energy transitions in nm, main configuration, theoretical peak assignment, oscillator strengths, *f*, experimental excitation energies of the lowest energy transitions in nm for $[Os(phen)_3]^{2+}$ and **Os-*n*T** (***n***=**0**–**4**), in water.

Os(II)-Compounds	Wavelength (nm)	Main Configuration (%)	Assignment	*f*	*Exp*
$[Os(phen)_3]^{2+}$	449	H→L+5 (72%)	MLCT	0.116	*478*
	436	H-1→ L+3 (91%)	MLCT	0.133	*431*
Os-0T	461	H-1→L+1 (45%) H-2 → L+2 (37%)	MLCT	0.130	*480*
	449	H → L+3 (75%)	MLCT	0.133	*431*
	429	H → L+4 (74%)	MLCT	0.155	
Os-1T	464	H-1→ L+1 (49%) H-2 →L+2 (41%)	MLCT	0.163	*484*
	450	H → L+4 (74%)	MLCT	0.131	*435*
Os-2T	468	H-2 → L+2 (44%)	MLCT	0.277	*486*
	431	H-2 → L+3 (58%)	MLCT	0.172	*432*
Os-3T	506	H-3 → L (48%)	MLCT	0.761	*≈506*
		H → L (38%)	ILCT		
	484	H → L+1 (48%)	ILCT	0.862	*487*
		H-3 → L (29%)	MLCT		
Os-4T	534 nm	H → L+1 (55%)	ILCT	2.134	*≈510*
	451 nm	H-1→ L+5 (52%)	MLCT	0.124	*436*

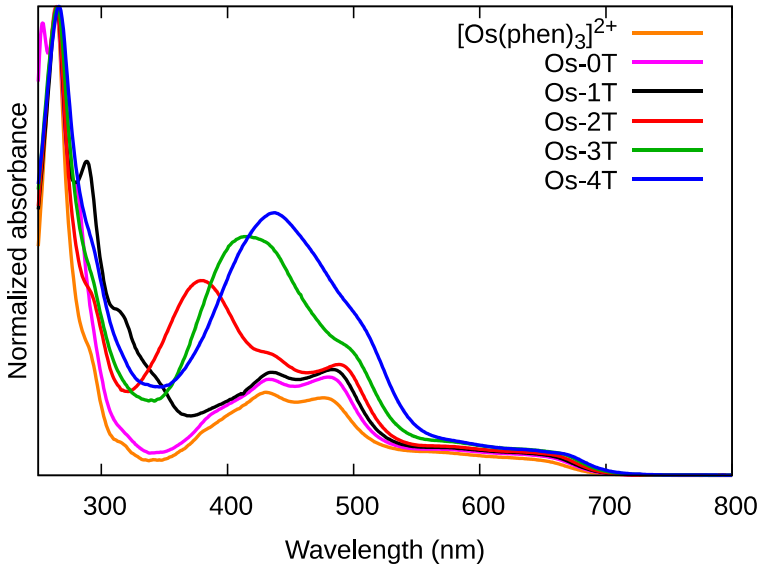

Figure S-34 UV-vis spectra of $[Os(phen)_3]^{2+}$ and **Os-*n*T** in water, normalized to the peak near 270 nm.

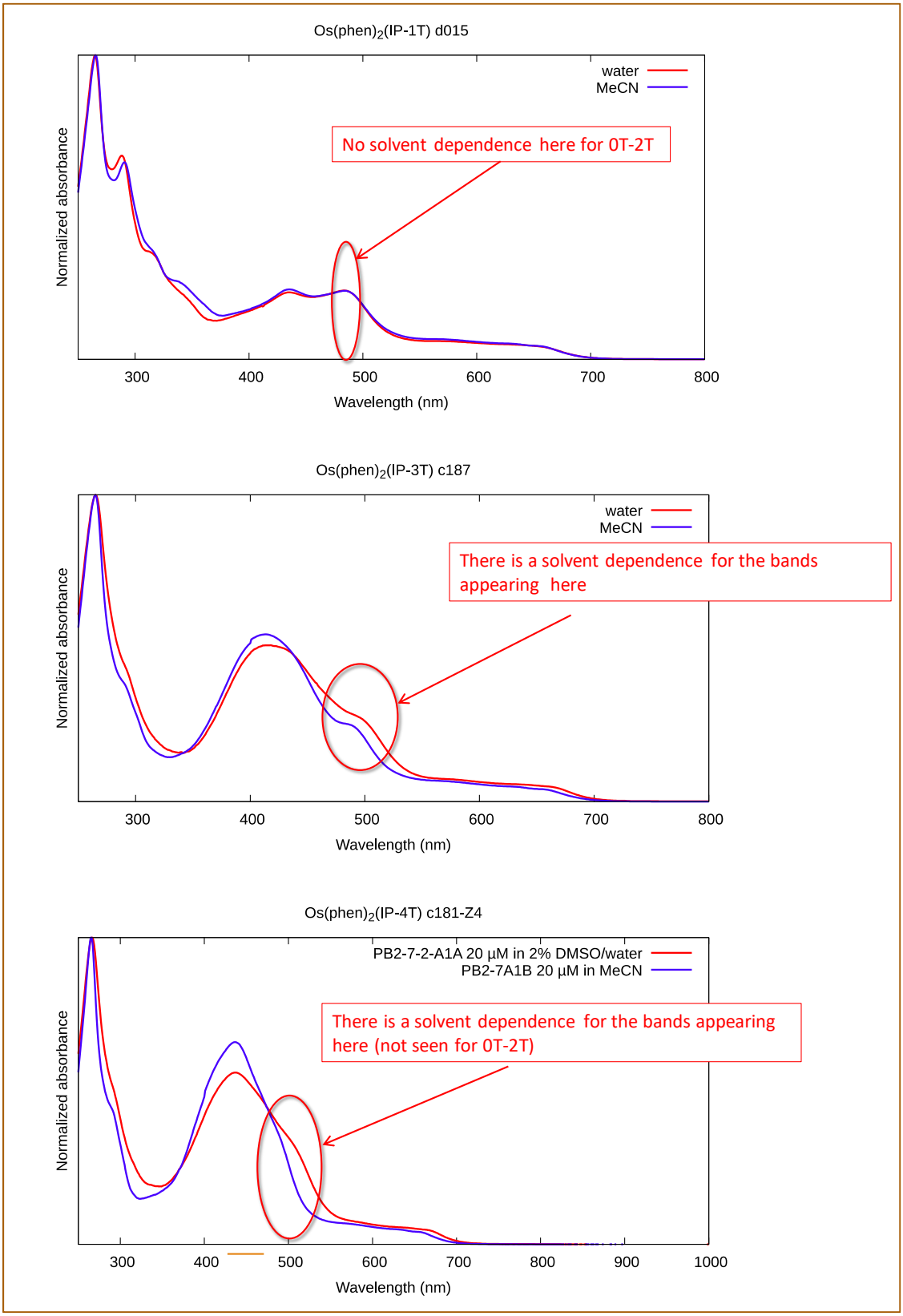

Figure S-35 The influence of solvent on the UV-Vis spectra.

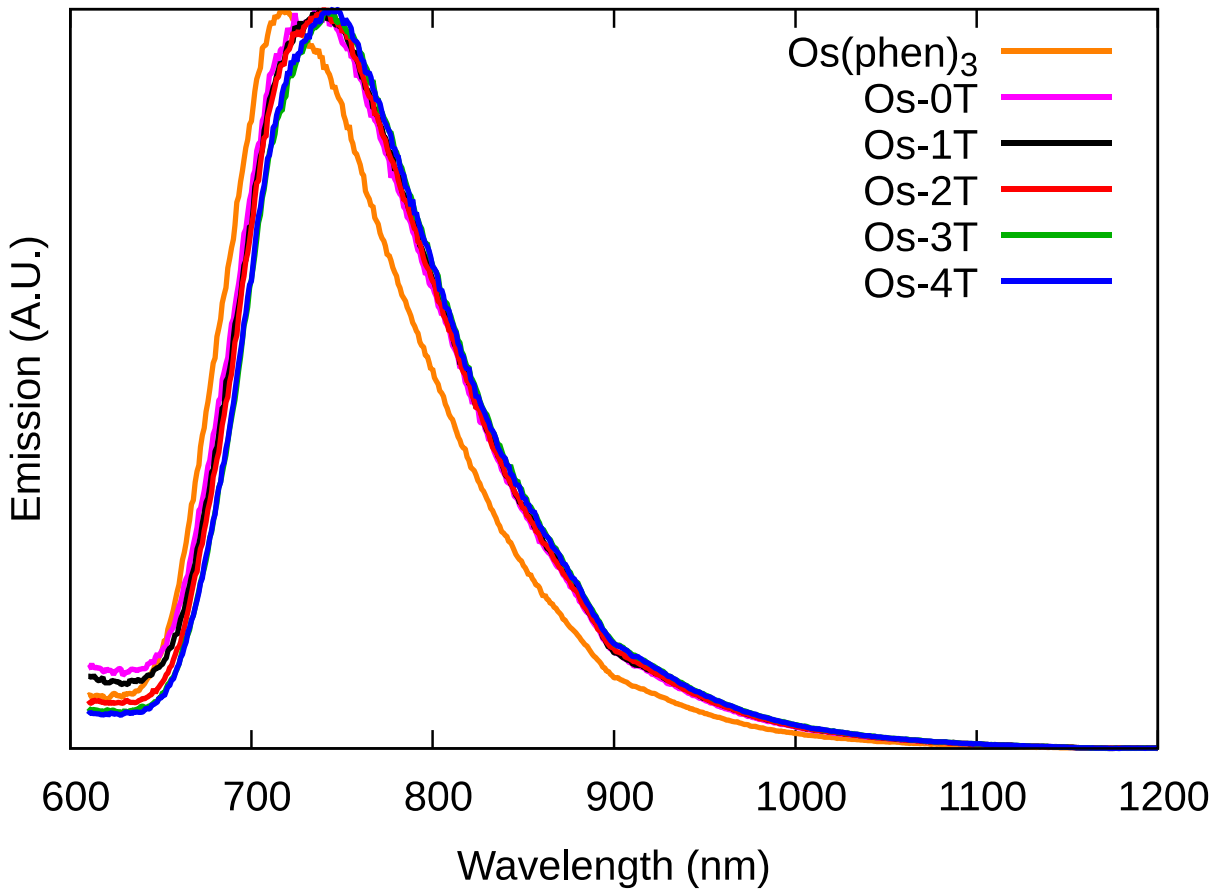

Figure S-36 Normalized emission spectra at room temperature in argon-sparged acetonitrile.

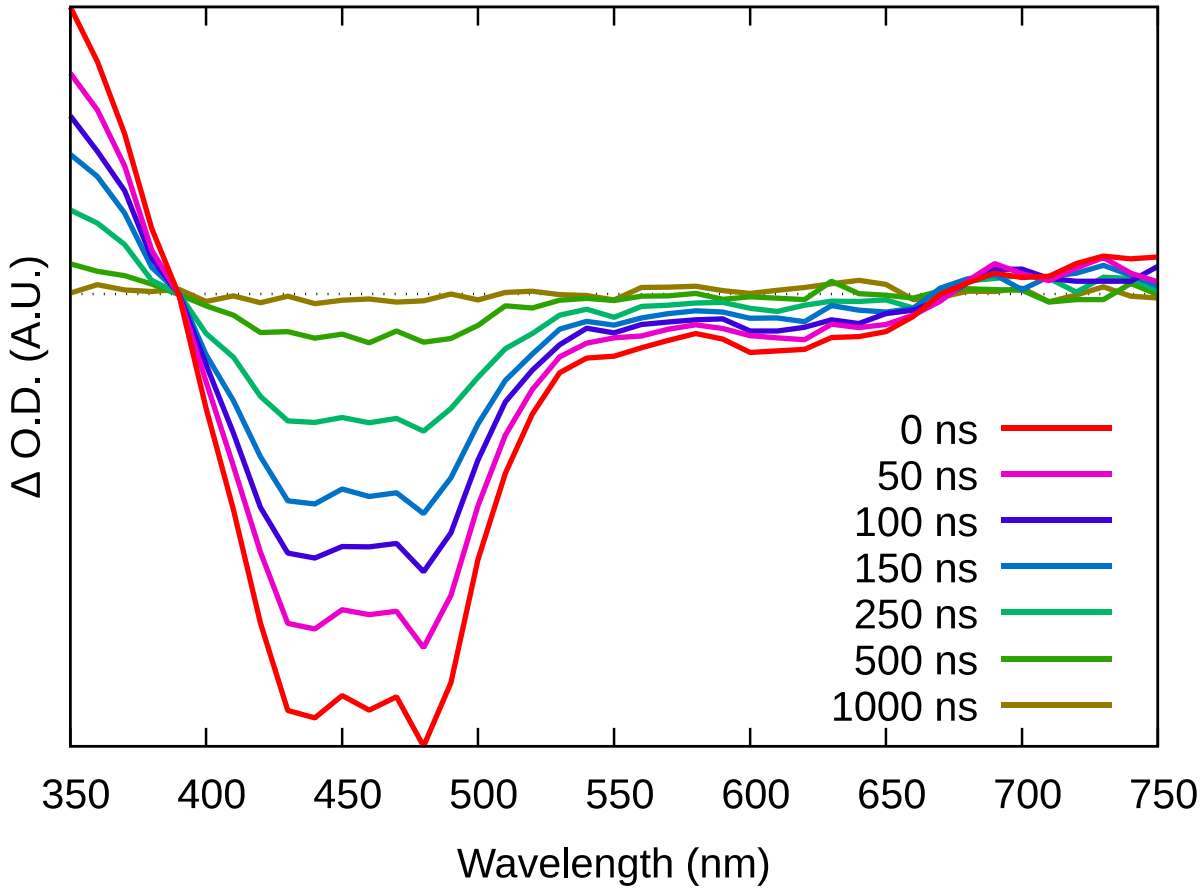

Figure S-37 Transient absorption spectrum of $[Os(phen)_3](PF_6)_2$ in deaerated MeCN at room temperature. Integration slices are 50 ns starting at the indicated time.

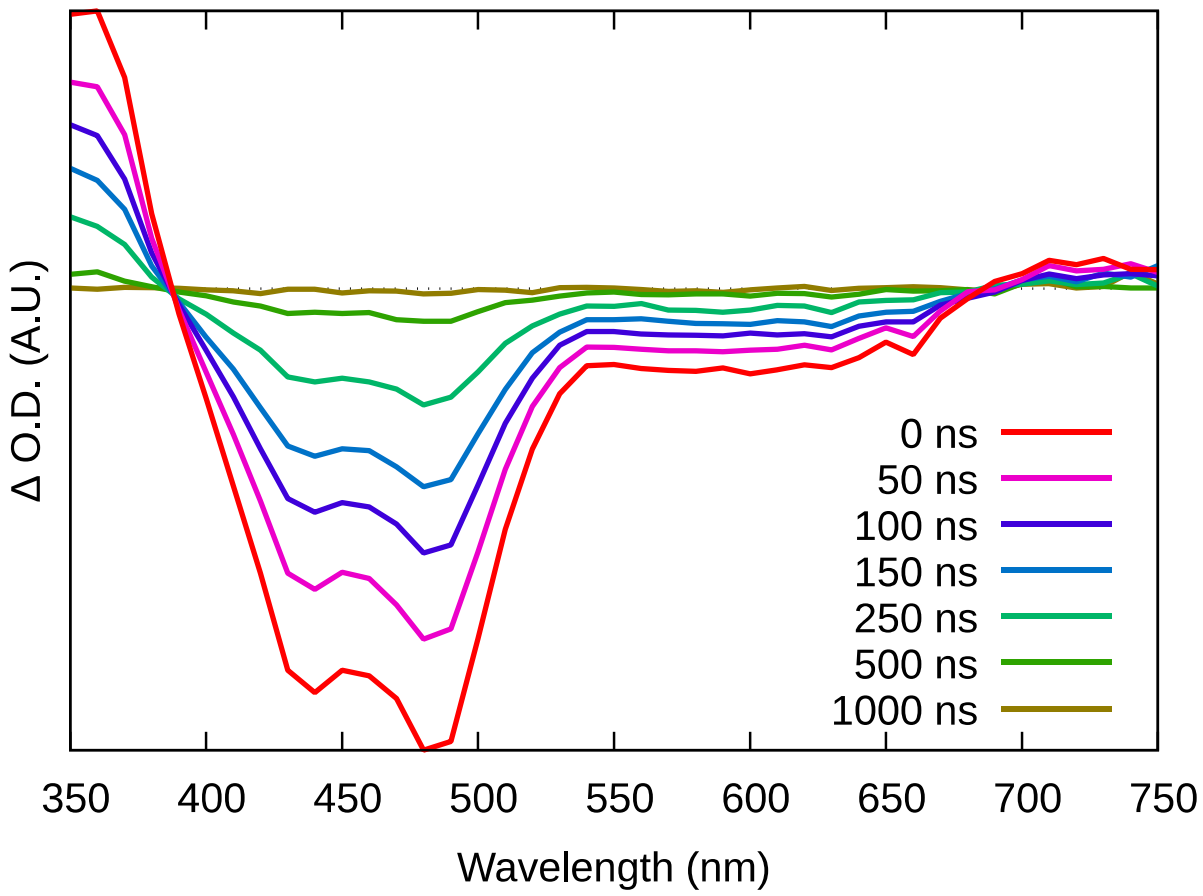

Figure S-38 Transient absorption spectrum of **Os-0T** in deaerated MeCN at room temperature. Integration slices are 50 ns starting at the indicated time.

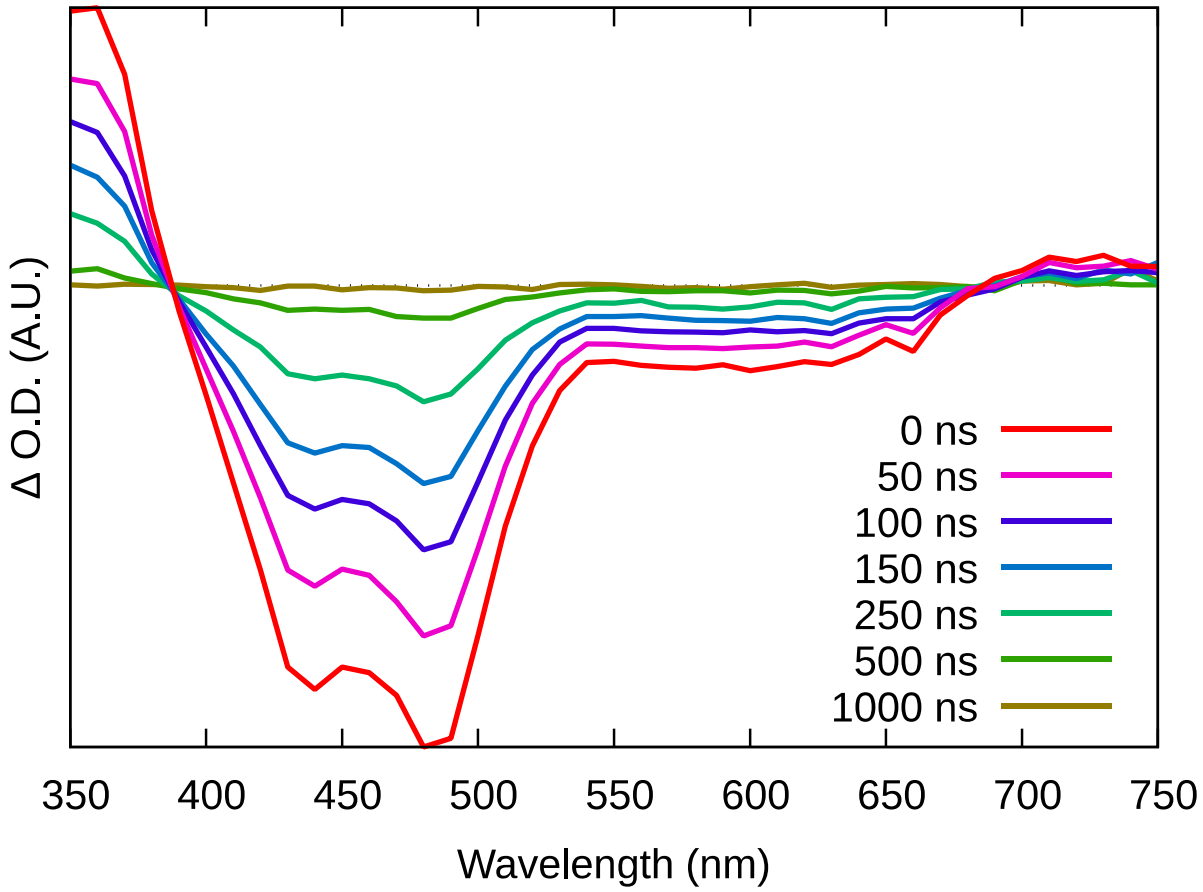

Figure S-39 Transient absorption spectrum of **Os-1T** in deaerated MeCN at room temperature. Integration slices are 50 ns starting at the indicated time.

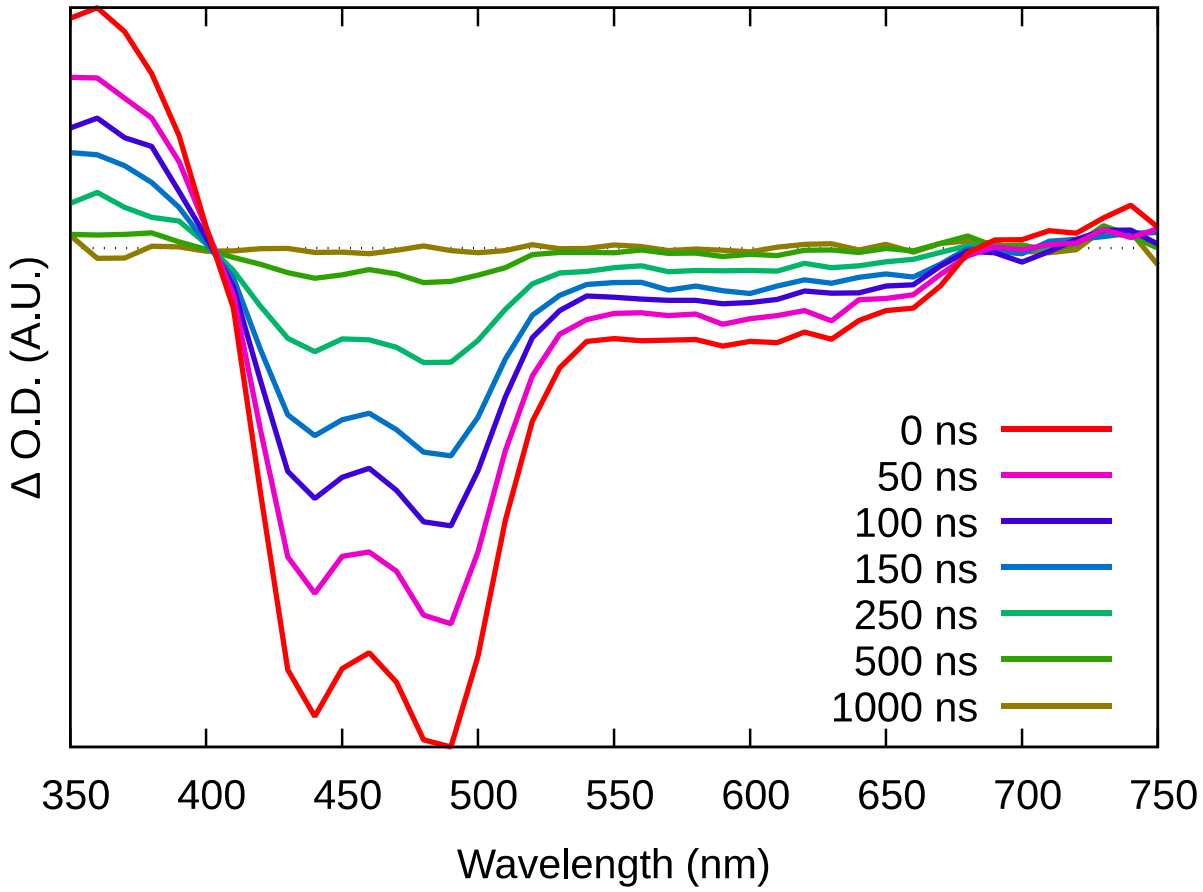

Figure S-40 Transient absorption spectrum of **Os-2T** in deaerated MeCN at room temperature. Integration slices are 50 ns starting at the indicated time.

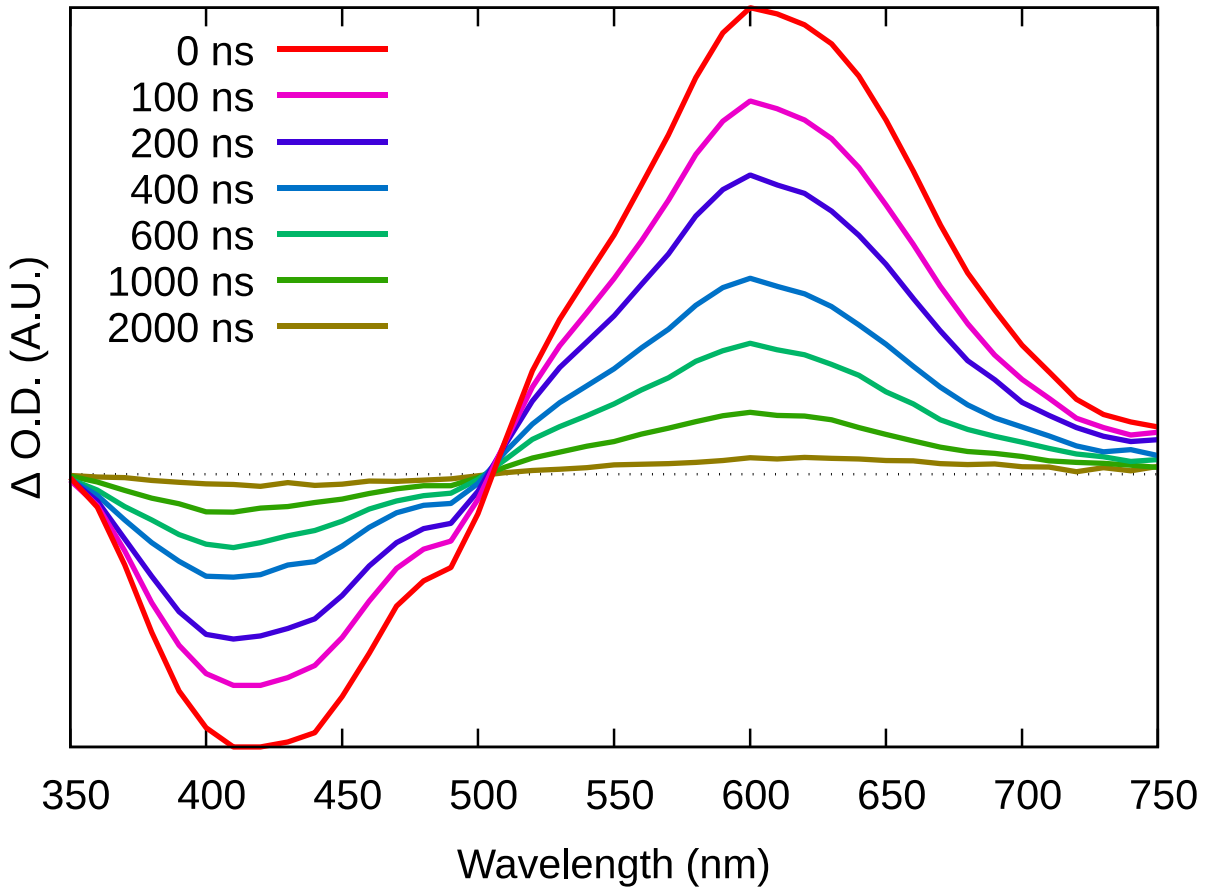

Figure S-41 Transient absorption spectrum of **Os-3T** in deaerated MeCN at room temperature. Integration slices are 100 ns starting at the indicated time.

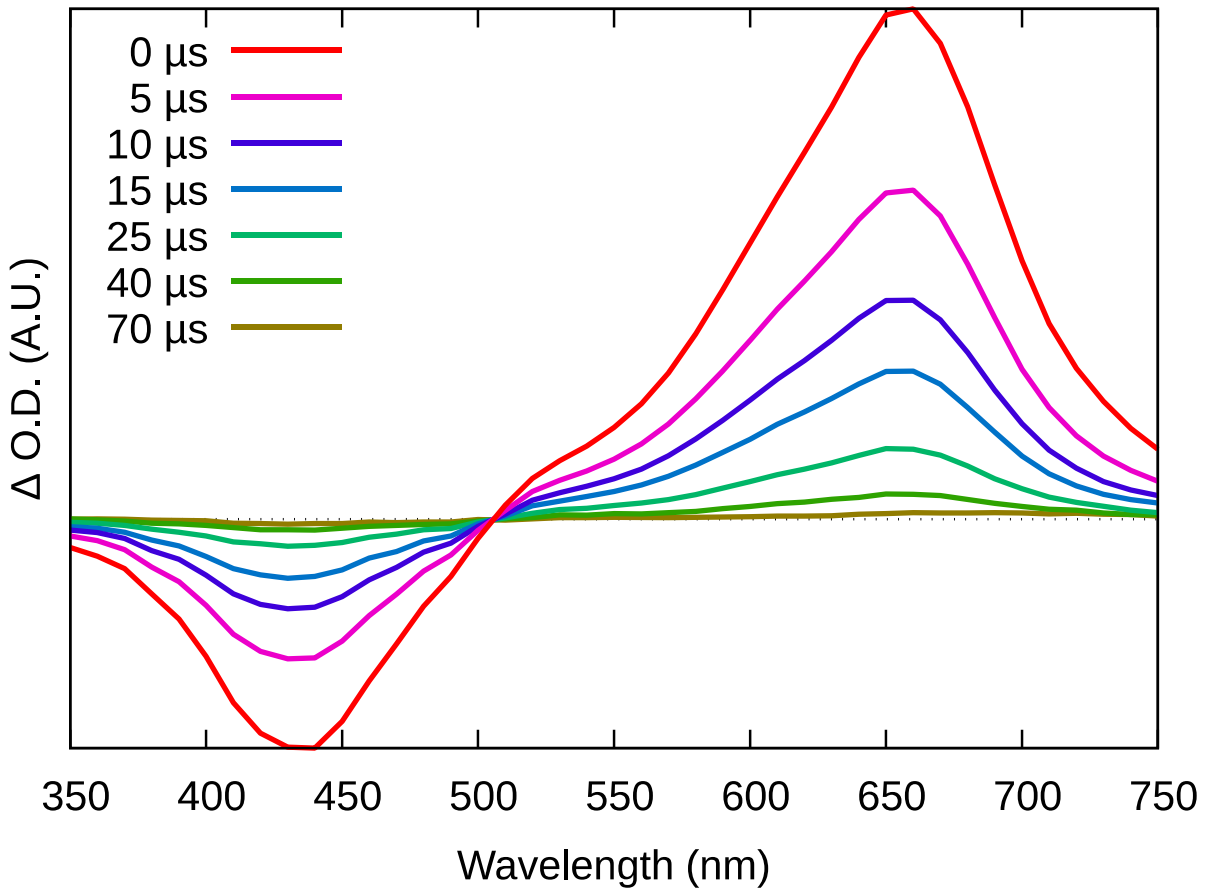

Figure S-42 Transient absorption spectrum of **Os-4T** in deaerated MeCN at room temperature. Integration slices are 5 µs starting at the indicated time.

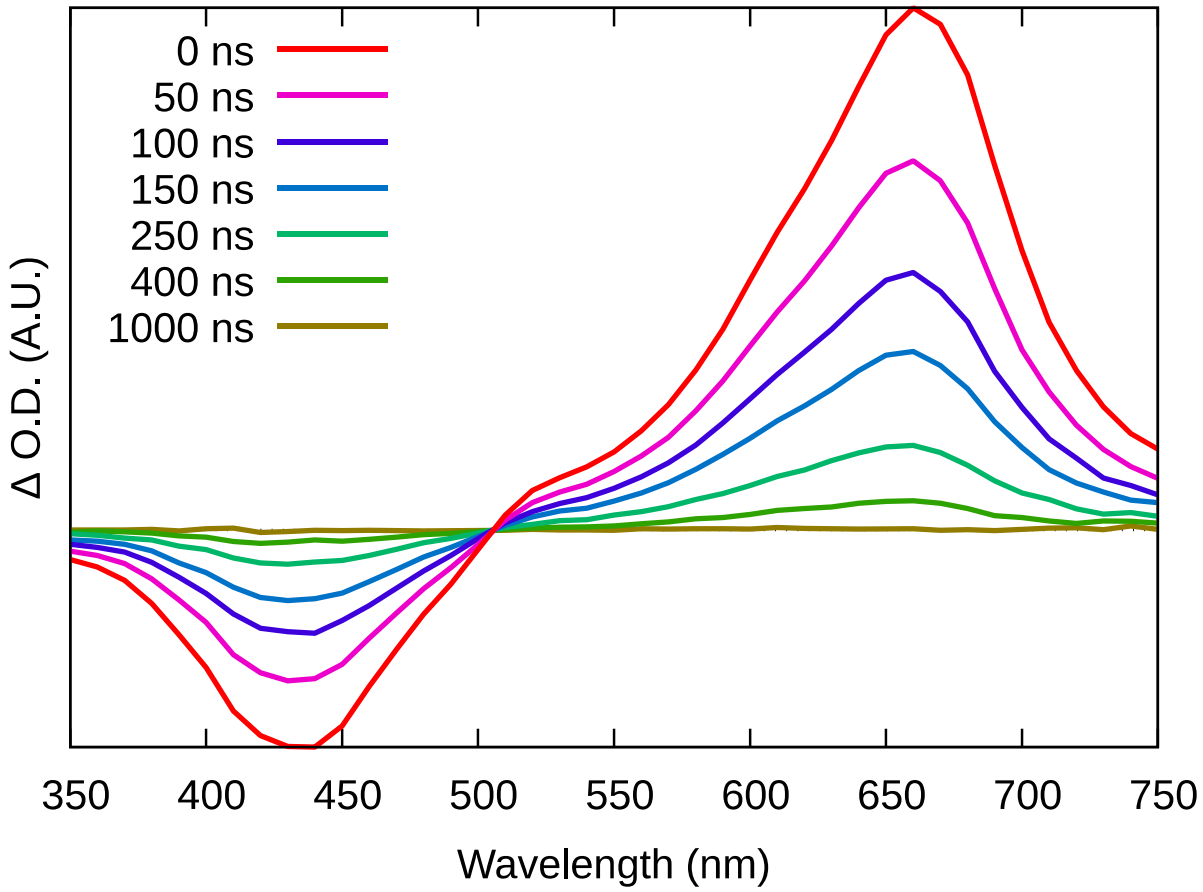

Figure S-43 Transient absorption spectrum of **Os-4T** in oxygen-containing MeCN at room temperature. Integration slices are 50 ns starting at the indicated time.

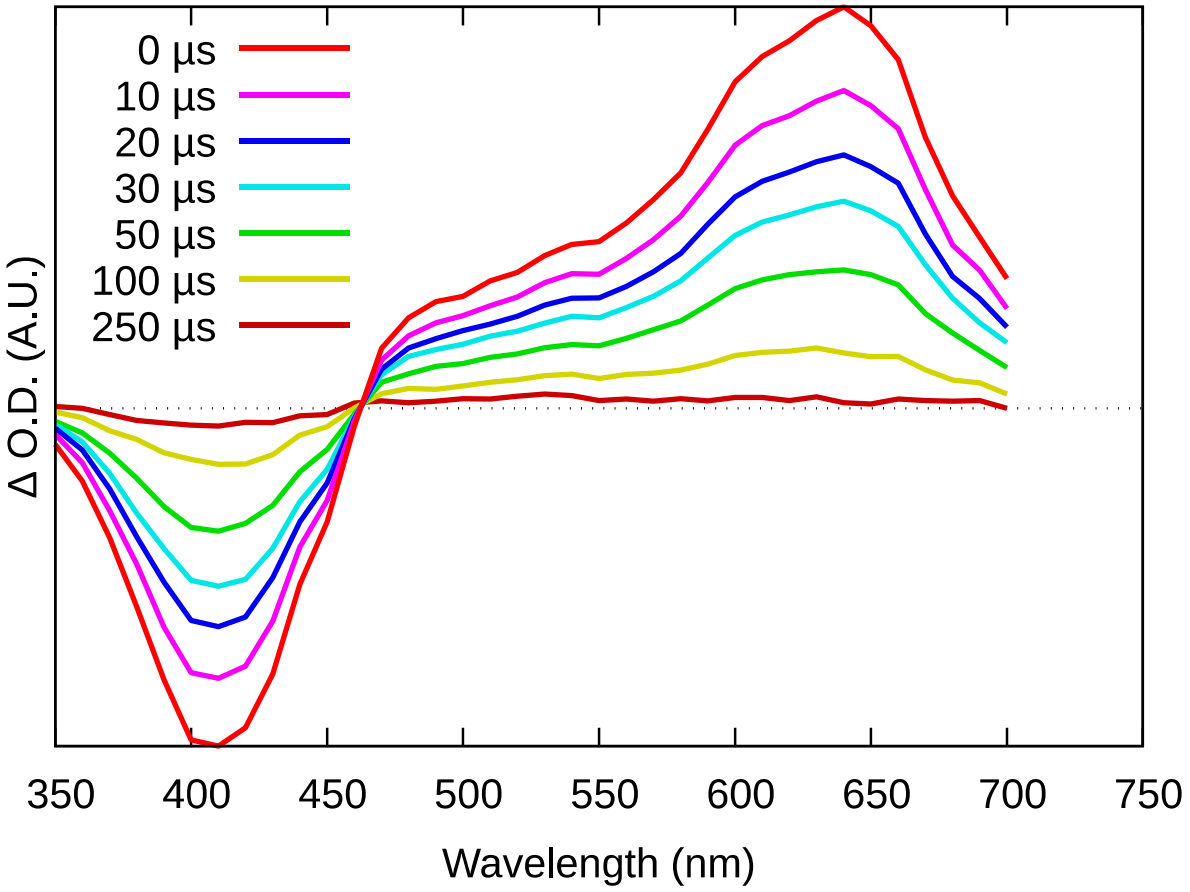

Figure S-44 Transient absorption spectrum of the **3T** ligand in deaerated DMSO at room temperature. Integration slices are 10 µs starting at the indicated time. τ=53 µs.

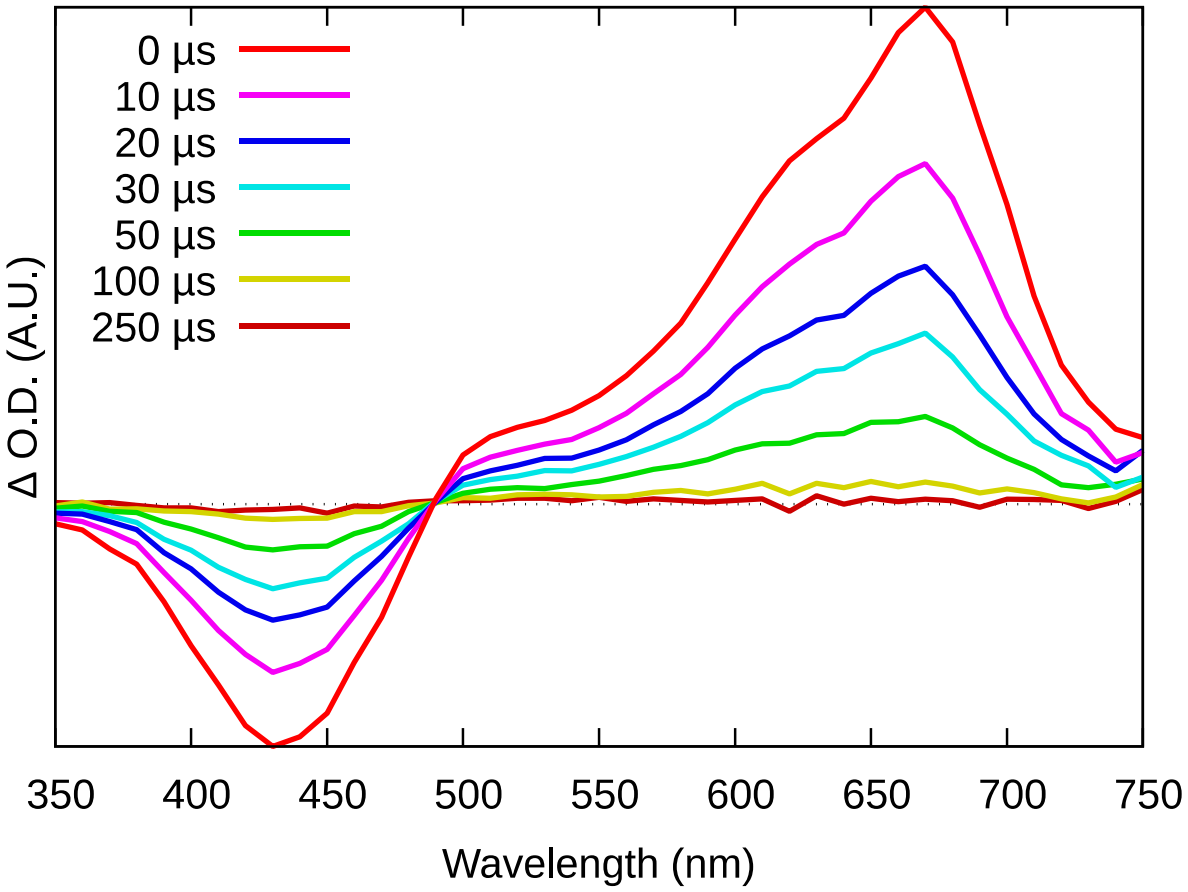

Figure S-45 Transient absorption spectrum of the **4T** ligand in deaerated DMSO at room temperature. Integration slices are 10 µs starting at the indicated time. τ=28 µs.

Table S-4 Cytotoxicity and photocytotoxicity of $[Os(phen)_3]Cl_2$ and **Os-*n*T** (***n*=0–4**) in normoxic-treated SK-MEL-28 amelanotic cells. Light treatments are approximately 100 J cm^{-2} delivered at 20 mW cm^{-2}. R_1 = $[Ru(bpy)_2(dppn)]Cl_2$, R_2 = cisplatin, [a] Cool white visible (400–700 nm), [b] green 523 nm, [c] red 633 nm, and [d] PI = phototherapeutic index. A dash (-) indicates that the conditions were not run. * indicates that no SEM was determined.

	Resazurin-Normoxia (18.5–21% O_2)						
	EC_{50} ± SEM (μM)				PI[d]		
Cmpd	Dark	Visible[a]	Green[b]	Red[c]	Visible[a]	Green[b]	Red[c]
$[Os(phen)_3]Cl_2$	158 ± 2	40.3 ± 1.5	86.1 ± 4.2	101 ± 5	4	2	2
Os-0T	116 ± 4	2.75 ± 0.09	11.9 ± 0.2	27.1 *	42	9	4
Os-1T	75.1 ± 1.2	2.98 ± 0.06	5.93 ± 0.07	9.84 ± 0.14	25	12	7
Os-2T	35.7 ± 3.2	1.43 ± 0.02	3.53 ± 0.15	3.94 ± 0.03	24	10	9
Os-3T	56.5 ± 1.2	0.153 ± 0.005	0.547 ± 0.150	0.678 ± 0.048	369	103	83
Os-4T	65.1 ± 1.3	(1.78 ± 0.05) $\times10^{-5}$	(1.16 ± 0.13) $\times10^{-3}$	0.010 ± 0.001	3.66×10^{6}	56120	6510
R_1	114 ± 3	3660.144 ± 0.001	0.165 ± 0.004	0.613 ± 0.036	791	690	185
R_2	3.12 ± 0.14	-	-	-	-	-	-

Table S-5 Cytotoxicity and photocytotoxicity of $[Os(phen)_3]Cl_2$ and **Os-*n*T** (***n*=0–4**) in hypoxic-treated SK-MEL-28 amelanotic cells. Light treatments are approximately 100 J cm^{-2} delivered at 20 mW cm^{-2}. R_1 = $[Ru(bpy)_2(dppn)]Cl_2$, R_2 = cisplatin, [a] Cool white visible (broad, 400–700 nm), [b] green 523 nm, [c] red 633 nm, and [d] PI = phototherapeutic index(=dark EC_{50} / light EC_{50}). [e] Red treated R_1 shows activity in hypoxia despite inactivity with more highly energetic light sources. A dash (-) indicates that the conditions were not run.

	Resazurin-Hypoxia (1% O_2)						
	EC_{50} ± SEM (μM)				PI[d]		
Cmpd	Dark	Visible[a]	Green[b]	Red[c]	Visible[a]	Green[b]	Red[c]
$[Os(phen)_3]Cl_2$	168 ± 2	187 ± 2	166 ± 2	172 ± 3	1	1	1
Os-0T	130 ± 3	45.7 ± 11.4	128 ± 3	144 ± 3	2	1	1
Os-1T	80.7 ± 1.7	86.2 ± 3.2	89.8 ± 2.3	88.4 ± 2.1	1	1	1
Os-2T	66.0 ± 2.4	58.0 ± 2.4	64.4 ± 1.9	68.2 ± 1.8	1	1	1
Os-3T	50.5 ± 0.8	39.6 ± 5.4	38.3 ± 3.4	52.5 ± 2.1	1	1	1
Os-4T	59.5 ± 1.4	0.651 ± 0.047	0.653 ± 0.02	0.835 ± 0.005	91	91	71
R_1	115 ± 3	117 ± 7	130 ± 10	6.54 ± 1.33	1	1	17[e]
R_2	3.35 ± 0.09	-	-	-	-	-	-

Table S-6 SRB parameters GI_{50}, LC_{50}, and TGI for normoxic treated SK-MEL-28 cells with $[Os(phen)_3]Cl_2$ and **Os-*n*T** (***n*=0–4**). GI_{50} measures 50% cell growth inhibition, LC_{50} references cytotoxicity (50% protein reduction compared to the beginning), and TGI is the concentration that leads to total growth inhibition (0% protein change compared to beginning). R_1 = $[Ru(bpy)_2(dppn)]Cl_2$, R_2 = cisplatin, [a] cool white visible (broad, 400–700 nm), [b] green 523 nm, and [c] red 633 nm. A dash (-) indicates that either the conditions were not run or a parameter could not be interpolated (95% CI) from the available data.

SRB-Normoxia (18.5–21% O_2)									
Treatment	Concentration (μM)	Compound							
		$[Os(phen)_3]Cl_2$	**Os-0T**	**Os-1T**	**Os-2T**	**Os-3T**	**Os-4T**	**R_1**	**R_2**
Dark	GI_{50}	125	46.8	21.5	23.4	-	-	30.2	1.11
	LC_{50}	-	-	-	55.2	-	-	-	1.45
	TGI	277	162	-	33.5	-	-	57.3	1.24
Red[a]	GI_{50}	15.2	10.6	5.01	2.00	0.303	0.00038	0.195	-
	LC_{50}	-	-	-	-	-	0.006	0.153	-
	TGI	32.9	25.8	-	3.01	0.469	0.001	0.199	-
Green[b]	GI_{50}	18.1	5.22	1.37	2.24	0.21	$(4.78)\times10^{-5}$	0.278	-
	LC_{50}	-	-	-	-	-	-	-	-
	TGI	49.3	8.60	1.79	3.30	0.351	0.00012	0.649	-
Vis[c]	GI_{50}	4.98	1.14	1.13	0.989	0.097	$(1.32)\times10^{-5}$	0.042	-
	LC_{50}	-	-	-	-	-	$(2.92)\times10^{-5}$	-	-
	TGI	13.5	1.36	1.40	1.02	0.124	$(1.58)\times10^{-5}$	0.136	-

Table S-7 SRB parameters GI_{50}, LC_{50}, and TGI for hypoxic (1% O_2) treated SK-MEL-28 cells with $[Os(phen)_3]Cl_2$ and **Os-*n*T** (***n*=0–4**). GI_{50} measures 50% cell growth inhibition, LC_{50} references cytotoxicity (50% protein reduction compared to the beginning), and TGI is the concentration that leads to total growth inhibition (0% protein change compared to beginning). R_1 = $[Ru(bpy)_2(dppn)]Cl_2$, R_2 = cisplatin, [a] cool white visible (broad, 400–700 nm), [b] green 523 nm, and [c] red 633 nm. A dash (-) indicates that either the conditions were not run or a parameter could not be interpolated (95% CI) from the available data.

SRB-Hypoxia (1% O_2)									
Treatment	Concentration (μM)	Compound							
		$[Os(phen)_3]Cl_2$	**Os-0T**	**Os-1T**	**Os-2T**	**Os-3T**	**Os-4T**	**R_1**	**R_2**
Dark	GI_{50}	127	68.2	61.2	31.7	-	-	37.9	1.88
	LC_{50}	-	-	-	-	0.001	-	-	3.59
	TGI	253	256	-	-	-	-	-	2.49
Red[a]	GI_{50}	87.5	51.4	49.7	22.1	-	0.139	4.20	-
	LC_{50}	-	-	88.1	-	-	0.604	-	-
	TGI	172	263	68.9	170	-	0.167	-	-
Green[b]	GI_{50}	144	53.7	-	31.2	-	0.116	-	-
	LC_{50}	-	-	-	-	-	-	-	-
	TGI	-	-	-	96.4	-	0.154	-	-
Vis[c]	GI_{50}	119	7.53	-	9.66	1.93	0.105	0.201	-
	LC_{50}	-	-	-	-	-	-	-	-
	TGI	275	20.7	-	65.0	-	0.136	-	-

Table S-8 Cytotoxicity and photocytotoxicity of **Os-4T** in normoxic-treated SK-MEL-28 amelanotic cells repeated over time. Light treatments are approximately 100 J cm^{-2} delivered at 20 mW cm^{-2} [a] Cool white visible (400–700 nm), [b] green 523 nm, [c] red 633 nm, [d] PI = phototherapeutic index (=dark EC_{50} / light EC_{50}), and *original run in repeat 0 from Table S-4.

	Resazurin-Normoxia (18.5–21% O_2) Os-4T Repeats						
	EC_{50} (μM)				PI[d]		
Repeat	Dark	Visible[a]	Green[b]	Red[c]	Visible[a]	Green[b]	Red[c]
0*	65.1	1.78×10^{-5}	1.16×10^{-3}	1.00×10^{-2}	3.66×10^{6}	5.61×10^{4}	6.51×10^{3}
1	60.1	1.01×10^{-4}	1.43×10^{-2}	3.00×10^{-2}	5.95×10^{5}	4.20×10^{3}	2.00×10^{3}
2	64.3	4.09×10^{-5}	9.44×10^{-3}	3.94×10^{-2}	1.57×10^{6}	6.81×10^{3}	1.63×10^{3}
3	67.5	2.88×10^{-5}	6.92×10^{-3}	1.41×10^{-2}	2.34×10^{6}	9.74×10^{3}	4.78×10^{3}
4	60.3	5.97×10^{-4}	2.54×10^{-2}	4.48×10^{-2}	1.01×10^{5}	2.38×10^{3}	1.35×10^{3}
5	62.2	8.91×10^{-3}	1.31×10^{-2}	4.62×10^{-2}	6.97×10^{3}	4.75×10^{3}	1.35×10^{3}
Mean ± SD	63.2 ± 2.9	$(1.62 \pm 3.58)\times10^{-3}$	$(1.17 \pm 0.82)\times10^{-2}$	$(3.08 \pm 1.56)\times10^{-2}$	$(1.38 \pm 1.43)\times10^{6}$	$(1.40 \pm 2.08)\times10^{4}$	$(2.94 \pm 2.18)\times10^{3}$
min	60.1	1.78×10^{-5}	1.16×10^{-3}	1.00×10^{-2}	6.97×10^{3}	2.38×10^{3}	1.35×10^{3}
max	67.5	8.91×10^{-3}	2.54×10^{-2}	4.62×10^{-2}	2.34×10^{6}	9.74×10^{3}	4.78×10^{3}

Summary of **Os-4T** interassay performance in SK-MEL-28 with reference from original run (repeat# 0). Repeats used different plate maps (all), different tips (Sartorius 790352 repeat #1, VWR 83007-352 repeats #2–3, low retention Sartorius LH-L790352 repeats #4–5), changed cell parent seed stock for repeats 4–5, and overhead lights were off in #5. Serum and consumable lots were identical for repeats 1–5. Cell passage numbers were equal. Run in parallel with hypoxic repeats.

Table S-9 Cytotoxicity and photocytotoxicity of **Os-4T** in hypoxic-treated (1% O_2) SK-MEL-28 amelanotic cells interassay performance. Light treatments are approximately 100 J cm^{-2} delivered at 20 mW cm^{-2}. [a] Cool white visible (400–700 nm), [b] green 523 nm, [c] red 633 nm, [d] PI = phototherapeutic index (=dark EC_{50} / light EC_{50}), *original run in repeat 0 from Table S-5, and [e] repeat 3 light treatments excluded due to higher O_2% than intended (as indicated by internal control).

	Resazurin-Hypoxia (1% O_2) Os-4T Repeats						
	EC_{50} (μM)				PI[d]		
Repeat	Dark	Visible[a]	Green[b]	Red[c]	Visible[a]	Green[b]	Red[c]
0*	59.5	0.651	0.653	0.835	91	91	71
1	58.5	0.508	0.616	0.351	115	95	167
2	67.6	0.573	0.722	0.786	118	94	86
3[e]	69.7	~~0.041~~	~~0.206~~	~~0.334~~	~~1689~~	~~338~~	~~208~~
4	61.4	0.617	0.764	0.492	99	80	125
5	57.5	1.26	1.8	1.62	46	32	36
Mean ± SD	62.4 ± 5.1	0.722 ± 0.305	0.910 ± 0.499	0.817 ± 0.493	94 ± 29	78 ± 27	97 ± 51
min	57.544	0.508	0.616	0.351	46	32	36
max	69.7	26	1.80	1.62	118	95	167

Summary of **Os-4T** interassay performance in SK-MEL-28 with reference from original run (repeat# 0). Repeats used different plate maps (all), different tips (Sartorius 790352 repeat #1, VWR 83007-352 repeats #2–3, low retention Sartorius LH-L790352 repeats #4–5), changed cell parent seed stock for repeats 4–5, and overhead lights were off in #5. Serum and consumable lots were identical for repeats 1–5. Cell passage numbers were equal. Run in parallel with normoxic repeats.

Table S-10 Cytotoxicity and photocytotoxicity of **Os-*n*T** (***n*=0–4**) in normoxic-treated SK-MEL-28 human amelanotic and B16F10 murine melanotic cell lines tested at Acadia University. Conditions include dark (no light) and 100 J cm^{-2} treatments as [a] visible BenQ projector (400–700 nm, 33 mW cm^{-2}) and [b] red (633 nm, 40 mW cm^{-2}). [c] PI is the phototherapeutic index (=dark EC_{50} / light EC_{50}).

	SK-MEL-28					**B16-F10**				
	EC_{50} ± SEM (μM)			PI[c]		EC_{50} ± SEM (μM)			PI[c]	
Cmpd	Dark	Visible[a]	Red[b]	Visible[a]	Red[b]	Dark	Visible[a]	Red[b]	Visible[a]	Red[b]
Os-0T	238 ± 20	1.74 ± 0.03	5.13 ± 0.05	136	46	139 ± 5	7.04 ± 0.32	51.2 ± 0.1	19	2
Os-1T	127 ± 3	2.11 ± 0.07	4.61 ± 0.0	60	27	136 ± 5	4.92 ± 0.01	4.88 ± 0.01	27	27
Os-2T	123 ± 5	1.13 ± 0.01	1.32 ± 0.01	108	93	136 ± 4	5.05 ± 0.04	1.16 ± 0.01	26	117
Os-3T	132	0.097 ± 0.001	0.161 ± 0.003	1359	819	190 ± 7	0.12 ± 0.01	0.14 ± 0.01	1583	1357
Os-4T	144 ± 4	(2.91 ± 0.19) $\times 10^{-3}$	(9.44 ± 0.03) $\times 10^{-3}$	49484	15254	>300	0.015 ± 0.001	0.016 ± 0.001	>20000	>18292

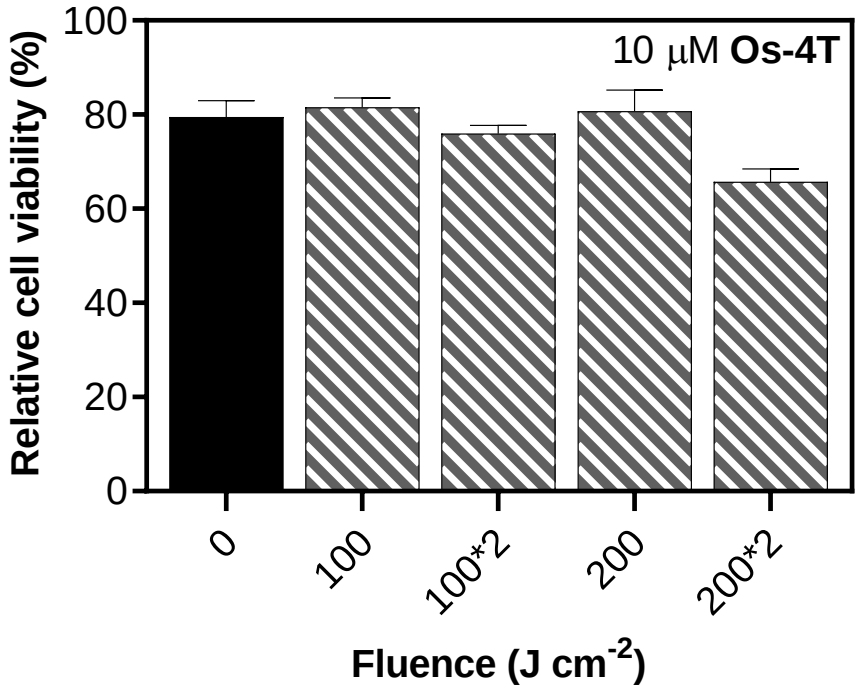

Figure S-46 Probing the near-infrared photocytotoxicity of 10 μM **Os-4T** at 753 nm (grey, diagonal stripes; 300 mW cm^{-2}) with dark control (left-most, no light, black bar) each in duplicate (± SD) on the ML8500 at 37°C with viability based on resazurin. An asterisk denotes separate treatments at the specified integer given at least an hour apart.

For data before normalization, the last point 200*2 J cm^{-2} was significant ($p<0.05$, $\alpha=0.05$) compared to the dark control (0 J cm^{-2}) in an ordinary one-way ANOVA and Dunnett's multiple comparison's test. There was a 14% reduction of the relative cell viability compared to dark for this treatment.

Abbreviations

Φ_Δ – singlet oxygen quantum yield
$^1O_2$ – singlet oxygen
ATCC – American Type Culture Collection
bpy – 2,2′-bipyridine
CH_2Cl_2 – methylene chloride
COSY – correlated spectroscopy
DFT – density functional theory
DI – deionized
DMEM – Dulbecco's Modified Essential Medium
DMSO – dimethyl sulfoxide
DPBS – Dulbecco's Phosphate-Buffered Saline
EC_{50} – effective concentration to affect sample population by 50%
EDTA – ethylenediaminetetraacetic acid
EMEM – Eagle's Minimum Essential Media
ESI+ – positive mode electrospray ionization
GI_{50} – 50% growth inhibition
GS – ground state
H_2O – water
HCl – hydrochloric acid
HMBC – heteronuclear multiple bond correlation
HOMO – highest occupied molecular orbital
HPLC – high performance liquid chromatography
HRMS – high resolution mass spectrometry
HSQC – heteronuclear single quantum coherence spectroscopy
IEFPCM – integral equation formalism polarizable continuum model
IL – intraligand
ILCT – intraligand charge transfer
IP – imidazo[4,5-*f*][1,10]phenanthroline
KNO_3 – potassium nitrate
KPF_6 – potassium hexafluorophosphate
LC_{50} – 50% lethal concentration or 50% protein reduction
log $D_{o/w}$ – lipophilicity index
LUMO – lowest occupied molecular orbital
MeCN – acetonitrile
MeOD – deuterated methanol
MLCT – metal-to-ligand charge transfer
MO – molecular orbital
NH_4OH – ammonium hydroxide
NMR – nuclear mass resonance
O_2 – oxygen
$O_2^{\cdot-}$ – superoxide
PBS – phosphate buffered saline
PDT – photodynamic therapy
phen – 1,10-phenanthroline
PI – phototherapeutic index

ppm – parts per million
PS – photosensitizer
RNS – reactive nitrogen species
ROS – reactive oxygen species
SD – standard deviation
SEM – standard error of the mean
SRB – sulforhodamine B
TA – transient absorption
TCA – trichloroacetic acid
TDDFT – time-dependent density functional theory
TGI – total growth inhibition concentration
UPLC – ultra-high performance liquid chromatography
UV-Vis – ultra-violet visible
VEA – vertical electron affinity
VIP – vertical ionization potential
XC – exchange-correlation